NUCLEAR HORMONE RECEPTOR-MEDIATED CHANGES OF CHOLESTEROL, TRIGLYCERIDE, AND BILE ACID PHYSIOLOGY IN RESPONSE TO ALTERATIONS IN CHOLESTEROL ABSORPTION AND BILE ACID POOL SIZE IN MICE

APPROVED BY SUPERVISORY COMMITTEE

Joyce Repa, Ph.D.

Jay Horton, M.D.

Rhonda Souza, M.D.

Ralf Kittler, Ph.D.

DEDICATION

To my wife Sarah, and our families. They have shared in all the sacrifices, and the joys that went into this work with unending support.

ACKNOWLEDGEMENT

I would like to acknowledge the many people who made this work possible. My deepest thanks go to my mentor Dr. Joyce Repa. Joyce is much more than a boss; she is a mentor in the truest sense of the word. She sacrificed many early mornings, late nights, and weekends to help me with experiments, and was always available to discuss science, going above and beyond what is expected of a mentor. Joyce ensured that I was exposed to many different aspects of metabolism and types of experiments, while also focusing on my dissertation research. This experience has given invaluable breadth as well as depth in my training. Thankfully, if Joyce's past trainees are any indication, her role as a mentor will not end with the completion of this dissertation. I would also like to thank the members of my dissertation committee, Drs. Jay Horton, Rhonda Souza, and Ralf Kittler. Their support and guidance have helped me with key aspects of my research, but more importantly they have helped me to develop into a better scientist.

I would also like to acknowledge the other members of my lab who have been instrumental in my training: Anna Taylor, Lilja Kjalarsdottir, Yelenis Mari, and Ernest Tong. Along the way they have all helped me with their technical knowledge, assisted with projects, and became my friends in addition to my colleagues. Additionally, much of this work would not have been possible without the continued support and collaboration of Dr. Stephen Turley and his laboratory. I spent many days doing experiments in the Turley lab, and his help and knowledge were invaluable components of this dissertation research. Additionally, I would like to thank former Repa lab members Mark Valasek and Jay Chuang for insightful discussions and collaborations.

NUCLEAR HORMONE RECEPTOR-MEDIATED CHANGES OF CHOLESTEROL, TRIGLYCERIDE, AND BILE ACID PHYSIOLOGY IN RESPONSE TO ALTERATIONS IN CHOLESTEROL ABSORPTION AND BILE ACID POOL SIZE IN MICE

by

RYAN DALE JONES

DISSERTATION

Presented to the Faculty of the Graduate School of Biomedical Sciences

The University of Texas Southwestern Medical Center at Dallas

In Partial Fulfillment of the Requirements

For the Degree of

DOCTOR OF PHILOSOPHY

The University of Texas Southwestern Medical Center

Dallas, Texas

June, 2013

NUCLEAR HORMONE RECEPTOR-MEDIATED CHANGES OF CHOLESTEROL, TRIGLYCERIDE, AND BILE ACID PHYSIOLOGY IN RESPONSE TO ALTERATIONS IN CHOLESTEROL ABSORPTION AND BILE ACID POOL SIZE IN MICE

RYAN DALE JONES, Ph.D.

The University of Texas Southwestern Medical Center at Dallas, 2013

JOYCE REPA, Ph.D.

The regulation of lipid metabolism is an interwoven series of pathways and events acting in concert to control the nutritional and metabolic needs of the body. When alterations in lipid balance occur they can result in disease, thus an understanding of the pathophysiology, as well as the molecular mediators of these alterations are vital to the advancement of treatment for these diseases. Many of these mediators are members of a class of proteins called nuclear hormone receptors, which respond to lipophilic compounds to regulate gene transcription. I have undertaken three separate, but related projects relating to lipid metabolism with a particular focus on nuclear hormone receptor function. First, I sought to understand how a drug that blocks cholesterol absorption can ameliorate the onset of hepatic steatosis. What I found was that in the early stages of disease onset, Ezetimibe prevents hepatic steatosis independently from the nuclear hormone receptor liver X receptor, and actually paradoxically stimulates hepatic lipogenesis despite decreased liver TG levels. Second, I determined the molecular and physiological changes that

occur with bile acid pool size restoration in mice that have a bile acid deficiency. This project highlighted the importance of bile acids in cholesterol absorption, the function of the bile acid-responsive nuclear hormone receptor farnesoid X receptor, and whole body lipid homeostasis. Additionally, we established a rationale for feeding low physiological amounts of bile acids to experimental animals, especially when those animals have a defect in bile acid production. Lastly, I studied the tissue distribution and nuclear hormone receptor-mediated regulation of a class of enzymes called carboxylesterases. This family of enzymes, which participate in neutral lipid hydrolysis, often came up on microarray analysis of metabolic studies, yet little was known about their regulation or function with regards to lipids. Therefore, I classified the tissue distribution of each of the carboxylestase family members in mice, and tested their gene expression upon treatment with synthetic agonists for the lipid-sensing NHRs. Thus, the information provided in this dissertation provides a valuable resource as the molecular mechanisms of disease and the role of nuclear hormone receptors begin to become clearer.

TABLE OF CONTENTS

PRIOR PUBLICATIONS

1. Fang S, Tsang S, **Jones R**, Ponugoti B, Yoon H, Wu S-Y, Chiang C-M, Willson TM, Kemper JK. The p300 acetylase is critical for ligand-activated farnesoid X receptor (FXR) induction of SHP. J Biol Chem. 2008;283:35086-95.

2. **Jones RD**, Repa JJ, Russell DW, Dietschy JM, Turley SD. Delineation of biochemical, molecular and physiological changes accompanying bile acid pool size restoration in Cyp7a1-/- mice fed low levels of cholic acid. Am J Physiol. 2012;303:G263-G74.

3. **Jones RD**, Taylor AM, Tong EY, Repa JJ. Carboxylesterases are uniquely expressed among tissues and regulated by nuclear hormone receptors in the mouse. Drug Metab Dispos. 2013;41(1):40-9. PMCID: 3533427.

LIST OF FIGURES

LIST OF TABLES

LIST OF APPENDICES

LIST OF ABBREVIATIONS

ABC, ATP-binding cassette transporter
ACAT (SOAT), acetyl-CoA acetyltransferase
ACCa, acetyl-CoA carboxylase alpha
ACOX2, acyl-CoA oxidase 2
ACSs, acetyl-CoA synthetases
ADRP, adipophilin
AKR1C4, aldo-keto reductase family 1, member C4
AMACR, alpha-methylacyl-CoA racemase
ANOVA, analysis of variance
ATGL (PNPLA2), adipose triglyceride lipase
BA, bile acids
BAAT, bile acid CoA: amino acid N-acyltransferase
BAT, brown adipose tissue
Bet1, blocked early in transport homologue 1
BSEP, bile salt export pump
bw, body weight
C, free (unesterified) cholesterol
CA, cholic acid
CAR, constitutive androstane receptor
CD36, fatty acid translocase
CDCA, chenodeoxycholic acid
cDNA, complementary Deoxyribonucleic acid
CE, cholesteryl ester
CES, carboxylesterase
CH25H, cholesterol 25-hydroxylase
ChREBP, carbohydrate-responsive element-binding protein
CM, chylomicrons
CoA, Coenzyme A
C_T, comparative cycle number at threshold
CYP7A1, Cholesterol 7α-hydroxylase
CYP, Cytochrome P450
DGAT, diacylglycerol acyltransferase
DM, diabetes mellitus
DMEM, Dulbecco's Modified Eagle Medium
ELISA, enzyme-linked immunosorbent assay
ER, endoplasmic reticulum
FA, fatty acids
FABPs, fatty acid binding poteins
FAS, fatty acid synthase
FATP4, fatty acid transport protein 4
FBS, fetal bovine serum
FGF, fibroblast growth factor
FGFR, fibroblast growth factor receptor
FH, Familial hypercholesterolemia
FLOT1/2, flotillins 1 and 2
FXR, farnesoid X receptor
GC, gas chromatography
h, hours

H & E, hematoxylin and eosin
HDL, high-density lipoprotein
HFD, high-fat diet
HFHCD, high-fat, high-cholesterol diet
HMG-CoA, 3-hydroxy-3-methyl-glutaryl-CoA
HNF4, hepatocyte nuclear factor 4 receptors
HSD3B7, 3 beta-hydroxysteroid dehydrogenase type 7
HSL, hormone sensitive lipase
IBAT (ASBT, Slc10a2), ileal bile acid transporter
IBABP, ileal bile acid binding protein
IDOL, inducible degrader of the LDL receptor
IL, interleukin
LDL, low-density lipoprotein
LDL-C, LDL associated cholesterol
LDLR, low-density lipoprotein receptor
LPS, Lipopolysaccharides
LRH-1, liver receptor homologue-1
LSS, lanosterol synthase
LXR, liver X receptor
LXR DKO, LXRα/LXRβ double knockout
MGATs, monoacylglycerol acyltransferases
mpk, mg/kg body weight
mRNA, messenger ribonucleic acid
MTP, microsomal triglyceride transport protein
Mylip, see IDOL
NAFLD, nonalcoholic fatty liver disease
NASH, nonalcoholic steatohepatitis
NHRs, nuclear hormone receptors
NMR, nuclear magnetic resonance
NPC, Niemann-Pick type C
NPC1L1, Niemann-Pick type C1-like protein 1
NTCP, sodium taurocholate transport protein
OATP, organic anion transporting polypeptide
OSBP, oxysterol binding protein
Ostα/β, organic solute transporter alpha and beta
PBS, phosphate buffered saline
PCR, polymerase chain reaction
PCSK9, proprotein convertase subtilisin/kexin type 9
PPAR, peroxisome-proliferator-activated receptor
PXR, pregnane X receptor
qPCR, quantitative real-time PCR\
RAR, retinoic acid receptor
RPL19, ribosomal protein L19
RPMI, Roswell Park Memorial Institute medium
RXR, retinoid X receptor
Sar1b, SAR1 homologue B
SCD1, stearoyl-Coenzyme A desaturase 1
SD, standard low-fat diet
Sec23, transport protein Sec23
SHP, small heterodimer partner

SEM, standard error of the mean
Slc, solute carrier family
SR-BI, scavenger receptor, class B member 1
SREBP, sterol regulatory element-binding protein
SRE, SREBP Response Elements ???????
TGR5 (Gpbar1), G protein-coupled bile acid receptor 1
TGs, triglycerides
TICE, transintestinal cholesterol efflux
TNF, tumor necrosis factor
TRα/β, thyroid hormone receptors alpha and beta
Vamp7, vesicle-associated membrane protein 7
VDR, Vitamin D receptor
VLDL, very-low-density lipoprotein
Vti1a, vesicle transport through interaction with t-SNAREs 1A
WAT, white adipose tissue
WT, wildtype

CHAPTER ONE:

Introduction

1.1 Introduction to Lipid Metabolism

Lipids are a broad family of naturally occurring molecules that vary in size and shape but carry some common features. One main distinction of lipids is that they are typically more soluble in non-polar solvents (e.g. chloroform or ethers) than in polar solvents (e.g. water). Many lipids play important roles in animals; they provide efficient energy storage, serve as signaling molecules, vitamins, hormones, and are structural components of plasma membranes. Some of the abundant physiologically relevant lipids are triglycerides (TGs), cholesterol, phospholipids, bile acids, steroid hormones, and sphingolipids. Though much is known about the chemical and functional roles of many lipids (an excellent resource is LIPID MAPS, www.lipidmaps.org), there is still much to be learned about the integrative physiology of how diverse classes of lipids affect each other at the molecular level. Lipid metabolism has been implicated along with glucose homeostasis in the diseases of obesity, metabolic syndrome, type 2 diabetes mellitus, and atherosclerosis. As I will discuss, the regulators of lipid metabolism impact numerous and varied pathways, and therefore an understanding of whole-body physiology of these processes is necessary to approach treatment options for these diseases.

Mouse models have proved invaluable to the study of lipid metabolism. With mice, one has the capacity to study the effect of specific diets, treatments, and most importantly genotype on the development and progression of disease. There are some caveats of using mice as model organisms for human disease, and data must be interpreted carefully. Some of these differences could confound the data presented in this dissertation. For instance, one major difference is that humans and mice both express the cholesterol transporter Niemann-Pick C1-Like 1 (NPC1L1) in the intestine where it mediates intestinal cholesterol absorption, however humans also express NPC1L1 in the liver to reclaim biliary cholesterol, whereas mice do not. Another difference is that humans and mice have a different chemical

makeup of their bile acid pools; one of the major primary bile acids in humans is chenodeoxycholic acid, but in mice this is modified to form muricholic acid. Additionally, mice appear to have many more carboxylesterase enzymes, which catalyze neutral lipid hydrolysis, compared to humans. Therefore the data presented in this dissertation may not fully recapitulate what is seen in human disease, and must be interpreted with this in mind.

The classes of lipids I will focus on in this dissertation are cholesterol, bile acids, and triglycerides. Specifically I will try to answer 3 main questions: 1) How does decreasing intestinal cholesterol absorption affect pathological triglyceride storage in the liver?; 2) What are the consequences of depleting an animal of endogenous bile acids, and the subsequent response to replenishment of specific bile acid species?; and 3) Within the family of carboxylesterases, a group of enzymes involved in neutral lipid hydrolysis, which members are transcriptionally regulated by known lipid-sensing transcription factors?. The physiological regulation of these lipids is central to all three projects, and this regulation is controlled to a large degree by a family of proteins called nuclear hormone receptors.

1.2 Nuclear Hormone Receptors

Nuclear hormone receptors (NHRs) comprise a superfamily of ligand-activated transcription factors. These receptors respond to lipophilic compounds to coordinate physiologic responses to nutritional, metabolic, or hormonal states. There are 48 NHRs in humans (49 in mouse) many of which were identified through sequence homology to known nuclear hormone receptors (Chawla et al., 2001). Most of these proteins contain a DNA-binding domain which recognizes receptor-specific DNA sequences providing target gene selection, and a ligand-binding domain which modulates receptor activity. NHRs recruit coregulators to exert their effect in increasing or decreasing promoter activity on their target genes, often achieved by altering chromatin structure. Classically, in the unliganded state corepressors are bound to the receptor residing on the DNA-response element. Upon ligand-binding, the corepressors are released, and coactivators are recruited to initiate target gene transcription.

The NHR superfamily can be further divided into subfamilies (see **Fig. 1.1)** of endocrine receptors (e.g. glucocorticoid receptor, estrogen receptors), lipid-sensing/adopted orphan receptors (e.g. liver X receptor, farnesoid X receptor), and orphan receptors for which there are no known endogenous ligands (e.g. small heterodimer partner) (Chawla et al., 2001). The endocrine receptors bind and respond to their respective ligands with very high affinity (pM-nM range). The adopted orphan receptors however have much lower affinity for their respective ligands (μM range). The ligands for this latter class of receptors are generally dietary-derived lipids participating in the nutritional homeostasis of the body, and therefore reach much greater concentrations compared to their endocrine counterparts.

One NHR, the retinoid X receptor (RXR) is unique because it forms heterodimers with many other NHRs, mainly from the adopted orphan receptor family, but also with retinoic acid receptor (RAR), vitamin D receptor (VDR), and thyroid hormone receptors (TRα/TRβ). These heterodimer partnerships can function permissively, where the pair can be activated by either RXR's ligand, or by its partner's ligand to stimulate gene transcription, and there is a synergistic effect with a combination of both ligands (e.g. LXRs, FXR, and PPARs). Alternatively, RXR can form ligand-independent non-permissive heterodimer partnerships in which target gene regulation is exclusively due to activation of the partner receptor (e.g. VDR, RAR). RXRs have also been observed to form homodimers, although target genes regulated by this complex have not yet been identified.

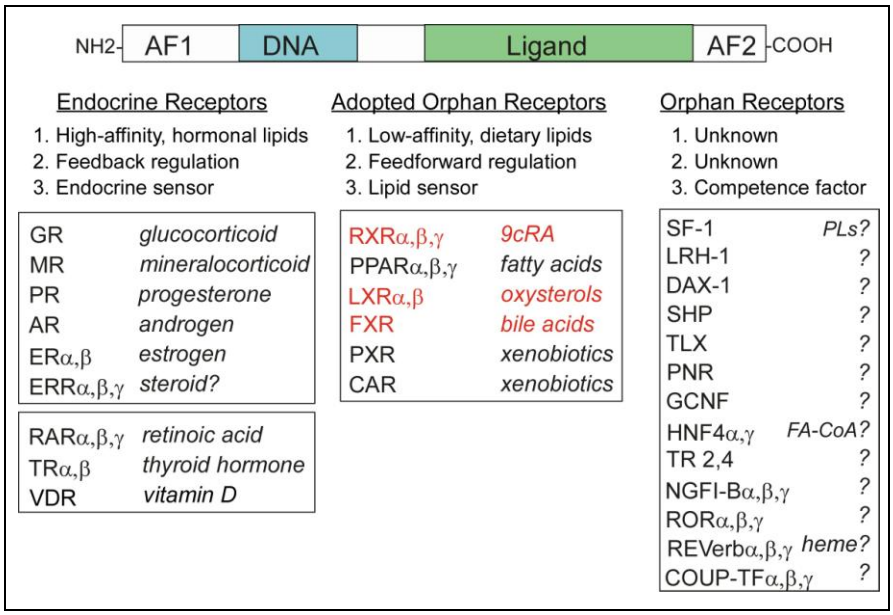

Fig. 1.1 The superfamily of nuclear hormone receptors. These transcription factors are displayed in three groups reflecting their roles as endocrine sensors, lipid sensors, and orphans. For each receptor, the physiologic ligand(s) are listed. The receptors shown in red are most relevant to work presented in this dissertation.

Liver X Receptors (LXRs)

The LXRs are members of the adopted orphan nuclear receptor subfamily. There are two LXR isoforms in both humans and mice, LXRα (NR1H3) and LXRβ (NR1H2). The endogenous ligands for these receptors are oxysterols, which are cholesterol metabolites present at very low concentrations within cells. The active oxysterols are generated by enzymatic processes, and include 24(*S*)-hydroxycholesterol (via CYP46), 22(*R*)-hydroxycholesterol which is the first intermediate in the reaction by the cytochrome P450 side chain cleavage enzyme (P450scc, also known as CYP11A1), 24(S),25-epoxycholesterol (via lanosterol synthase (LSS)) and perhaps 27-hydroxycholesterol (via CYP27) (Fu X. et al., 2001; Janowski B. A. et al., 1999; Janowski B. A. et al., 1996; Lehmann et al., 1997). More recently the cholesterol biosynthetic intermediate desmosterol has also been shown to be a ligand for LXRs (Yang et al., 2006). LXRα and LXRβ both function as permissive heterodimers with RXR and recognize the same DNA hexanucleotide response element, a direct repeat (AGGTCA) with 4 intervening spacer nucleotides (DR4) which are present in the promoter/enhancer regions of LXR target genes. The main difference between the two isoforms of LXR is their pattern of expression. LXRα expression is high in metabolically active

tissues such as liver, adipose, small intestine, kidney, and lung. LXRβ is much more ubiquitous in its expression pattern and generally less prominent than LXRα in the tissues where both are present, especially the liver (Lu et al., 2001).

Oxysterol concentrations tend to increase under conditions where cellular cholesterol is increased, and therefore LXRs are activated. Many of the targets genes act to promote cholesterol lowering, and some stimulate lipogenesis through multiple strategies: 1) through cellular cholesterol efflux via the action of ATP-binding cassette transporters (ABC) members A1, G1, G5, and G8; 2) to convert cholesterol into bile acids through increased expression of cholesterol 7α-hydroxylase (CYP7A1); 3) through inducible degradation of the LDL-receptor (LDLR) via expression of the gene myosin regulatory light chain interacting protein (MYLIP, also called IDOL); or 4) by increasing fatty acid synthesis through activation of fatty acid synthase (FAS), stearoyl-Coenzyme A desaturase (SCD1), and other lipogenic transcription factors sterol regulatory element-binding protein 1c (SREBP-1c) and carbohydrate response element-binding protein (ChREBP) (Cha and Repa, 2007; Chawla et al., 2001; Repa et al., 2002a; Repa et al., 2000a; Zelcer et al., 2009). It is unclear if increasing fatty acid synthesis reduces the cholesterol burden on cells, but it may 1) reduce the rates of *de novo* cholesterol biosynthesis through reduction of the initial substrate acetyl-CoA, and/or 2) provide preferred fatty acids needed for the esterification of free cholesterol. Free cholesterol is more damaging to cells than cholesteryl esters, which can be safely stored in lipid droplets, and transported out of the cell into lipoprotein particles.

Whole body cholesterol homeostasis is highly regulated, and aside from the nervous system which is largely self-contained with regards to cholesterol metabolism, can be divided into three separate but related components. These components are the liver, the intestine, and other peripheral tissues.

The liver is the main regulatory organ for cholesterol homeostasis. It is the largest producer of newly synthesized cholesterol, and it is also the main site for elimination of cholesterol from the body. It is responsible for the ultimate clearance of chylomicron remnant particles, as well as LDL- and HDL-

cholesterol. Bile acids are produced exclusively in the liver and represent a major excretory route for cholesterol. In addition, hepatic cholesterol transporters ABCG5/8 are upregulated by LXR to promote secretion of unesterified cholesterol directly into bile.

The small intestine is responsible for the absorption of dietary and biliary cholesterol as well as the reuptake of bile acids. 5% of bile acids are lost everyday representing a major route of cholesterol elimination. Dietary cholesterol mixes with biliary cholesterol and phospholipids to form mixed micelles in the small intestine to allow transit across the unstirred water later adjacent to the enterocyte. Only approximately 50% of this cholesterol is absorbed. Cholesterol is transported into enterocytes by the apical membrane-bound transporter Niemann-Pick C1-Like 1 (NPC1L1, see **Fig. 1.2**). The enterocyte can sense this cholesterol which can then be recycled back into the intestinal lumen through the action of the LXR-responsive cholesterol transporters ABCG5/8. Alternatively, the enterocyte can package cholesterol into chylomicrons, or into HDL-particles through the LXR-responsive transporter ABCA1. There are also reports suggesting that the intestine can undergo reverse cholesterol transport through a process known as transintestinal cholesterol efflux (TICE) (Temel and Brown, 2010; van der Velde et al., 2010; van der Velde et al., 2008; Vrins, 2010). TICE would contribute to the fecal neutral sterol pool in addition to biliary cholesterol to contribute to excretion of cholesterol from the body, though the physiological relevance of this pathway is still controversial. Nevertheless, the small intestine is very important in the regulation of whole body cholesterol homeostasis.

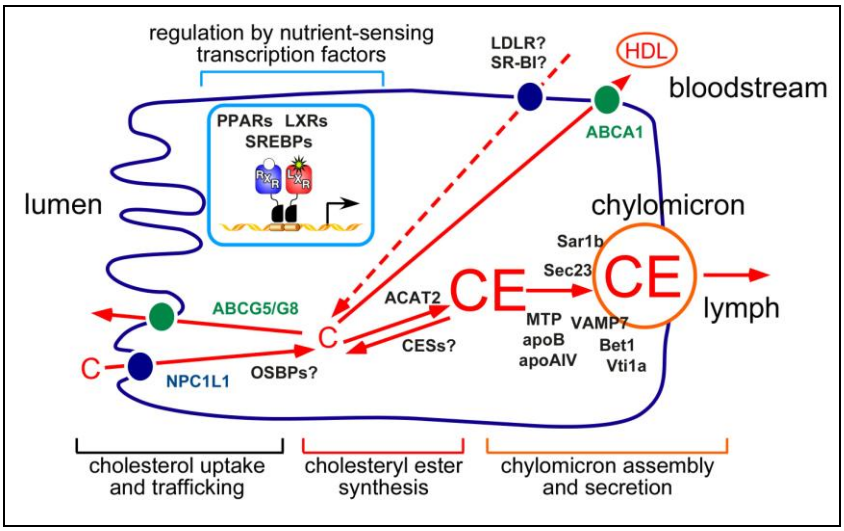

Fig. 1.2 Cholesterol trafficking in the enterocyte. An enterocyte of the proximal jejunum is pictured, with apical (left) and basolateral (right) orientation. Unesterified cholesterol (C) is transported into the cell, esterified (CE) and packaged into chylomicrons that are secreted into lymph. The novel, yet controversial, TICE (transintestinal cholesterol efflux) is shown by the dotted line. Full descriptions of these processes are provided in the text and reviewed in (Abumrad and Davidson, 2012). Abbreviations: ABC, ATP binding cassette transporter; ACAT2, acyl-CoA: cholesterol acyltransferase 2; Bet1, Blocked early in transport homolog 1 ; CESs, carboxylesterases; MTP, microsomal triglyceride transferase; NPC1L1, Niemann Pick C 1 Like-1; OSBPs, oxysterol-binding proteins; Sar1b, SAR1 homolog B ; Sec23, transport protein Sec23 ; SR-BI, scavenger receptor BI; VAMP7, vesicle-associate membrane protein 7 ; Vti1a, vesicle transport through interaction with t-SNAREs 1 homolog.

Peripheral tissues have the capacity to synthesize their own cholesterol, and can also take up circulating cholesterol through LDL-particle receptor-mediated endocytosis. This peripheral tissue cholesterol is necessary for certain cellular functions, but excess cholesterol must eventually be removed to maintain necessary levels. The main route of peripheral cholesterol elimination is through reverse cholesterol transport to HDL-particles partly through the action of LXR-responsive ABCA1. These HDL-particles are then processed by the liver. Thus, LXR has proven to be critical for whole body cholesterol homeostasis by its actions in the liver, intestine, and peripheral tissues.

Due to the beneficial effects of LXR-activation on cholesterol metabolism, this system represents a potential mechanism for the treatment of cholesterol-related disorders. Highly specific agonists for LXR have been synthesized (including T0901317 (Repa et al., 2000b; Schultz et al., 2000), and GW3965 (Collins et al., 2002) reviewed in (Goodwin B. J. et al., 2008)), and have been shown to promote reverse cholesterol transport from the periphery to the liver for processing, reduce atherosclerotic plaque size,

decrease cholesterol absorption, and stimulate the conversion of cholesterol to bile acids reviewed in (Calkin and Tontonoz, 2012). Unfortunately, LXR-activation also results in robust activation of hepatic lipogenesis causing severe hepatic steatosis precluding these agonists from use as first-line therapeutic agents (Repa et al., 2000a; Schultz et al., 2000). Efforts have been made to find an LXRβ-specific agonist to promote reverse cholesterol transport, without the negative side-effects of hepatic steatosis where LXRα predominates, however to my knowledge, this effort has been unsuccessful thus far. It is possible that LXR-agonist administration could be useful for short-term therapy or through localized delivery (e.g. agonist-coated stents placed in atherosclerotic arteries) to stimulate reverse cholesterol transport, without causing irreversible liver damage, but to my knowledge these approaches have not yet been tested.

Farnesoid X Receptor (FXR) and Bile Acids

FXR (NR1H4) is another member of the adopted orphan nuclear receptor subfamily. There is only one FXR isoform in humans, while there are two in mice, FXRα and FXRβ (NR1H5). The importance of FXRβ in mice is unclear and will not be discussed. FXR was originally described (and so named) as a sensor for farnesol, an intermediate of cholesterol metabolism, however this interaction occurred at supraphysiologic levels (Forman et al., 1995). It was later discovered that bile acids are the endogenous ligands for FXR (Makishima et al., 1999; Parks et al., 1999). Both of the main bile acid species in humans, cholic acid (CA) and chenodeoxycholic acid (CDCA) have been described as FXR ligands. FXR is most abundantly expressed in liver, intestine, kidney, and adrenal glands. FXR forms a permissive heterodimer with RXR on target genes, which can be activated by both FXR and RXR agonists. The FXR/RXR heterodimer recognizes and binds to an inverted repeat of the canonical hexanucleotide sequence AGGTCA with a one nucleotide spacer (IR1) (Forman et al., 1995). When FXR is activated, it modulates expression of target genes involved in bile acid homeostasis, as well as some genes involved in other pathways such as cholesterol and glucose homeostasis. Some of the effects of

FXR are to repress gene expression, often through the action of small heterodimer partner (SHP) and liver receptor homologue 1 (LRH1). Animals have developed multiple sensors for bile acids including FXR, the xenobiotic-sensing receptors pregnane X receptor (PXR) and constitutive androstane receptor (CAR), vitamin D receptor (VDR) as well as the G protein-coupled bile acid receptor 1 (TGR5 also known as Gpbar1). Therefore, isolating the effects of FXR is challenging and benefits from the use of mice lacking FXR (Sinal et al., 2000), as well as specific synthetic FXR agonists (e.g. GW4064).

When bile acids are produced they are typically conjugated to amino acids (taurine or glycine). This increases their solubility, but prohibits their diffusion across cell membranes. Thus tissues (liver, kidney, intestine) harbor specific bile acid transporters for bile acid uptake and efflux. They are then stored in the gall bladder where they are kept until food is ingested, signalling the gall bladder to release its contents into the duodenum. Bile acids are necessary to form mixed micelles in the intestine facilitating the absorption of dietary lipids, including cholesterol and fat-soluble vitamins. In addition, the production and excretion of bile acids represents a primary method for cholesterol elimination from the body. Bile acids undergo significant enterohepatic circulation, with 5% of the total pool size lost each day. At high concentrations bile acids are toxic to cells, and therefore feedback regulation is very important to prevent overproduction.

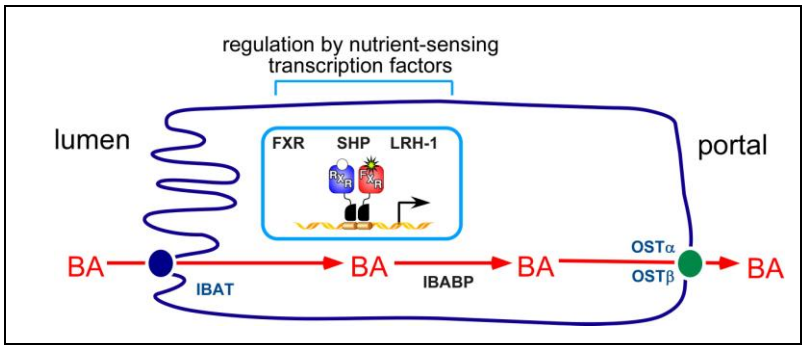

Fig. 1.3 Bile acid trafficking in the enterocyte. An enterocyte of the ileum is pictured, with apical (left) and basolateral (right) orientation. Bile acids (BA) are transported into the cell by the bile acid transporter, (IBAT), bound and carried by the ileal bile acid binding protein (IBABP), and secreted into the portal circulation via the organic solute transporters, OSTα/OSTβ.

FXR is one of the key regulators of bile acid metabolism. In the liver, when the bile acid pool size is high, FXR acts to inhibit further production of bile acids. Hepatic FXR utilizes a feedback loop through induction of SHP which interacts with LRH1 to form a heterodimer. This interaction results in the repression of cholesterol 7α-hydroxylase (CYP7A1), the rate-limiting enzyme in the classical pathway of bile acid biosynthesis (Jelinek et al., 1990; Russell D. W., 2003). In the small intestine FXR also drives expression of the circulating peptide fibroblast growth factor 19 (FGF19) in humans, or its ortholog FGF15 in mice. FGF15/19 is secreted from the intestine and travels to the liver via enterohepatic circulation acting on FGF receptor 4 (FGFR4) to initiate signal transduction pathways that ultimately repress CYP7A1 expression (Inagaki et al., 2005). Thus, both the intestine and the liver participate in regulating the amount of bile acids being produced by providing feedback information about the bile acid pool size.

When bile acids are produced they are exported from the liver to the gall bladder through the action of the FXR-responsive protein bile salt export pump (BSEP, ABCB11) and emptied into the lumen of the small intestine upon ingestion of a meal. In the distal small intestine (see **Fig. 1.3**), bile acids are transported into enterocytes via the ileal bile acid transporter (IBAT, also known as ASBT and SLC10A2). These bile acids are sensed by FXR which drives expression of ileal bile acid-binding protein (IBABP) promoting the transit of bile acids to the basolateral side of the enterocyte. They are then released into the portal venous system for return to the liver via the action of FXR-responsive organic solute transporters (OSTα and OSTβ). The liver then receives the recycled bile acids through sodium taurocholate cotransporting polypeptide (NTCP) and organic anion transporting polypeptide (OATP). NTCP and OATP are repressed by FXR to prevent bile acids from accumulating to unsafe levels in the liver. Bacteria in the distal small intestine and colon often modify primary bile acids producing secondary bile acids that differ in their affinity for bile acid sensors (DCA and LCA have decreased affinity for FXR, but LCA is a potent activator of PXR, VDR, and TGR5).

Bile acids have an apparent relationship with glucose homeostasis, as well as with hepatic insulin resistance. This association may act through both FXR-dependent and independent pathways (Kobayashi et al., 2007; Li et al., 2010; Watanabe et al., 2011; Zieve et al., 2007). Thus, bile acids are re-emerging as an important system to study as their function in whole body metabolic homeostasis goes well beyond their role as simply detergents to solubilize fats and vitamins in the small intestine.

1.3 Cholesterol

Cholesterol is an integral component of every cell type, and is essential for the proper functioning of mammalian life. Cholesterol serves a structural role in cell membranes effecting permeability and fluidity, and also interacts with several proteins inside and outside of cells. It acts as the substrate for the production of several important compounds including bile acids, steroid hormones (e.g. testosterone and estrogen), and vitamin D. The transport, synthesis, breakdown, and storage of cholesterol are tightly controlled processes regulated by a variety of transcription factors as well as the post-translational control of critical protein levels and activity. However, problems still arise where cholesterol has been implicated in the pathophysiology of disease states. These include hypercholesterolemia and resulting cardiovascular disease; non-alcoholic fatty liver disease; lysosomal storage diseases defined by trapped lysosomal cholesterol; and cholelithiasis. Overwhelming evidence implicates increased circulating levels of cholesterol-rich low density lipoproteins (LDL) as the most prominent risk factor for atherosclerotic plaque development and cardiovascular disease (Expert Panel on Detection, 2001). Current guidelines recommend LDL-cholesterol levels of lower than 100 mg/dL for patients at risk for cardiovascular disease (Costet, 2010; Grundy S. M. et al., 2004). Additionally, there is genetic evidence supporting the benefits of lifelong lowering of plasma LDL cholesterol concentrations (Cohen et al., 2006). Thus, treatments designed to lower the cholesterol burden on the body have been developed to lower circulating LDL-cholesterol levels. The most widely prescribed among these are statins which block the rate-limiting enzyme in *de novo* synthesis of cholesterol, 3-hydroxy-3-methylglutaryl coenzyme A (HMG-

CoA) reductase. Another strategy is to prevent the intestinal absorption of cholesterol from both dietary and biliary sources through the use of the drug Ezetimibe.

The function of cholesterol

Cholesterol is a component of diet, but it can also be synthesized by virtually every cell of the body. It is an integral component of plasma membranes, and provides the precursor to bile acids and steroid hormones. Dietary cholesterol, as well as biliary cholesterol travel through the small intestine solubilized in mixed micelles with bile acids. The protein Niemann-Pick C1-Like 1 (NPC1L1), located on the apical membrane of intestinal enterocytes, then binds to and facilitates the transport of cholesterol into the enterocyte (see **Fig. 1.2**). Within the enterocyte, cholesterol is esterified by the addition of a fatty acyl side chain via the enzyme acyl CoA:cholesterol acyl transferase 2 (ACAT2), and packaged into chylomicrons (CM). CMs are TG-rich lipoprotein particles which travel through the lymph until they are released into the bloodstream. CMs release TGs to various tissues until they decrease in size and become CM remnants. These are then internalized by hepatocytes where the liver then processes the contents of the CM remnant. The liver also has the capacity to secrete very-low-density lipoprotein (VLDL) particles, which are TG- rich lipoproteins also containing cholesterol. VLDL is eventually converted into low-density lipoproteins (LDL) in the blood stream which are classically considered the "bad" cholesterol. When cells are deficient in cholesterol they increase the amount of LDL uptake by increasing the amount of the protein low-density lipoprotein receptor (LDLR). However, when blood levels of LDL get too high, the risk of developing atherosclerosis is greatly increased. Cholesterol within high-density lipoprotein (HDL) particles is commonly referred to as "good" cholesterol. HDL particles can claim cholesterol stored in peripheral tissues such as atherosclerotic macrophages, and transport the cholesterol back to the liver for further processing. The nervous system is unique in that the blood-brain barrier is impermeable to cholesterol-carrying lipoproteins, and therefore it must synthesize and process all of its own cholesterol, a significant fact, as the brain contains roughly 25% of the body's total cholesterol.

The pathophysiology of cholesterol-related disorders.

Hypercholesterolemia and atherosclerosis. The most prevalent cholesterol-related disorder is atherosclerosis resulting from cholesterol deposition into macrophages in arteries eventually leading to plaque formation. Eventually, these plaques can rupture leading to thrombosis and occlusion of the artery. When this happens in the major arteries of the heart, it can lead to a myocardial infarction. When this occurs in the carotid arteries, it can result in ischemic stroke.

Familial Hypercholesterolemia (FH). This disease most commonly results from loss-of-function mutations in the LDLR. Homozygous FH, caused by a complete loss of LDLR through the inheritance of two mutant LDLR alleles results in severe LDL-cholesterol accumulation in the body, often exceeding 650 mg/dL. The incidence for homozygous FH is very rare (1:1,000,000). Homozygous FH patients often suffer heart attacks during early childhood, in addition to the deposition of cholesterol-laden xanthomas on the skin and tendons. More commonly (1:500), patients inherit one mutant copy of the LDLR gene, and are thus termed heterozygous FH. Patients with heterozygous FH have plasma LDL-cholesterol concentrations ranging from 350-550 mg/dL, and increased risk for early cardiovascular events (Goldstein et al., 1995).

Nonalcoholic Fatty Liver Disease Another cholesterol-related disorder is nonalcoholic fatty liver disease (NAFLD) which will be discussed in greater detail below.

Lysosomal storage diseases There are some rare, yet extremely severe diseases that result from defects in the intracellular handling of cholesterol. These diseases occur due to the entrapment of lysosomal cholesterol. In the most serious disease of lysosomal cholesterol storage Neimann-Pick type C (NPC) disease, a mutation in either the Neimann-Pick type C1 or C2 (NPC1 or NPC2) proteins results in increased unesterified cholesterol within the lysosome. Patients with this disease suffer from progressive neurodegeneration, as well as hepatic and pulmonary disease, ultimately resulting in premature death, typically around the time of adolescence.

Neurodegenerative disorders Cholesterol has also been implicated in several neurological diseases such as Parkinson Disease, Huntington Disease, and Alzheimer Disease (reviewed in (Vance, 2012), but this will not be discussed further.

Cholesterol Metabolism

The synthesis, storage, efflux and breakdown of cholesterol are all very tightly regulated processes controlled by two opposing transcription factors, the sterol regulator element-binding protein 2 (SREBP-2) which is active when the sterol burden is low and the LXRs discussed previously which respond to increased sterol concentrations. Cholesterol is synthesized *de novo* from acetyl-CoA precursors through a series of biochemical processes. The rate-limiting enzyme in this pathway is HMG CoA Reductase, which reduces HMG-CoA to form mevalonate. Additional enzymes participate to eventually produce cholesterol with its characteristic four rings and 27 carbons. The expression of these cholesterol biosynthetic enzymes are all regulated by the SREBP-2 transcription factor. SREBP-2 is one member of the SREBP family of transcription factors. These proteins are synthesized as inactive precursors, and reside in the endoplasmic reticulum (ER). There are two mammalian SREBP genes. The *srebp-1* gene produces two distinct proteins, SREBP-1a and 1c, which are produced by alternative promoters resulting in distinct first exons. The *srebp-2* gene produces only one protein, SREBP-2. Upon conditions of sterol-depletion SREBP-2 is transported to the golgi apparatus where it is proteolytically cleaved. A soluble N-terminal fragment then enters the nucleus where it binds to sterol regulatory elements (SREs) to drive transcription of cholesterol biosynthetic genes, as well as LDLR to increase internalization of extracellular cholesterol (Horton et al., 2002). When cellular cholesterol is increased, SREBP-2 is detained in the ER in its precursor form to prevent activation of the cholesterol biosynthetic machinery.

Treatments for cholesterol-related disorders

Decreased dietary cholesterol intake is the first-line therapy for the treatment of hypercholesterolemia. Unfortunately, as the body is fully capable of synthesizing cholesterol, this is often

not sufficient to achieve the recommended lowering of LDL-cholesterol, especially for patients with underlying genetic or metabolic disease. Therefore, pharmaceutical agents have been developed as secondary therapies for the treatment of cholesterol-related diseases. For hypercholesterolemia statins are the most widely prescribed therapy. Statins act as competitive inhibitors of HMG CoA Reductase, the rate-limiting enzyme in cholesterol biosynthesis. Although a sustained decrease of cholesterol synthesis is usually not achieved, there is a lasting effect on plasma LDL-cholesterol reductions. This is likely due to SREBP2-mediated transcriptional activation of the LDLR which internalizes plasma LDL. The use of statins has provided substantial evidence for the beneficial effects of lowering plasma LDL-cholesterol levels (Grundy S. M. et al., 2004).

Other treatments that result in LDL-cholesterol reduction are: niacin (Vitamin B3); fibrates, which act through the NHR peroxisome proliferator-activated receptor α (PPARα); bile acid binding resins (e.g. cholestryramine), which cause fecal loss of bile acids resulting in greater turnover of cholesterol into bile acids; and plant sterols.

Finally, another drug commonly prescribed to lower LDL-cholesterol is Ezetimibe. This drug blocks intestinal cholesterol absorption through its action on the protein NPC1L1. Ezetimibe can either be used alone (Zetia) or in combination with a statin (Vytorin, Ezetimibe plus Simvastatin; Liptruzet, Ezetimibe plus Atorvastatin). The benefits of Ezetimibe use on mortality rates due to coronary heart disease compared with statins have not yet been established through clinical trials, yet it remains a good option for patients who do not achieve recommended LDL-cholesterol levels on statins alone as LDL-cholesterol lowering is enhanced by this combination therapy. Ezetimibe will be discussed in more detail below.

Ezetimibe

The drug Ezetimibe was developed by the company Schering-Plough Research Institute (Kenilworth, NJ) in the late 1990's and the early 2000's. While much of the pharmaceutical industry focused on "rational drug design" applying new biochemical technologies to known molecular targets, the discovery

of Ezetimibe followed a different path. Researchers at Schering-Plough were searching for novel inhibitors of acyl-CoA cholesterol acyltransferase (ACAT) as a means to reduce the accumulation of cholesteryl esters, and perhaps cholesterol absorption. The rationale for this had only been established in rodents, and it was not known what the effects in primates and humans would be. They identified a compound that not only reduced hepatic cholesteryl ester accumulation, but also reduced plasma cholesterol concentrations, and even more surprisingly, seemed to act independently of ACAT. At the time, the molecular mechanism for cholesterol absorption was unknown, it was unclear whether it was a protein-mediated process, or uptake into the enterocyte occurred by passive diffusion across the apical membrane (Clader, 2004). It was later discovered that the mechanism of action of Ezetimibe was to block cholesterol absorption, by binding to a putative cholesterol transporter in the apical membrane of enterocytes (Kosoglou et al., 2005). The development of this drug subsequently led to the discovery of its molecular target NPC1L1, as well as the observation that NPC1L1 is required for cholesterol absorption (Altmann et al., 2004; Garcia-Calvo et al., 2005). This is an excellent example of scientific discovery being made after careful physiological observations while testing novel compounds, instead of the traditional approach of identifying molecular targets first.

Ezetimibe is a member of the azetidinone family of chemicals, and acts primarily in the small intestine. It undergoes enterohepatic circulation, and is metabolized to a more active glucuronide form of the compound in both enterocytes and hepatotyes, and from the liver, gets secreted into the bile (Kosoglou et al., 2005). The circulating concentration outside of the enterohepatic circulation is very low. Interestingly mice express the molecular target for Ezetimibe, NPC1L1, only in the intestine, whereas humans also express NPC1L1 in the liver. Thus, in humans Ezetimibe acts to inhibit cholesterol absorption in the intestine, as well as biliary cholesterol reuptake in the liver.

1.4 Triglycerides and Obesity

Triglycerides (TGs) are molecules made up of three fatty acids bound as esters onto a glycerol backbone. TGs are used extensively in eukaryotic physiology as a primary means for energy storage. TGs are very energy dense providing 9 kcal/g, compared to 4.5 and 4 kcal/g for carbohydrates and proteins respectively. TGs are primarily stored in adipocytes, where they can accumulate without many negative consequences due to the fact that they are insoluble in water producing very little osmotic pressure.

As a dietary component, TGs in the intestinal lumen must be hydrolyzed by lipases to allow internalization of components (fatty acids, monoacylglycerides, and glycerol) by enterocytes. Within enterocytes the free fatty acids reform TGs, and through the action of microsomal triglyceride transfer protein (MTP) are packaged into chylomicrons and excreted into the intestinal lymphatics (see **Fig. 1.4**). The lymph is eventually released into the bloodstream where TGs are hydrolyzed by lipoprotein lipase and free fatty acids released for uptake into peripheral tissues.

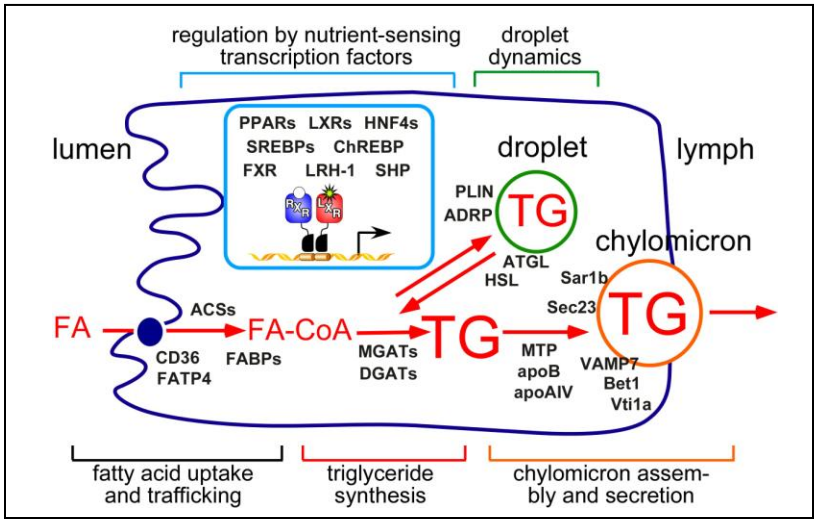

Fig. 1.4 Fatty acid trafficking in the enterocyte. An enterocyte of the jejunum is pictured, with apical (left) and basolateral (right) orientation. Free fatty acids (FA) are transported into the cell, modified by the addition of a coenzymeA (FA-CoA), esterified (TG) and packaged into chylomicrons that are secreted into lymph. There is evidence of transient formation of lipid droplets. Full descriptions of these processes are provided in the text and reviewed in (Abumrad and Davidson, 2012; Hussain et al., 2005; Xiao et al., 2011). Abbreviations: ACSs, Acyl-CoA synthetases; ADRP, adipophilin: ATGL, adipose triglyceride lipase; Bet1, Blocked early in transport homolog 1; CD36, fatty acid translocase; DGATs, diacylglycerol acyltransferases; FABPs, fatty acid binding proteins; FATP4, fatty acid transport protein 4; HSL, hormone-sensitive lipase; MGATs, monoacylglycerol transferases; ; MTP, microsomal triglyceride transferase; Sar1b, SAR1 homolog B ; Sec23, transport protein Sec23; VAMP7, vesicle-associate membrane protein 7 ; Vti1a, vesicle transport through interaction with t-SNAREs 1 homolog.

TGs can also be synthesized *de novo* by acetyl-CoA substrates to form fatty acids. This process is regulated by a myriad of proteins and transcription factors such as LXR, SREBP-1c, ChREBP, fatty acid synthase (FAS), and acetyl-CoA carboxylase alpha (ACCa). Some of the humoral factors that stimulate lipogenesis are insulin, and carbohydrate availability, in order to efficiently store energy as it becomes available. TGs are synthesized primarily in the liver and adipose tissue, although low rates of lipogenesis are observed in many tissues. The majority of the acetyl-CoA substrate necessary to initiate the lipogenic process comes from the catabolism of carbohydrates (Hillgartner et al., 1995).

TGs and fatty acids can be mobilized in the body depending on energy needs. The liver can secrete TG-rich very-low density lipoprotein particles (VLDLs) for delivery to peripheral tissues. This process again involves lipoprotein lipase to release fatty acids from the TGs. Additionally, under periods of energy deficiency, adipocytes can secrete free fatty acids released from stored TGs catalyzed by the sequential actions of adipose triglyceride lipase (ATGL, also known as PNPLA2), and hormone-sensitive lipase (HSL).

The human body stores energy very efficiently as TGs in adipose, which has been very beneficial in the history of our evolutionary ancestors during periods of energy deficiency. However, in developed nations energy-dense food is readily available, and people often consume this energy in excess of what they need. The body simply stores this energy as adipose, and this has led to a dramatic rise in the incidence of obesity in our country. Obesity increases the risk factors for many diseases such as metabolic syndrome, type 2 diabetes mellitus, and cardiovascular disease. Additionally, obesity and insulin resistance are associated with the increased incidence of another disorder called nonalcoholic fatty liver disease (NAFLD).

Type 2 Diabetes Mellitus and the McGarry Hypothesis

Diabetes mellitus (DM) is the most common insulin disorder, and can be subdivided into two main types. Insulin is a peptide hormone secreted from pancreatic beta cells in the Islets of Langerhans. Insulin is central to energy homeostasis in the body, as it is secreted with increased glucose levels. It has wide-ranging systemic effects through increasing the following: glucose uptake into cells, TG synthesis, TG storage in adipocytes, and the storage of glucose as glycogen. Type 1 DM (representing approximately 10% of DM cases) is an autoimmune condition resulting in the destruction of pancreatic beta cells. This condition often occurs as a sudden onset in childhood, and is life-threatening without insulin supplementation. Type 2 DM is much more common, and is often associated with obesity. In obese patients, insulin resistance occurs in peripheral tissues (e.g. muscle, liver, adipose) resulting in decreased glucose uptake, and the need for greater amounts of insulin to achieve plasma glucose-lowering. This insulin resistance leads to beta cell proliferation, and eventually can cause beta cell exhaustion and death. This failure results in severe hyperglycemia, and the consequences may be life-threatening without therapeutic intervention.

As pioneered by the late Dennis McGarry, there is an emerging emphasis within the study of type 2 DM that it must be viewed not only as disease of glucose metabolism, but also of lipid metabolism (McGarry, 2002). As insulin has the capacity to drive lipogenesis in the liver, the increased circulating insulin during stages of early type 2 DM causes an overproduction of fatty acids and TGs in the liver which are then secreted in VLDL. TGs are then delivered to peripheral tissues such as muscle and WAT where they are stored, and contribute to worsening insulin resistance. The liver actually maintains a selective insulin resistance, by maintaining its sensitivity to insulin's lipogenic effects, but becoming resistant to the inhibition of the gluconeogenisis response to insulin (Brown M. S. and Goldstein, 2008). This selective insulin resistance results in the classic clinical triad of hyperglycemia, hyperinsulinemia, and hypertriglyceridemia, all hallmarks of type 2 DM. This metabolic derangement leads to a vicious cycle where the high TGs lead to increased insulin resistance, the high glucose leads to higher insulin, and the high insulin leads to higher TGs.

Nonalcoholic Fatty Liver Disease

NAFLD is a disease of TG storage in the liver, and encompasses the downstream consequences of that storage. The NAFLD process begins with abnormal accumulation of TGs in the liver, a condition termed hepatic steatosis, and is generally a benign and reversible process. TGs are normally stored in adipocytes, and excess storage in the liver is not typical. Therefore in NAFLD, it is thought that there is a defect in the regulatory mechanisms of hepatic triglyceride levels, which are established by lipid acquisition (from diet, from adipose (fatty acids), and via *de novo* lipogenesis) and loss (VLDL secretion, and oxidation of component fatty acids). In humans hepatic steatosis is currently defined as a hepatic TG level greater than the 95^{th} percentile observed in lean healthy individuals, or roughly above 55 mg/g liver (Szczepaniak et al., 2005). In patients with hepatic steatosis there is a greater chance for further progression to more severe forms of NAFLD such as: nonalcoholic steatohepatitis (NASH) characterized by inflammatory infiltrates, hepatocyte ballooning degeneration, cell death, and/or fibrosis; cirrhosis, defined by excessive collagen deposits resulting in severe fibrosis; and hepatocellular carcinoma (Cohen et al., 2011). These sequelae of hepatic steatosis are emerging as leading causal factors requiring liver transplantation in the United States. Diagnosis of NAFLD can be achieved through imaging techniques to determine the presence of TGs in the liver, however definitive staging of the disease requires a tissue biopsy. Treatment options for NAFLD are limited, and therefore there is an impending need for the development of new therapeutic agents (Cohen et al., 2011). Hepatic steatosis has a strong association with obesity and insulin resistance. Therefore, with the rise in obesity and metabolic syndrome in developed nations, there is also a related rise in the incidence of NAFLD (Browning et al., 2004).

Cholesterol Absorption and NAFLD

There have been several recent reports which suggest that inhibiting intestinal cholesterol absorption, either through therapeutic intervention such as Ezetimibe or by genetic deletion of the intestinal cholesterol transporter NPC1L1 in mice, protects against diet-induced hepatic steatosis (Chan et al., 2010;

de Bari et al., 2011; Deushi et al., 2007; Filippatos and Elisaf, 2011; Fukuda et al., 2010; Jia et al., 2010; Muraoka et al., 2011; Park et al., 2011; Repa et al., 2005; Zheng et al., 2008). Ezetimibe is a widely prescribed small-molecule therapeutic agent used for the treatment of hypercholesterolemia. It acts by binding to and inhibiting the action of the protein Niemann-Pick C1-Like 1 (NPC1L1) in the intestine to reduce cholesterol absorption (Altmann et al., 2004; Garcia-Calvo et al., 2005). Ezetimibe has very few off-target effects, and the observed protection from hepatic steatosis, and improved hepatic insulin sensitivity are both likely related to its ability to decrease intestinal cholesterol absorption.

1.5 Carboxylesterases

In addition to the synthesis, transport and storage of lipids, the breakdown of lipids is also an important process to understand in evaluating mechanisms regulating lipid balance. For many systems, the molecular mediators of hydrolysis and catabolism of lipids is unclear. Thus, I decided to also study a family of proteins called carboxylesterases (CES) as they were recently renamed and categorized based on sequence homology. In addition, CES genes were highly represented in microarray analyses we performed to evaluate pathways regulating hepatic steatosis.

CES comprise a family of proteins that catalyze neutral lipid hydrolysis (Holmes and Cox, 2011; Hosokawa et al., 2007; Williams et al., 2010). Substrate specificity among CES is often broad, overlapping, or yet to be identified leading to difficulty in performing comprehensive functional assays (Staudinger et al., 2010). Still, certain CES have long been recognized to play important roles in the biotransformation of ester- and amide-containing compounds to affect the detoxification and/or activation of a variety of xenobiotics, narcotics, and pharmacologic agents in liver and intestine (Satoh and Hosokawa, 1998; Satoh and Hosokawa, 2006). In addition, growing evidence suggests that some CES enzymes may contribute to aspects of lipid metabolism through triglyceride, cholesteryl ester, or retinyl ester hydrolysis (Ghosh, 2012; Parathath et al., 2011; Quiroga and Lehner, 2011b; Schreiber et al., 2009).

The CES family has been organized into five isoenzyme classes based on sequence similarity and gene structure (Holmes and Cox, 2011; Holmes et al., 2010b; Hosokawa et al., 2007; Williams et al., 2010). The six human *CES* genes, including one pseudogene, reside on chromosome 16; and the 20 mouse *Ces* genes, also including one pseudogene, are located on chromosome 8. The large number of *Ces* genes in rodents is believed to have arisen by tandem duplication. Thus, the sequence similarities of mouse *Ces* mRNA species and protein products are quite high, particularly within an isoenzyme class, which complicates the selective detection of *Ces* members *in vivo*.

One of the carboxylesterase functions of particular interest is the potential role in cholesterol ester hydrolysis. Inside the cell unesterified cholesterol can be toxic, so it is often esterified through the action of acyl CoA:cholesterol acyl transferase 1 and 2 (ACAT1, ACAT2, also known as SOAT1 and SOAT2). There is clearly a dynamic shift between stored cholesterol ester and unesterified cholesterol, and while ACATs are responsible for esterification, there is no definitive esterase for the reverse reaction. It is likely that cholesterol ester hydrolysis is facilitated by one or more of the CES genes, and therefore I set out to identify the major CES gene products in a variety of tissues important in cholesterol metabolism, most notably the small intestine (SI), liver, and macrophage. In addition, I measured NHR-mediated regulation of CES enzymes, and their role in chronic lipid overload resulting in obesity and insulin resistance.

1.6 Rationale

The regulation of lipid metabolism is an interwoven series of pathways and events acting in concert to control the nutritional and metabolic needs of the body. When alterations in lipid balance occur they can result in disease, thus an understanding of the pathophysiology, as well as the molecular mediators of these alterations are vital to the advancement of treatment for these diseases. I have undertaken three separate, but related projects relating to lipid metabolism. First, I sought to understand how a drug that blocks cholesterol absorption can ameliorate the onset of hepatic steatosis. What I found was that in the

early stages of disease onset, Ezetimibe prevents hepatic triglycerides independently from the NHR LXR, and actually paradoxically stimulates hepatic lipogenesis. Second, I determined the molecular and physiological changes that occur with bile acid pool size restoration in mice that have a bile acid deficiency. This project highlighted the importance of bile acids in cholesterol absorption, and whole body lipid homeostasis. Additionally, we established a rationale for feeding low physiological amounts of bile acids to experimental animals, especially when those animals have a defect in bile acid production. Lastly, I studied the tissue distribution and NHR-mediated regulation of a class of enzymes called carboxylesterases. This family of enzymes, which participate in neutral lipid hydrolysis, often came up on microarray analysis of metabolic studies, yet little was known about their regulation or function with regards to lipids. Therefore, I classified the tissue distribution of each of the carboxylestase family members in mice, and tested their gene expression upon treatment with synthetic agonists for the lipid-sensing NHRs. Thus, the information provided in this dissertation provides a valuable resource as the molecular mechanisms of disease begin to become clearer.

CHAPTER TWO:

Ezetimibe suppresses high-fat diet induced hepatic steatosis independent of LXR activity and changes in *de novo* fatty acid synthesis rates

2.1 ABSTRACT

Fatty liver disease affects one third of the adult population in the United States, and its sequelae (cirrhosis and hepatocellular carcinoma) are emerging causes of liver related morbidity and mortality. The pathogenesis of hepatic steatosis is not yet well defined, and there are limited treatment options for this disease. However, several reports have now suggested that inhibiting intestinal cholesterol absorption may protect against hepatic steatosis.

The Liver X Receptors (LXRs) are sterol-sensing transcription factors that regulate hepatic lipogenesis. Thus experiments were performed to test the hypothesis that limiting cholesterol absorption (by Ezetimibe treatment) restricts the delivery of intestine-derived sterols to the liver, thereby reducing LXR activity and concomitant *de novo* lipogenesis. Wildtype and *LXRα/β*$^{-/-}$ mice were fed either a low-fat, a high-fat (31% fat, 0.02% cholesterol), or a high-fat high-cholesterol (31% fat, 0.2% cholesterol) diet for 12 days with or without Ezetimibe. All mice, regardless of the genotype, receiving high-fat diets exhibited elevated hepatic triglyceride levels, which were normalized by Ezetimibe treatment. *In vivo* lipid balance studies confirmed the effects of Ezetimibe treatment on cholesterol homeostasis, but revealed that Ezetimibe administration did not result in reduced hepatic fatty acid synthesis rates. These findings demonstrate that the mechanism(s) linking Ezetimibe action to reduced hepatic steatosis are LXR-independent and do not rely on reduced hepatic lipogenesis.

2.2 INTRODUCTION

Hepatic steatosis is a variant of a broader class of disease called nonalcoholic fatty liver disease (NAFLD). The NAFLD disease process begins with abnormal accumulation of triglycerides (TGs) in the liver termed hepatic steatosis and is generally a benign and reversible process. In humans hepatic steatosis is currently defined as a hepatic TG level greater than the 95th percentile observed in lean healthy individuals, or roughly above 55 mg/g liver (Szczepaniak et al., 2005). In patients with hepatic steatosis there is a greater chance for further progression to more severe forms of NAFLD such as: nonalcoholic steatohepatitis (NASH) characterized by inflammatory infiltrates, hepatocyte ballooning degeneration, cell death, and/or fibrosis; cirrhosis, defined by excessive collagen deposits resulting in severe fibrosis; and hepatocellular carcinoma (Cohen et al., 2011). These sequelae of hepatic steatosis are emerging as leading causal factors requiring liver transplantation in the United States. Diagnosis of NAFLD can be achieved through imaging techniques to determine the presence of TGs in the liver, however definitive staging of the disease requires a tissue biopsy. Treatment options for NAFLD are limited, and therefore there is an impending need for the development of new therapeutic agents (Cohen et al., 2011). Hepatic steatosis has a strong association with obesity and insulin resistance. Therefore, with the rise in obesity and metabolic syndrome in developed nations, there is also a related rise in the incidence of NAFLD (Browning et al., 2004).

Hepatic triglyceride levels are established by lipid acquisition (from diet, from adipose (fatty acids), and via *de novo* lipogenesis) and loss (VLDL secretion, and oxidation of component fatty acids). There have been several recent reports which demonstrate that inhibiting intestinal cholesterol absorption, either through therapeutic intervention such as Ezetimibe or by genetic deletion of the intestinal cholesterol transporter Npc1l1 in mice, protects against diet-induced hepatic steatosis (Chan et al., 2010; de Bari et al., 2011; Deushi et al., 2007; Filippatos and Elisaf, 2011; Fukuda et al., 2010; Jia et al., 2010; Muraoka et al., 2011; Park et al., 2011; Repa et al., 2005; Zheng et al., 2008). Ezetimibe is a widely prescribed small-molecule therapeutic agent used for the treatment of hypercholesterolemia. It acts by binding to and

inhibiting the action of the protein Niemann-Pick C1-Like 1 (NPC1L1) in the intestine to reduce cholesterol absorption (Altmann et al., 2004; Garcia-Calvo et al., 2005). Ezetimibe has very few off-target effects, and the observed protection from hepatic steatosis, and improved hepatic insulin sensitivity are both likely related to its ability to decrease intestinal cholesterol absorption. Hepatic cholesterol balance is maintained by acquisition (via intestinal absorption (diet and biliary sterol), lipoprotein uptake, and *de novo* synthesis), and loss (through biliary secretion, lipoprotein secretion, and conversion and secretion as bile acids) (Repa and Mangelsdorf, 2000). Within enterocytes cholesterol is esterified by acyl CoA:cholesterol acyl transferase 2 (ACAT2) and packaged into chylomicrons through the action of microsomal triglyceride transfer protein (MTP). Chylomicrons travel through lymph, are released into the bloodstream, and ultimately the liver then clears the chylomicron remnants (Iqbal and Hussain, 2009; Wang D. Q., 2007).

An emerging, yet untested, hypothesis for the Ezetimibe/NPC1L1-related protection from hepatic steatosis is that blocking delivery of intestine-derived sterol to the liver reduces hepatic lipogenesis through decreased activity of the sterol-sensing transcription factor Liver X Receptor (LXR) (de Bari et al., 2011; Jia et al., 2010). LXR is a nuclear hormone receptor with two isoforms (LXRα and LXRβ) which are bound and activated by oxysterols to regulate gene transcription (Janowski B. A. et al., 1996). Many LXR-regulated genes act to decrease the cholesterol burden within cells either through cellular export or conversion to bile acids. In addition LXR regulates two key lipogenic transcription factors, the sterol regulatory element-binding protein-1c (SREBP-1c) and the carbohydrate response element-binding protein (ChREBP) (Cha and Repa, 2007; Repa et al., 2000a). Beyond the transcriptional regulation by LXR, these lipogenic transcription factors are also sensitive to components of the carbohydrate metabolic pathway, specifically glucose for ChREBP, and insulin for SREBP1c (Horton et al., 2002; Uyeda and Repa, 2006).

The initial reports revealing the protective effects of Ezetimibe or *Npc1l1* ablation on hepatic steatosis utilized long-term feeding studies. Under these conditions, hepatic steatosis was assessed as much as 24

weeks after the introduction of high-fat diets to mice (Jia et al., 2010). Due to the protective effect of Ezetimibe and *Npc1l1* deletion on hepatic insulin resistance, at the time of tissue harvest the livers from *Npc1l1*$^{-/-}$ mice, which do not absorb cholesterol, remain insulin sensitive, while the *Npc1l1*$^{+/+}$ mice develop insulin resistance. Thus, the reported decrease in *de novo* lipogenesis in *Npc1l1*$^{-/-}$ mice associated with the long-term high-fat feeding could be due to multiple factors: the decreased hepatic sterol delivery being sensed through LXR in *Npc1l1*$^{-/-}$ mice, by the increase in insulin and glucose associated with increased hepatic insulin resistance in the *Npc1l1*$^{+/+}$ mice, by a combination of these factors, or by an alternate pathway. What is lacking from these previous studies is an assessment of the initiating factors driving the state of triglyceride storage in the liver. Insulin resistance consists of a vicious cycle in which hyperglycemia, triglyceride production, and beta-cell failure feed into a self-reinforcing series of events which leads to the development of type-2 diabetes mellitus (McGarry, 2002). The key to understanding the effect of Ezetmibe on this process is to assess hepatic triglyceride storage and lipogenesis at an early timepoint before overt obesity and insulin resistance feed into this cycle.

The focus of these studies was to determine the early molecular mechanisms linking cholesterol absorption and hepatic steatosis, and to assess the importance of LXR in this regulatory pathway. The results clearly demonstrate that inhibition of cholesterol absorption decreases hepatic steatosis independent of LXR, under both high-fat, and high-fat high-cholesterol dietary conditions. Furthermore, in some groups Ezetimibe treatment leads to a paradoxical increase in *de novo* lipogenesis, despite reduced hepatic TG levels, after 12 days on high fat diet. Taken together, these data point to an alternative mechanism for Ezetimibe-associated protection from high-fat diet-induced hepatic steatosis.

2.3 MATERIALS AND METHODS

Animal, diets, and study designs. Mice lacking LXRα (NR1H3) and LXRβ (NR1H2) and wildtype controls on a mixed strain background (C57Bl/6:A129/SvJ) have been previously described (Kalaany et al., 2005). Mice were individually housed in plastic colony cages with wood shavings in a temperature-controlled environment with 12h light/dark cycles (light: 06:00-18:00) and allowed free access to food and water. Male mice of 3-7 months of age were used in all studies. All experiments were approved by the Institutional Animal Care and Use Committee of the University of Texas Southwestern Medical Center in accordance with the Guide for the Care and Use of Laboratory Animals as adopted and promulgated by the National Institutes of Health.

Mice were provided *ad libitum* a cereal-based standard rodent diet (**SD**, which contains 4% lipid, 0.02% cholesterol; #7001, Teklad Diets, Madison, WI), a high-fat diet (**HFD**, #7001 supplemented with 264g/kg palm oil and 16g/kg corn oil to achieve 60% kCal from fat) or a high fat/high-cholesterol diet (**HFHCD**, the HFD further supplemented with cholesterol (Sigma, St. Louis MO) to achieve 0.2% wt/wt). Ezetimibe (Sequoia Research Products, Pangbourne, United Kingdom) was supplied in the diets to provide 5 mg/kg body weight/day (mpk).

In all studies that culminated in obtaining blood and tissues for chemical measurements, histology, and RNA, food was removed at 06:00 and mice were anesthetized at 10:00 following this 4h fast, exsanguinated and tissues were obtained. For experiments in which lipid synthesis rates were determined by the tritiated water method (see below), food was removed at 06:00, the mice were injected at 08:00 with [^{3}H]water, and tissues were obtained 1h later for analysis.

To monitor processes related to the development of hepatic steatosis, one cohort of mice was fed respective diets for only 12 days. Body composition was assessed on day12 by NMR (Bruker minispec). To determine the efficacy of Ezetimibe on preexisting hepatic steatosis, another cohort of mice was fed the HFD for 8 weeks. One set of these mice (n=4/group) was euthanized at this point to confirm fatty

liver and the remaining mice (n=5-6 mice/group) were continued on HFD with or without 5mpk Ezetimbe for another 4 weeks. Finally a third cohort of mice was fed HFD with or without 5mpk Ezetimbe and were analyzed as follows: on d10 blood was drawn (fed-state), then mice were fasted overnight for morning blood-draw (fasting state) followed by 4h feeding of respective diets (refed state) to establish plasma triglyceride levels under these dietary conditions; on d14 mice received an oral bolus of [^{14}C]-triolein/[^{3}H]-sitostanol to assess triglyceride absorption (see method below); on d21 mice were fasted overnight then injected with Tyloxapol (ip, 500 mpk) to monitor plasma triglyceride levels and assess VLDL secretion; on d35 mice received a Tyloxapol injection (ip, 500 mpk) followed by administration of corn oil (200µl/25g body weight) by oral gavage to monitor plasma triglyceride levels and assess chylomicron appearance.

Hepatic triglyceride concentration. Aliquots of liver were extracted with folch (2:1 chloroform:methanol v/v) solution along with the recovery standard [^{14}C]triolein (American Radiolabeled Chemicals, Inc., St. Louis, MO). Aliquots of this extract were dried under air and the residue was dissolved in 1 ml of hexane: methyl-t-butyl ether (100:1.5, v/v). Cholesterol esters were separated using silica-based columns (Sep-Pac Vac RC: WAT036950, Waters Corporation, Milford, MA), then the solvent was switched to hexane: methyl-t-butyl either (96:4, v/v) to elute the triglycerides then dried under air. Following resuspension in folch solution, aliquots were dried and used for scintillation counting to detect the recovery standard, and analyzed using the Infinity triglyceride reagent kit (TR22321, Thermo, Middletown, VA) to measure triglyceride mass. All samples were compared against glycerol standards. (Repa et al., 2005)

Concentrations of total cholesterol in liver. Aliquots of liver were saponified and extracted and total cholesterol concentrations were measured by GC using stigmastanol as an internal standard (Schwarz et al., 1998).

Rates of cholesterol and fatty acid synthesis in liver and small intestine. The rates of cholesterol and fatty acid synthesis were assessed in vivo using [^{3}H]water as previously described (Schwarz et al., 1998). Mice received approximately 40 mCi of [^{3}H] water by intraperitoneal injection, and 1h later, the liver and small intestine (flushed, and divided into 3 equal parts) were removed, rinsed, blotted, and weighed. Tissues were then saponified, the labeled sterols were extracted and the amount of digitonin-precipitatable sterols were quantified as described (Schwarz et al., 1998). The rate of cholesterol synthesis in each organ was calculated as the nmol of [^{3}H] water incorporated into sterols per hour per g of tissue after correction for plasma specific activity of [^{3}H]. The aqueous phase was then acidified and labeled fatty acids extracted and quantitated as described (Shimano et al., 1996). The rate of fatty acid synthesis in each organ was calculated as the μmol of [^{3}H] water incorporated into fatty acids per hour per g of tissue.

Relative mRNA expression analysis. Total RNA was isolated from tissue samples using RNA STAT-60 (Tel-Test, Inc., Friendswood, TX) as previously described (Kurrasch D. M. et al., 2004b). RNA concentration was determined by absorbance at 260 nm, and RNA quality by the 260/280 ratio. Quantitative real-time PCR (qPCR) was performed using an Applied Biosystems 7900HT sequence detection system as described (Kurrasch D. M. et al., 2004b; Valasek and Repa, 2005). Briefly, total RNA was treated with Dnase I (RNase-free; Roche Molecular Biochemicals) and reverse-transcribed with random hexamers using SuperScript II (Invitrogen) to generate cDNA. Each qRT-PCR was analyzed in duplicate and contained in a final volume of 10 μl: 25 ng of cDNA, each primer at 150 nM, and 5 μl of 2x SYBR Green PCR Master Mix (Applied Biosystems). Results were evaluated by the comparative cycle number at threshold method (Schmittgen and Livak, 2008) using ribosomal protein L19 (RPL19) as the invariant reference gene (Dheda et al., 2004; Kosir et al., 2010). RPL19 was chosen after software analysis (Biogazelle, Zwijnaarde, Belgium) to establish the optimal invariant housekeeping gene.

Fecal neutral sterol measurements and lipid content. Mice were individually housed, and stools were collected over a period of 3 days. These samples were dried, weighed, and ground. To determine the

neutral sterol content, a 1-g aliquot was subjected to alkaline hydrolysis at 120-130°C for 12h, then dried and resuspended in 10 ml of water and 10 ml of ethanol, then extracted in 15 mL petroleum ether containing 1.0 mg of the internal standard 5-cholestene (Sigma, St. Louis, MO). The amounts of cholesterol, coprostanol, and cholestanone were quantified by gas chromatography. The lipid content of the stools were determined gravimetrically following a folch (2:1 chloroform:methanol, v/v) extraction (Schwarz et al., 1998).

Plasma measurements (triglycerides, Glucose, cholesterol, Insulin, PCSK9). Mice were exsanguinated using heparin-coated syringes, and samples were immediately centrifuged at 10,000g for 10 min at 4°C to obtain plasma. Plasma triglycerides and glucose concentrations were determined using the Vitros 250 system (Mouse Metabolic Phenotyping Core at UT Southwestern). For Tyloxapol studies, plasma triglyceride levels were measured using the Infinity triglyceride reagent kit (TR22321, Thermo, Middletown, VA), and all samples were compared against glycerol standards. Plasma cholesterol was measured with gas chromatography following saponification and petroleum ether extraction (Schwarz et al., 1998). Insulin was measured using a rat radioimmunoassay kit (RI-13K, Millipore, Billerica, MA). Plasma levels of proprotein convertase subtilisin/kexin type 9 (PCSK9) were detected using an ELISA assay (provided by Jay Horton, UT Southwestern).

Microarray analysis. Liver and duodenum RNA samples from the 12-day HFD cohort of mice were analyzed using the Illumina MouseWG-6 V2 BeadChip platform. For each group (n=6) equal quantities of RNA were pooled for 2 mice to yield 3 independent samples per treatment group. Results were analyzed using BeadStudio software (Illumina, San Diego, CA), Ingenuity Pathway Analysis software (Ingenuity Systems, Redwood City, CA), and Genesifter software (Geospiza, Inc., Seattle, WA).

Histology. For the long-term HFD study, a section of liver from each mouse was removed immediately after exsanguination and drop-fixed in 10% neutral-buffered formalin. After 3 days, samples were switched to 10% sucrose solution overnight, and then stored in an 18% sucrose solution. Livers were

frozen sectioned, then stained using hematoxylin and eosin (H&E) or Oil Red O by the Molecular Pathology Core of UT Southwestern.

Data analysis. All data are reported as means ± SEM, for the number of mice as specified in each figure legend. GraphPad Prism 5 software (GraphPad, San Diego, CA) was used to perform all statistical analyses. Differences between means were tested for statistical significance ($P < 0.05$) by one-way analysis of variance, followed by the Newman-Keuls multiple-comparison post-hoc test. Transformed data were used if unequal variance among groups was evident by Bartlett's test.

2.4 RESULTS

Ezetimibe has no effect on body weight in wild-type mice, and it prevents weight gain in LXR-DKO mice fed a high-fat diet (Fig. 2.1 A-C). A short-term (12 day) feeding regimen was employed to study the early development of hepatic steatosis. All mice receiving the standard diet (SD) with or without Ezetimibe experienced little change in body weight (**Fig. 2.1A**) over this time period, and the 1-4% weight loss observed was likely attributable to the switch from pelletted to powder forms of this low-fat diet. Wild-type mice fed the high-fat diet (HFD) gained significant weight (~6%) regardless of the presence or absence of Ezetimibe (**Fig. 2.1B)**. However, LXR-DKO mice fed HFD gained substantial weight (8.8%) only in the absence of Ezetimibe, LXR-DKO mice displayed virtually no change in body weight (0.8%) when fed the HFD containing Ezetimibe. Consistent with a previous study (Kalaany et al., 2005), the addition of dietary cholesterol (HFHCD, **Fig. 2.1C**) prevented the robust weight gain observed in LXR-DKO mice fed high-fat (HFD). In all mice fed HFHCD, the inclusion of Ezetimibe had no effect on cumulative body weight gain. Thus, in wildtype mice, Ezetimibe administration had no impact on body weight gain regardless of diet type. In LXR-DKO mice, Ezetimibe administration prevented weight gain only in mice receiving the HFD.

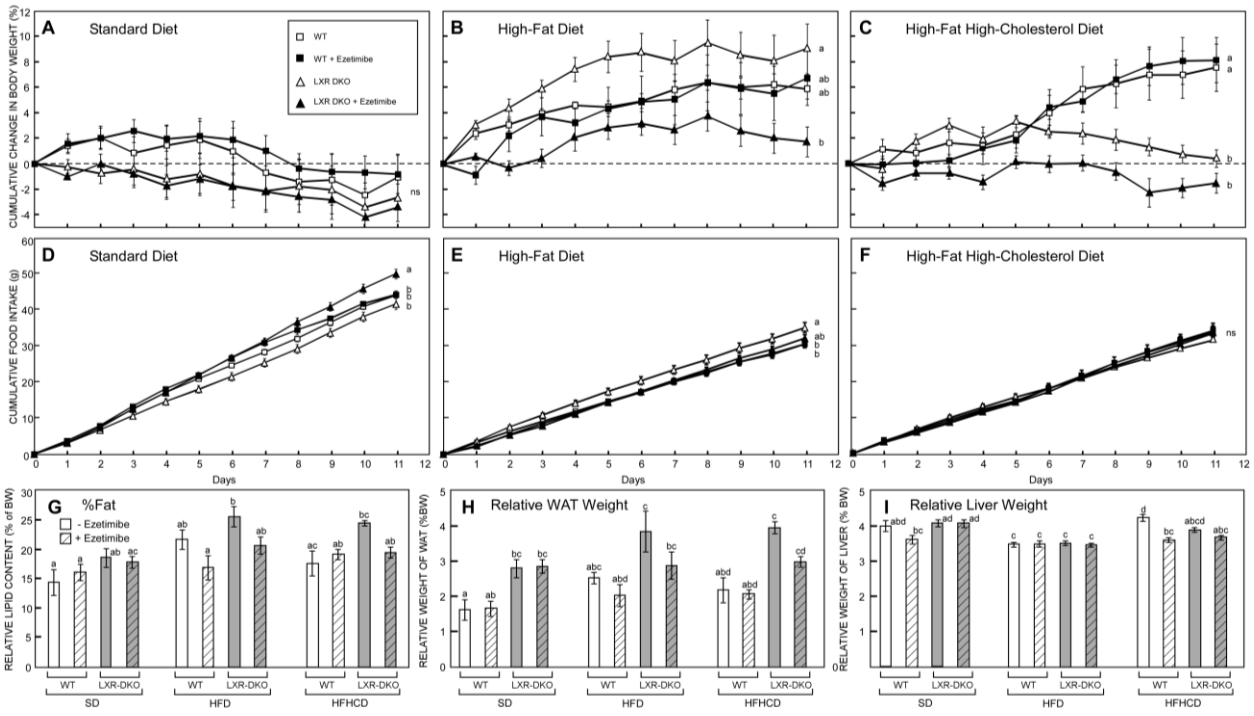

Fig. 2.1 Effects of Ezetimibe feeding on food intake, weight gain, and body composition. Adult, male wildtype (WT) and LXRα/LXRβ-double knockout mice (LXR-DKO) were provided ad libitum a standard low-fat rodent diet (SD), a high-fat diet (HFD), or a high-fat, high cholesterol diet (HFHCD) with or without 5mpk Ezetimibe for 12 days. Cumulative weight gain (A-C) and food intake (D-F) were evaluated over 11 days (Mice were fasted 4h prior to euthanasia on d12). G. Percent body fat was measured by NMR prior to fasting on d12, and relative white adipose tissue ((H) WAT, epididymal fat pad) and liver weights (I) were measured following the 4h fast on d12. Values represent the mean ± SEM of 6 mice per group. Significant differences ($P<0.05$) were determined by one-way ANOVA with Neuman-Keuls post-hoc test, and different letters denote groups that are significantly different.

Ezetimibe treatment has no effect on cumulative food intake in the wild-type mice (Fig. 2.1D-F). The inclusion of Ezetimibe had no impact on the cumulative food intake of wild-type mice under any of the dietary treatments tested (**Fig. 2.1 D-F**). However, inclusion of Ezetimbe had modest effects on food intake in LXR-DKO mice, and these changes in food intake did not necessarily correlate with the observed changes in body weight gain. LXR-DKO mice fed the SD (which experienced the greatest weight loss) had the highest apparent cumulative food intake among mice receiving this diet (**Fig. 2.1A, D**). LXR-DKO mice receiving the HFD showed both the greatest food intake, though not reaching statistical significance, and the greatest body weight gain (**Fig. 2.1B, E**). Finally, despite the disparate body weight gains observed between wild-type and LXR-DKO mice fed the HFHC diets, cumulative food intake was similar for these four groups of mice (**Fig. 2.1C, F**).

Ezetimibe has minimal effects on body fat, white adipose weight and relative liver weight in mice fed diets of varying lipid composition (Fig. 2.1G-I). Body composition was determined by nuclear magnetic resonance analysis, and relative lipid content (**Fig. 2.1G**) of mice receiving high-fat diets (HFD and HFHCD) was modestly reduced by Ezetimibe treatment. As the NMR method can only determine total body lipid content, and not localization, we also measured the weights of adipose (WAT, epididymal depot, **Fig. 2.1H**) and liver (**Fig. 2.1I**) relative to body mass. The relative WAT weight among the different groups exhibited nearly the same pattern as that observed from whole body lipid content. Thus these data suggest that Ezetimibe treatment mitigates the expansion of WAT in mice, both wild-type and LXR-DKO, fed HFD and HFHCD. Very modest changes were observed in relative liver weights among groups (**Fig. 2.1I**), and the only significant effect of Ezetimibe was observed in wild-type mice receiving the HFHCD. Of note, in all mice receiving the HFD with or without Ezetimibe (this diet group was later used for extensive measures of lipid balance), relative liver weights were unaffected by genotype or Ezetimibe.

Ezetimibe mitigates the hepatic triglyceride (TG) accumulation upon feeding HFD and HFHCD in both wild-type and LXR-DKO mice (Fig. 2.2A). Despite the short-term feeding regimen and modest changes in body weight and composition, feeding mice HFD and HFHCD clearly resulted in increased hepatic TG concentrations (**Fig. 2.2A**). Importantly, this was observed in both wild-type and LXR-DKO mice. Feeding mice the SD (low-fat, and therefore high-carbohydrate) did not result in elevated hepatic TG, and Ezetimibe had no impact on TG levels. When provided with the high-fat diet, wild-type mice exhibited a hepatic TG concentration of 23.5 mg/g (compared to 12.12 mg/g observed in SD-fed mice) that was reduced to 18.9 with Ezetimibe treatment. Although these differences did not reach statistical significance, the trends are consistent with reports using extended feeding periods (Repa et al., 2005; Zheng et al., 2008). LXR-DKO fed the HFD displayed a more robust and significant increase in hepatic TG (39.7 mg/g), which was significantly reduced in the presence of Ezetimibe (18.9 mg/g). Inclusion of 0.2% cholesterol in the HFD (i.e. the HFHCD) resulted in enhanced hepatic TG accumulation in wild-

type mice (49.8 mg/g), with no further increase observed in LXR-DKO mice (42.09 mg/g). Again, Ezetimibe treatment nearly restored basal hepatic TG levels in mice of both genotypes receiving the HFHCD. These data clearly show that the 12-day feeding paradigm is sufficient to drive early hepatic triglyceride accumulation, and that Ezetimibe treatment mitigates this lipid accumulation regardless of genotype. Thus, LXR is not required to mediate Ezetimbe's effect on hepatic steatosis.

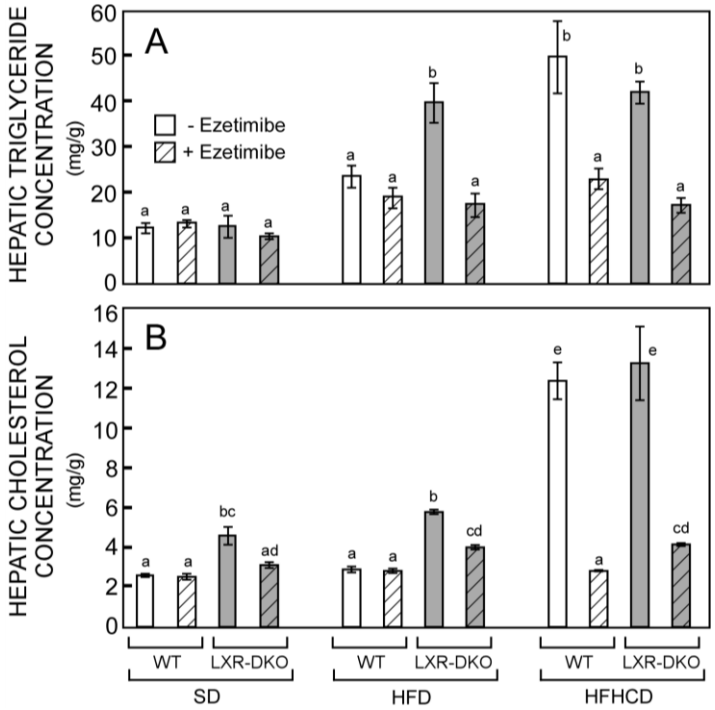

Fig. 2.2 Ezetimibe administration normalized hepatic triglyceride and cholesterol levels in mice fed HF and HFHC diets. Adult, male (WT, white bars) and LXRα/LXRβ-double knockout mice (LXR-DKO, grey bars) were provided ad libitum a standard low-fat rodent diet (SD), a high-fat diet (HFD), or a high-fat, high cholesterol diet (HFHCD) with or without 5mpk Ezetimibe (hatched bars) for 12 days. Triglyceride (A) and cholesterol (B) concentrations are expressed as mg per g liver. Values represent the mean ± SEM of 6 mice per group. Significant differences ($P<0.05$) were determined by one-way ANOVA with Neuman-Keuls post-hoc test, and different letters denote groups that are significantly different.

Reduced hepatic cholesterol concentrations in mice receiving Ezetimibe confirm the ability of this agent to limit the delivery of intestinal sterols to the liver (Fig. 2.2B). Hepatic cholesterol concentrations of wild-type mice fed the SD were all within the normal range for male mice (2.4-2.6 mg/g), and Ezetimibe had no impact on these levels. Interestingly, the LXR-DKO mice fed SD displayed higher liver total cholesterol concentrations (4.5 mg/g), which were significantly reduced (to 3.1 mg/g) upon Ezetimibe

feeding. Similar results were observed in animals receiving the HFD (no added cholesterol), and analysis of the levels of free and esterified cholesterol in liver samples from these mice clearly showed that changes in total hepatic sterol were due to alterations in the esterified cholesterol fraction (data not shown). The results observed for mice fed the HFHCD clearly demonstrate the efficacy of Ezetimibe treatment to limit hepatic cholesterol accumulation, as the elevated levels observed in mice receiving the HFHCD without Ezetimibe (wild-type, 12.4 mg/g; LXR-DKO, 13.2 mg/g) were reduced to levels consistent with those in mice fed the SD.

Plasma glucose and insulin levels suggest that mice fed HF diets for only 12 days were not insulin resistant; plasma lipid levels were modestly impacted by LXR genotype, but not Ezetimibe (Fig. 2.3 A-D). Plasma glucose concentrations (taken after a 4h fast) exhibited a trend toward reduced levels in LXR-DKO mice on all diets, but were independent of Ezetimibe treatment (**Fig. 2.3A**). Plasma insulin levels were unaffected by diet, Ezetimibe and LXR genotype (**Fig. 2.3B**). Cumulatively these glucose and insulin levels suggest that mice receiving HF diets for only 12 days were not yet insulin resistant, and therefore this condition would not confound interpretation of analyses of hepatic lipid metabolism. Plasma TG concentrations in wild-type mice fed HFD and HFHCD were significantly decreased compared to wild-type mice fed the SD (**Fig. 2.3C**), plasma TG levels of LXR-DKO mice were unaffected by diet, and Ezetimibe treatment had no impact on plasma TG concentrations for any of the twelve groups of mice. Plasma cholesterol concentrations were significantly lower in LXR-DKO mice (**Fig. 2.3D**), as previously reported (Kalaany et al., 2005). Ezetimibe treatment had no impact on plasma cholesterol levels in LXR-DKO mice, but appeared to modestly reduce (although not reaching statistical significance) cholesterol concentrations in wild-type mice on all diets.

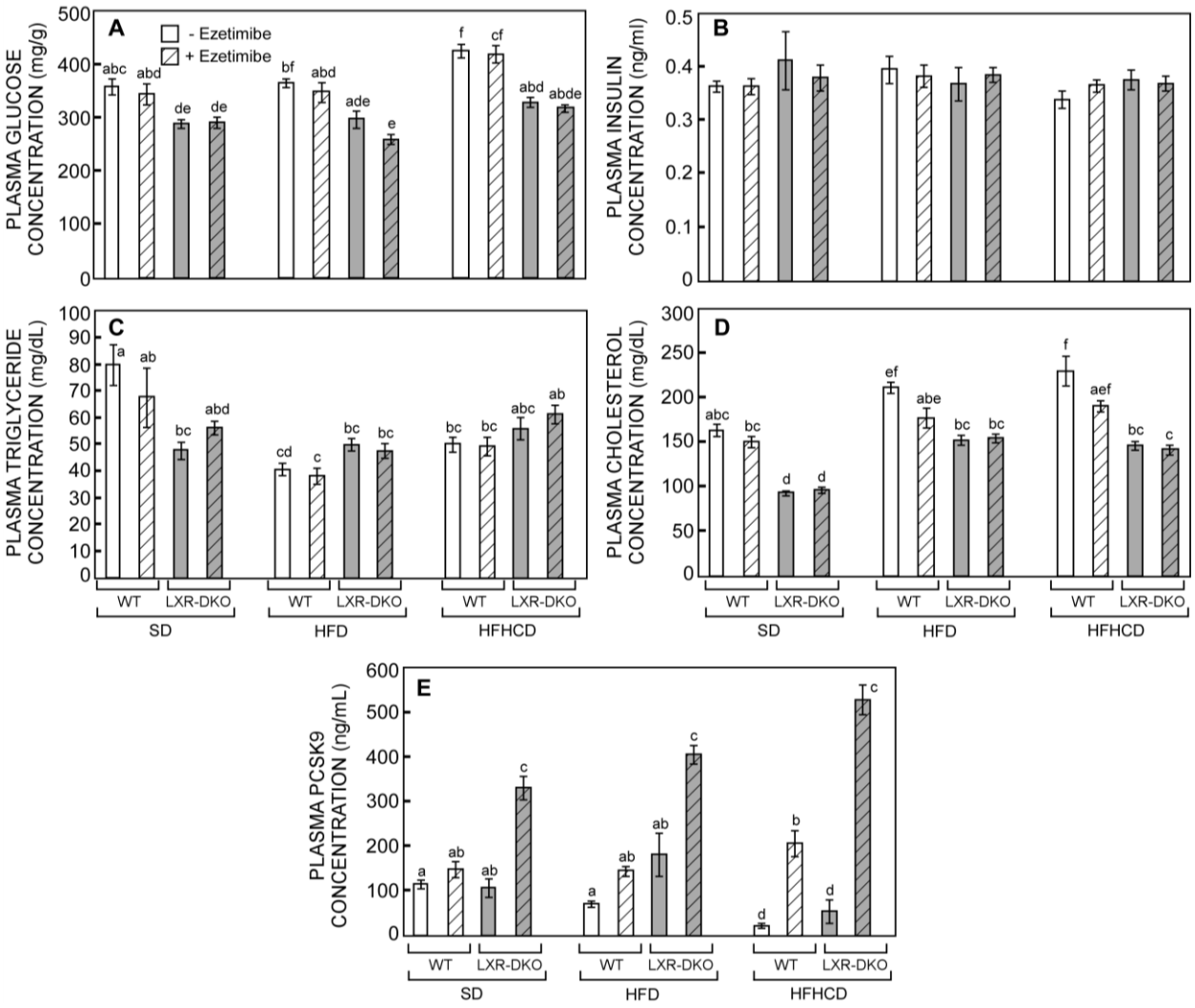

Fig. 2.3 Dietary lipids and Ezetimibe have minimal effects on plasma glucose and insulin; LXR genotype impacts plasma triglyceride and cholesterol levels; and changes in plasma PCSK9 concentrations reveal diet, genotype, and Ezetimibe interactions. Adult, male (WT, white bars) and LXRα/LXRβ-double knockout mice (LXR-DKO, grey bars) were provided ad libitum a standard low-fat rodent diet (SD), a high-fat diet (HFD), or a high-fat, high cholesterol diet (HFHCD) with or without 5mpk Ezetimibe (hatched bars) for 12 days. Values represent the mean ± SEM of 6 mice per group. Significant differences ($P<0.05$) were determined by one-way ANOVA with Neuman-Keuls post-hoc test, and different letters denote groups that are significantly different.

Plasma PCSK9 levels were dramatically affected by diet, genotype, and Ezetimibe and serve as sensitive biomarkers of hepatic sterol synthesis rates. Proprotein convertase subtilisin/kexin type 9 (PCSK9) is a secreted protein that binds to and degrades LDL receptor (LDLR) protein, thus affecting plasma LDL concentrations. PCSK9 is transcriptionally regulated by SREBP2 and is therefore responsive to changes in cellular cholesterol levels. In wild-type mice provided diets without Ezetimibe, plasma PCSK9 levels

displayed a sequential decline from 114 ng/ml (SD) to 70 ng/ml (HFD) and 20 ng/ml (HFHCD) (**Fig. 2.3E**). PCSK9 concentrations were increased in all groups receiving Ezetimibe, regardless of genotype, and the most robust increases were observed in animals fed HFHCD with Ezetimibe, particularly in LXR-DKO mice (reaching 529 ng/ml). These plasma PCSK9 levels exhibited changes in a reciprocal manner to hepatic cholesterol levels (**Fig. 2.2B**) and consistent with in vivo measures of hepatic sterol synthesis rates (**Fig. 2.4A**).

Changes in hepatic and intestinal sterol synthesis rates confirm the impact of Ezetimibe treatment on sterol balance (Fig. 2.4A, B). In vivo sterol synthesis rates were determined by the tritiated water method (Dietschy and Spady, 1984). The pattern of hepatic sterol synthesis rates was similar in mice fed diets lacking added sterol, the SD and HFD (**Fig. 2.4A**). In wild-type mice of these dietary groups, in the absence of Ezetimibe, sterol synthesis rates were 358 and 408 nmol/h/g for SD and HFD groups, and increased 5.5-fold and 6.6-fold, respectively, when Ezetimibe was included in the diet. The inclusion of 0.2% cholesterol in the HF diet (i.e. the HFHCD) resulted in a decline in hepatic sterol synthesis rates for wild-type (to 20.5 nmol/h/g liver) and LXR-DKO (to 334 nmol/h/g) mice compared to mice receiving SD or HFD. However, the inclusion of Ezetimibe to the HFHCD erased these declines, and the sterol synthesis rates were comparable to those of SD and HFD receiving Ezetimibe. Thus the mice fed HFHCD exhibited Ezetimibe-associated changes of 83-fold (wild-type) and 19-fold (LXR-DKO) in hepatic sterol synthesis rates. Of note, the LXR-DKO mice exhibited sterol synthesis rates higher than their wild-type counterparts under virtually all dietary conditions. Similar changes in sterol synthesis were observed for small intestine (**Fig. 2.4B**), although the absolute values for sterol synthesis tended to be lower for intestine than those measured for liver (note differing y-axis scales), and the increases in sterol synthesis rates observed in Ezetimibe-treated mice were not as robust (2-4 fold changes). Overall, these findings are consistent with previous reports demonstrating that blocking intestinal cholesterol absorption by Ezetimibe results in enhanced sterol synthesis in intestine, and reduced delivery of dietary sterol to liver

resulting in compensatory increases in hepatic sterol synthesis rates (Repa et al., 2002b; Repa et al., 2005; Valasek et al., 2008).

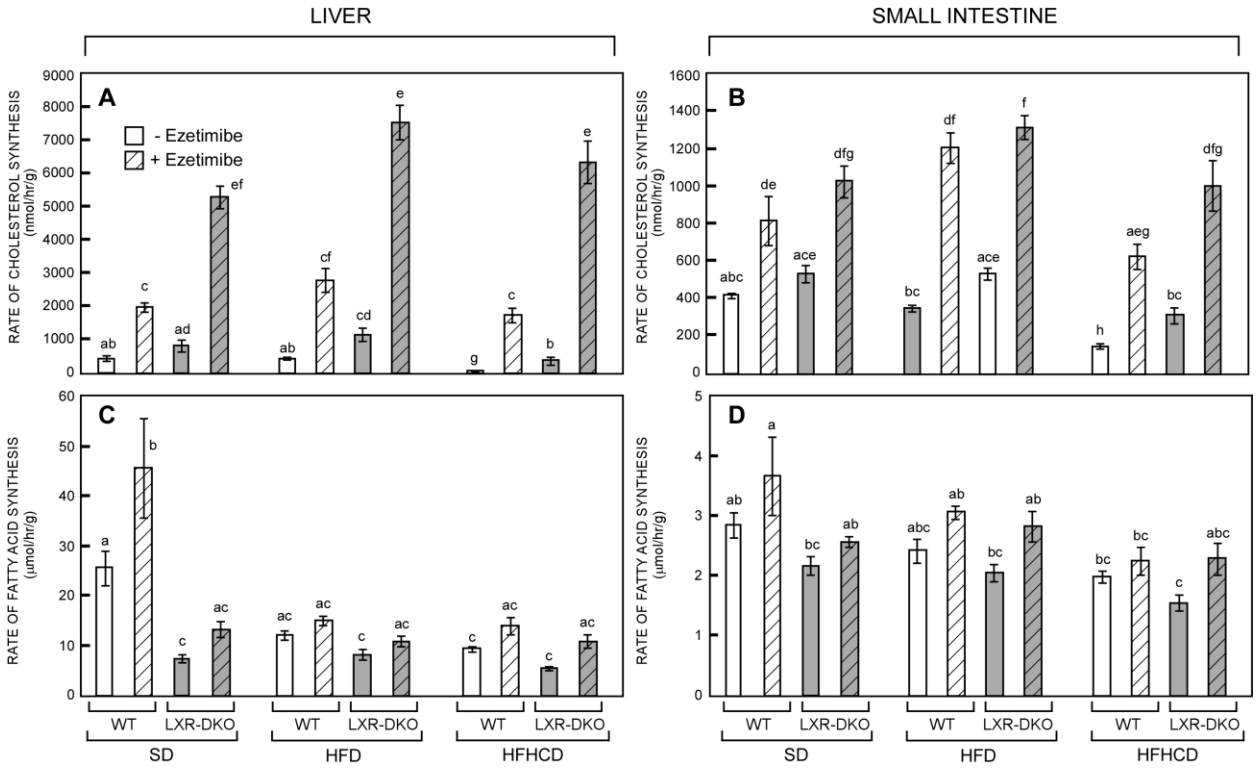

Fig. 2.4 Cholesterol and fatty acid synthesis rates in liver and intestine reveal significant effects and interactions between dietary lipid content, Ezetimibe treatment and LXR genotype. Importantly, inclusion of Ezetimibe does not reduce hepatic lipogenesis, despite the reduction in triglyceride content (Fig. 2.2B). Adult, male (WT, white bars) and LXRα/LXRβ-double knockout mice (LXR-DKO, grey bars) were provided ad libitum a standard low-fat rodent diet (SD), a high-fat diet (HFD), or a high-fat, high cholesterol diet (HFHCD) with or without 5mpk Ezetimibe (hatched bars) for 12 days. Values represent the mean ± SEM of 4 mice per group. Significant differences ($P<0.05$) were determined by one-way ANOVA with Neuman-Keuls post-hoc test, and different letters denote groups that are significantly different.

Despite the Ezetimibe-associated lowering of hepatic TG levels (Fig.2. 2A), there is no reduction observed in fatty acid synthesis rates in liver or intestine (Fig 2.4C, D). In vivo fatty acid synthesis rates were determined by the tritiated water method (Shimano et al., 1996), using saponified tissue samples to capture all free fatty acids, and all fatty acids conjugated to other lipid species that were generated during the 1h exposure to $[^3H]_2O$. As previously reported, the hepatic fatty acid synthesis rates of LXR-DKO mice are reduced compared to wild-type mice when fed SD (**Fig. 2.3C**, (Kalaany et al., 2005; Repa et al., 2000a). When wild-type mice received HF diets, hepatic fatty acid synthesis rates were reduced by

roughly half, and thus comparable to rates seen in LXR-DKO mice. In all cases, for wild-type and LXR-DKO mice, Ezetimibe treatment did not result in lower hepatic fatty acid synthesis rates, despite our previous observation that hepatic triglyceride concentrations were significantly reduced by Ezetimibe in mice fed high-fat diets (**Fig. 2.2A**). Fatty acid synthesis rates of the small intestine (**Fig. 2.4D**) were largely unaffected by diet, genotype, and Ezetimibe treatment in mice, and of much lower magnitude (compare y-axes) than rates observed in liver.

Relative mRNA levels in liver reveal differential gene expression in response to diet, genotype and Ezetimbe administration (Fig. 2.5A). To assess the potential molecular mechanism(s) relating Ezetimibe treatment to hepatic steatosis, relative mRNA levels were measured by quantitative real-time PCR in liver (**Fig. 2.5A**). Expression of LXRα and LXRβ mRNA in liver confirm the appropriate genotypes of mice, and reveal that none of the conditions affect expression of these nuclear hormone receptors. This is consistent with reports that LXRα is not autoregulated in mouse, as it is in human cells (Laffitte et al., 2001; Whitney et al., 2001). The relative mRNA levels of hepatic SREBP-2 and its target genes, HMG CoA synthase (Hmgcs1), LDLR, and PCSK9 were affected by dietary sterol, as reduced mRNA levels were observed in wild-type mice fed HFHCD without Ezetimibe. In livers from all mice receiving Ezetimibe, a compensatory rise in mRNA levels for this collection of genes was evident. These changes are consistent with the *in vivo* sterol synthesis rates (**Fig. 2.4A**) and the plasma PCSK9 levels (**Fig. 2.3E**) previously determined. Evaluation of key lipogenic transcription factors revealed that hepatic SREBP-1c mRNA levels were reduced in LXR-DKO mice, consistent with earlier reports (Repa et al., 2000a), and ChREBP levels were unchanged by diet, genotype, or Ezetimibe (data not shown). Patterns similar to SREBP-1c were observed for stearoyl CoA desaturase 1 (SCD1), and for both SREBP-1c and SCD1 a decline in mRNA levels was observed by Ezetimbe treatement of HFHCD-fed wild-type mice, and a modest increase was observed in LXR-DKO mice receiving Ezetimibe in their diets. Despite these changes, FAS mRNA levels tended to increase upon Ezetimibe treatment, particularly in HFHCD-fed mice, consistent with the changes observed in fatty acid synthesis rates (**Fig. 2.4C**). As hepatic TG levels

declined by Ezetimibe treatments, despite no change or an increase in lipogenesis, we also evaluated mRNA levels for proteins involved in lipoprotein production: hepatic MTP mRNA levels were enhanced in the LXR-DKO mice, with no change due to diet or Ezetimibe; and no changes were observed for apoB, MGAT1, and HNF1α (data not shown). A global gene expression profile was performed by microarray analysis in mice receiving HFD, and two of the most regulated genes were carboxylesterases, Ces1d and Ces1e. Confirmation of the microarray results revealed that the mRNA levels of these two lipid hydrolases were abundantly expressed in liver, and lower in LXR-DKO mice.

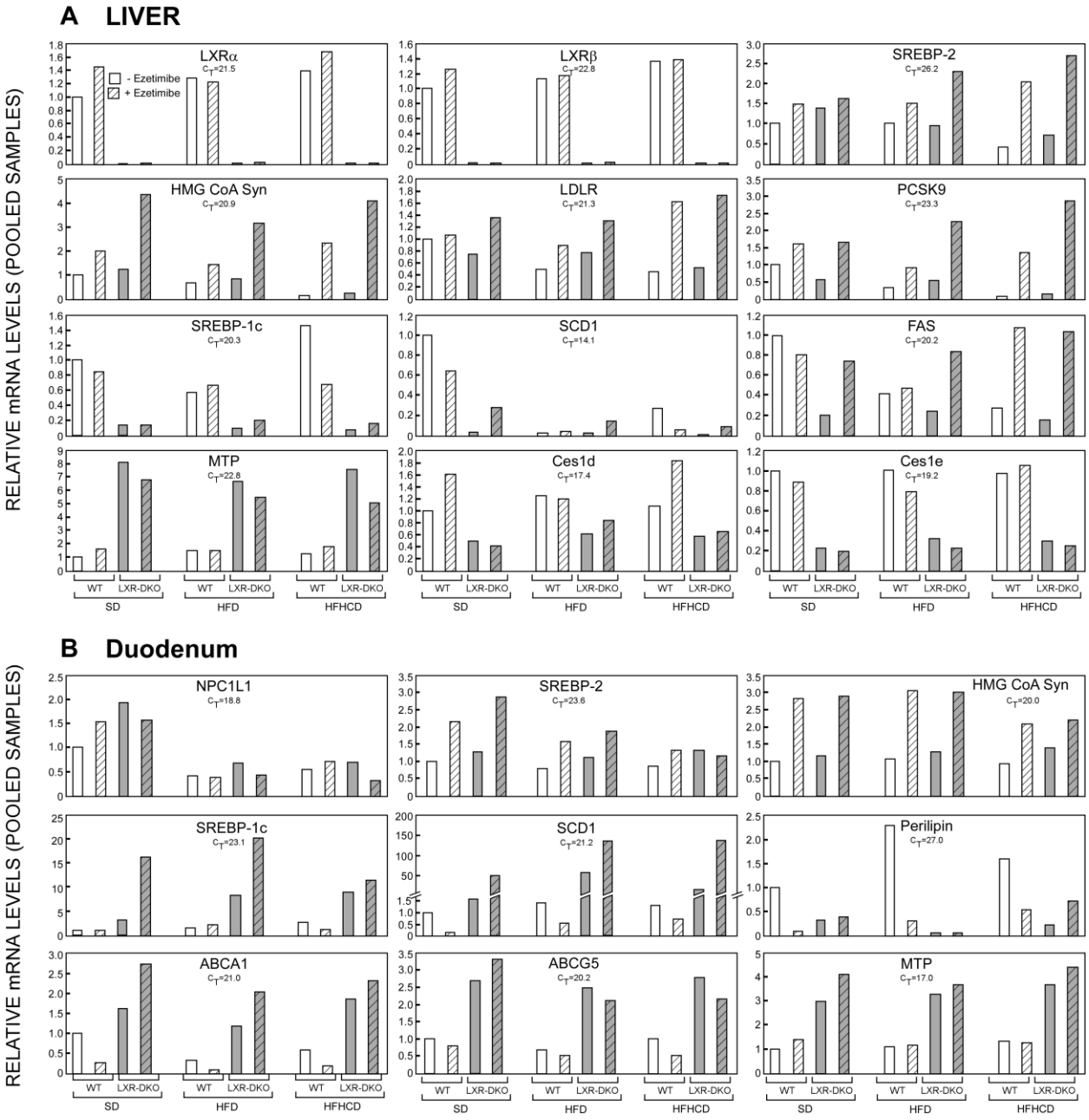

Fig. 2.5 The changes in relative mRNA levels in liver and intestine confirm genotypes of mice, actions of Ezetimibe, and support the lipid synthesis rates previously measured (Fig. 2.4). Adult, male wildtype (WT, white bars) and LXRα/LXRβ-double knockout mice (LXR-DKO, gray bars) were provided ad libitum a standard low-fat rodent diet (SD), a high-fat diet (HFD), or a high-fat, high-cholesterol diet (HFHC) with or without 5 mpk Ezetimibe (hatched bars) for 12 days. Equal quantities of RNA (6 mice per group) were pooled and measured by quantitative real-time PCR, and relative mRNA levels were established using the comparative Ct method and *Rpl19* as the invariant housekeeping gene. The cycle number at threshold (Ct) for the SD without Ezetimibe-fed group (leftmost white bar) is provided for each RNA to illustrate relative abundance of each gene product.

Relative mRNA levels in duodenum reveal differential gene expression in response to diet, genotype and Ezetimbe administration (Fig. 2.5B). RNA levels for the target of Ezetimibe, NPC1L1, were unaffected by genotype or Ezetimibe treatment, but were consistently lower in mice receiving HF diets. This is consistent with a previous report that the lipid-sensing nuclear hormone receptor, PPARα, represses *Npc1l1* gene expression in mice (Valasek et al., 2007). Changes in mRNA levels for SREBP-2 and target gene, HMGCS1, mirrored those observed in liver, and were consistent with altered sterol synthesis rates in the mouse intestine (**Fig. 2.4B**). The mRNA levels for SREBP-1c and SCD1 in intestine are much lower than those in liver, but changes were observed by genotype (levels higher in LXR-DKO mice), and were enhanced in this mouse strain upon Ezetimibe treatment under all dietary conditions. ABCA1 and ABCG5 mRNA levels were increased in duodenum of LXR-DKO mice, as previously reported (Repa et al., 2002a; Repa et al., 2000b), and were reduced only in wild-type mice receiving Ezetimibe treatement of the various diets. Finally, again two genes implicated in fatty acid/TG handling in the enterocyte, the lipid droplet protein perilipin, and MTP were identified by microarray analysis. Perilipin mRNA levels sharply declined in wild-type mice receiving Ezetimbe, and again MTP levels were elevated in LXR-DKO mice. Ezetimibe had no effect on gene expression of proteins involved in intestinal fatty acid uptake (CD36, FATP4), TG synthesis (DGAT1 or 2, MGAT2), or chylomicron assembly (apoAIV, apoB, Sarb1, Vti1a), (see **Fig. 1.4,** and reviewed in (Abumrad and Davidson, 2012). In summary, changes in mRNA levels of liver and duodenum confirm the *in vivo* measures of fatty acid and sterol synthesis rates, and suggest that altered lipid handling by enterocytes and/or liver may contribute to changes in hepatic TG levels.

Ezetimibe treatment causes an increase in fecal neutral sterol loss without affecting non-sterol lipid absorption (Fig. 2.6A-C). Further studies to determine lipid balance were performed in mice receiving the HFD, as both genotypes of mice experienced body weight gain under this dietary regimen (Fig. 2.1B). Fecal neutral sterol excretion was determined in stool samples collected over the last three days of the 12-day feeding period. As expected, treating mice with Ezetimibe, a cholesterol absorption inhibitor,

resulted in significantly greater sterol excretion in all mice (**Fig. 2.6A**). This increase in sterol excretion was further enhanced in the LXR-DKO mice, likely due to increased expression of ABCG5/ABCG8, which promote biliary sterol secretion and efflux of cholesterol from enterocytes back into the intestinal lumen to inhibit cholesterol absorption (Repa et al., 2002a). When total fecal lipid was measured, and arithmetically adjusted to eliminate the contribution by sterol, there were no significant differences in lipid output by mice, regardless of genotype or Ezetimibe treatment (**Fig. 2.6B**). Finally, fecal bile acid excretion was determined in mice fed the HFD. Ezetimibe had no impact on fecal bile acid excretion, but excretion was significantly lower in LXR-DKO mice (**Fig. 2.6C**). This could occur by more efficient reclamation of bile acids in the lower small intestine, or by a reduced bile acid pool size in LXR-DKO mice. The latter would be consistent with the observed decrease in sterol absorption (i.e. increase in fecal sterol loss (**Fig. 2.6A**)) evident in LXR-DKO mice.

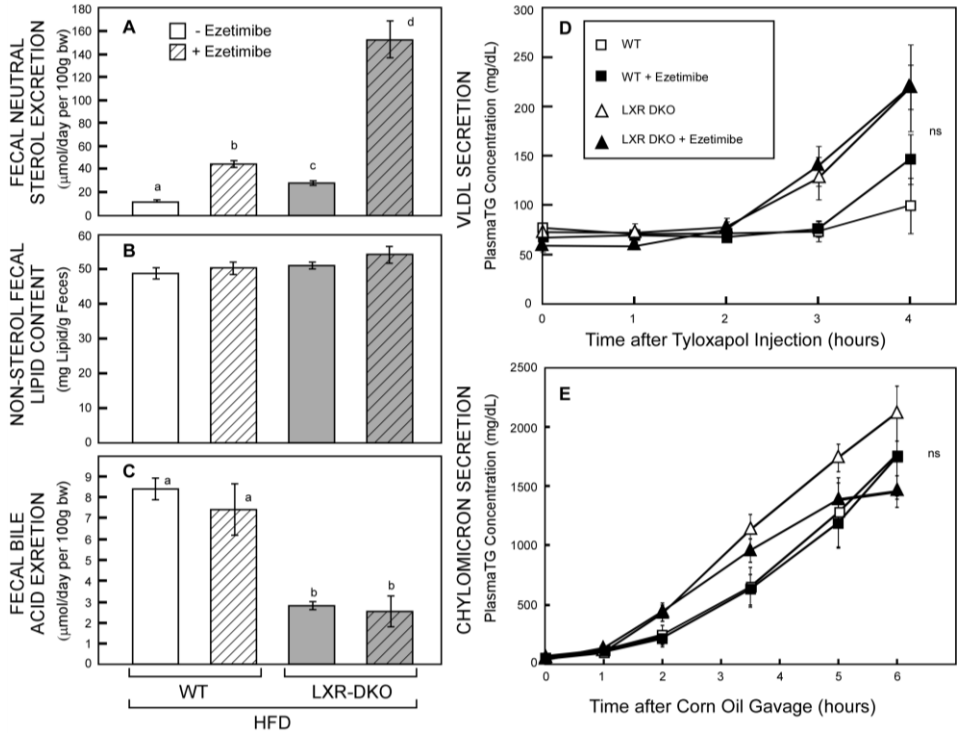

Fig. 2.6 Ezetimibe exerts dramatic effects on sterol excretion, but does not impact lipid or bile acid excretion, or triglyceride secretion as a component of VLDL or chylomicron particles. Adult, male wildtype (WT, white bars in left panels, squares in right panels) and LXRα/LXRβ-double knockout mice (LXR-DKO, gray bars in left panels, triangles in right panels) were provided ad libitum a high-fat diet (HFD) with or without 5 mpk Ezetimibe (hatched bars in left panels, black symbols in right panels). Fecal neutral sterol (A), lipid (B) and bile acid excretion were determined in stool samples collected during the final 72h of the 12d feeding regimen. Plasma TG was measured following Tyloxapol administration to fasted mice (D, VLDL secretion) or to mice receiving an oral lipid gavage (E, Chylomicron secretion). Values represent the mean ± SEM of 4-6 mice per group. Significant differences ($P<0.05$) were determined by one-way ANOVA with Neuman-Keuls post-hoc test, and different letters denote groups that are significantly different.

Triglyceride secretion from liver and intestine, as a component of VLDL particles or chylomicrons, is unaffected by Ezetimibe treatment (Fig. 2.6D.E). To determine whether a change in hepatic triglyceride could be the result of either enhanced VLDL secretion, or reduced delivery of dietary TG to liver via lower chylomicron production, lipoprotein lipase was inhibited in mice by Tyloxapol administration in the fasted state (VLDL, **Fig. 2.6D**) or fed-state (corn oil gavage, chylomicron, **Fig. 2.6E**). The results of these analyses did not reveal significant changes in VLDL or chylomicron secretion by Ezetimibe treatment of HF-fed mice. There was a trend toward enhanced VLDL and chylomicron secretion by LXR-DKO, consistent with increased MTP expression.

Ezetimibe can relieve lipid accumulation in livers of wild-type and LXR-DKO mice with preexisting steatosis (Fig. 2.7A-E). Previous studies revealed that Ezetimibe can prevent TG accumulation in both wild-type and LXR-DKO mice during the development of hepatic steatosis (12-day study). We also addressed whether Ezetimibe could relieve TG accumulation in mice with existing steatosis. Wild-type and LXR-DKO mice were fed the HFD for 8 weeks. One set of mice was evaluated at this time to establish hepatic TG levels. Additional mice were continued on HFD or HFD supplemented with Ezetimibe for 4 weeks. As observed in the 12-day study, LXR-DKO mice accumulated greater amounts of hepatic TG than wild-type mice (**Fig. 2.7A**). Introduction of Ezetimibe during the last 4 weeks reduced hepatic triglyceride levels in wild-type mice (from 40.8 mg/g to 26.9 mg/g, not reaching significance p=0.068) and LXR-DKO mice (from 92.2 mg/g to 46.7 mg/g, $p<0.0015$). These changes in hepatic lipid were confirmed by Oil Red O staining of livers from these mice (**Fig. 2.7B-E**). The enhanced hepatic lipid accumulation by LXR-DKO mice compared to wild-type mice was evident (panel C versus panel B), wherein the LXR-DKO mice treated for 12 weeks on high-fat diet exhibited pan-lobular steatosis on Oil Red O staining, while the corresponding WT mice accumulated somewhat less steatosis in a predominantly centrizonal pattern. Rare ballooning cells were identified in an LXR-DKO 12 week HFD fed mouse on routine histologic stain (data not shown). No significant inflammatory infiltrates were seen in any of the groups. In mice of both genotypes Ezetimibe administration during the last 4 weeks of this 12-week HF feeding study qualitatively reduced hepatocyte lipid accumulation (compare panels B and D for wild-type; C and E for LXR-DKO).

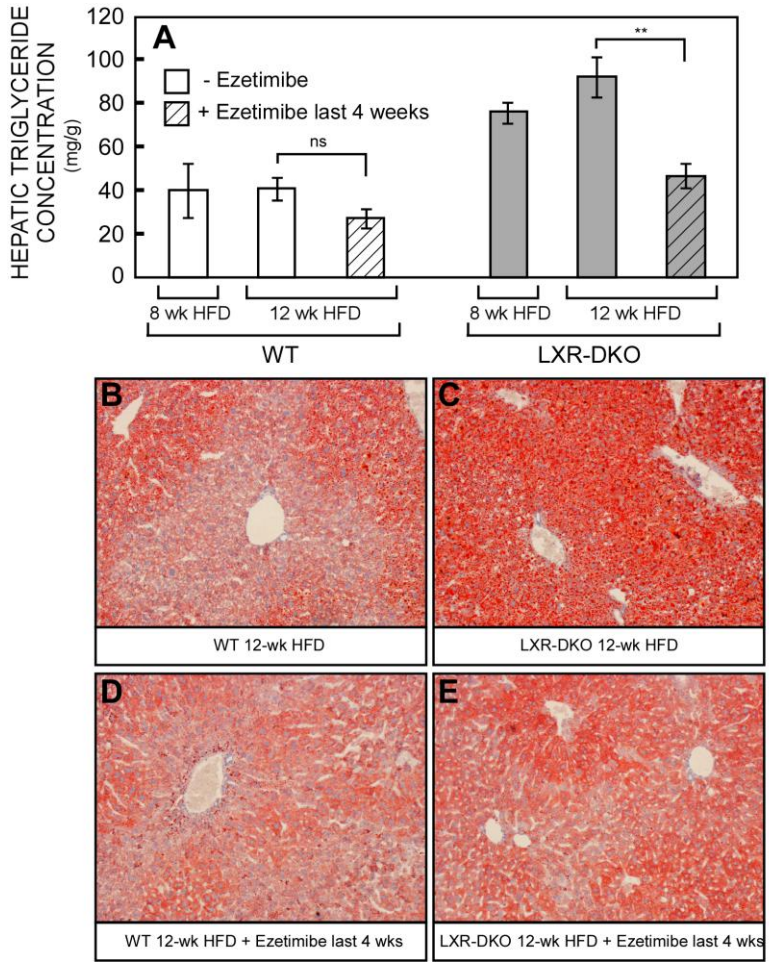

Fig. 2.7 Ezetimibe treatment can ameliorate existing steatosis in high-fat fed mice, independent of LXR. Adult, male wildtype (WT, white bars) and LXRα/LXRβ-double knockout mice (LXR-DKO, gray bars) were provided ad libitum a high-fat diet (HFD) for 8 weeks (one set of mice evaluated at this timepoint), then continued on the HFD with or without 5 mpk Ezetimibe (hatched bars) for an additional 4 weeks. Hepatic triglyceride concentrations (A) and visualization of neutral lipid accumulation by Oil Red O staining (B-C) were evaluated. All images were visualized at 100x. Values in (A) represent the mean ± SEM of 4-6 mice per group. **, $P<0.01$ as determined by Student's t-test.

2.5 DISCUSSION

The main purpose of these studies was to address whether LXR is the mediator of Ezetimibe-associated protection from hepatic steatosis. Several reports have demonstrated that Ezetimibe treatment of HF-fed mice reduces hepatic steatosis, and nearly all have invoked a putative role for LXR in this process (de Bari et al., 2011; Jia et al., 2010; Ushio et al., 2013). These previous studies typically involved long-term feeding studies (ranging from 1-7 months). Thus in addition to hepatic steatosis, the experimental animals also often developed differential degrees of confounding factors, including increased body weight, white adipose expansion and insulin resistance. Our studies were designed to assess the role of LXR while reducing confounding factors by utilizing two different feeding strategies.

The first strategy aimed to examine the development of hepatic steatosis. By studying these mice after only 12 days of high-fat feeding concurrent with Ezetimibe treatment, the initiating events in the development of hepatic steatosis, as well as the roles of LXR and *de novo* lipogenesis could be assessed before the mice developed overt insulin resistance and obesity. Indeed, as shown in **Fig. 2.3A-B**, plasma glucose levels were unchanged due to Ezetimibe treatment, and insulin levels remained normal across all groups. These studies revealed that Ezetimibe's ability to mitigate high-fat diet-induced hepatic steatosis did not depend on LXR. Perhaps more importantly, by removing the confounding factors of obesity and insulin resistance, it became clear that lipogenesis was not decreasing with Ezetimibe treatment despite the reduction in hepatic TG concentration.

The 12 week long-term high-fat feeding strategy aimed to study the effect of Ezetimibe administration to mice with pre-existing hepatic steatosis and equivalent insulin resistant states. This study allowed us to evaluate the efficacy of Ezetimibe to relieve fatty liver in both the wildtype and LXR-DKO mice. These results clearly showed that Ezetimibe can rescue existing hepatic steatosis independently of LXR. This is an important point, because if Ezetimibe were employed as a therapy in human patients with NAFLD, it would most likely be in patients with concurrent obesity and insulin resistance.

Two other factors regarding the chosen experimental design warrant further elaboration. The first is the choice of diets in these studies. There have been several dietary models employed in mice to induce hepatic steatosis in an effort to recapitulate the human form of this disease including high-fat diets, high-cholesterol/cholate diets, high-fructose diets, and diets with a deficiency of methionine and choline (reviewed in (Hebbard and George, 2011). The methionine and choline deficient diet induces rapid development of hepatic steatosis, however there is no weight gain or insulin resistance and the deficiency of these nutrients blocks hepatic β-oxidation and VLDL production. Thus it does not appear to recapitulate the human pathophysiology of NAFLD, and was not selected for use in our studies. A recent report revealed that Ezetimibe does not prevent steatosis induced by high-fructose feeding (Ushio et al., 2013) so this diet was not selected. The majority of studies involving Ezetimibe's effect on hepatic steatosis utilize high-fat diet induction of fatty liver. Thus, we elected to use high-fat feeding, and chose a HF diet rich in palm oil, as this regimen was particularly efficacious in studies by Jia and colleagues. Additionally, a high-fat diet with added cholesterol was included in our study design to further exacerbate conditions that may impact the sterol-sensing transcription factor, LXR.

The choice to use mice with global deletions of both LXRα and LXRβ was another important decision in the experimental design of these studies. Although LXRα is the predominant LXR subtype in the liver, LXRα and β are both expressed in intestine. Therefore, as a first analysis, global deletion of these transcription factors was utilized.

Finally, two other interesting observations warrant mention. First, we observed greater hepatic sterol synthesis in the face of greater hepatic cholesterol concentration in LXR-DKO mice. SREBP-2 and SREBP-1c have different functions, however when SREBP-1c is absent, there could be compensation by SREBP-2 which activates the cholesterol biosynthetic pathway (Liang et al., 2002). The hepatic expression of SREBP-1c is dramatically reduced in LXR-DKO mice, which could lead to this compensation which would explain the increase in cholesterol synthesis. However, cholesterol synthesis rates are also increased in the intestine of the LXR-DKO mice, which have a higher expression of

SREBP-1c compared to wildtype mice (data not shown). An alternative explanation is that some target gene of LXR could be involved in intracellular transport or hydrolysis of cholesterol esters, and when LXR is missing, the cell loses its capacity to accurately gauge its cholesterol levels. Two genes, *Ces1d* and *Ces1e*, were expressed at significantly lower levels in LXR-DKO mice, and it is possible that these could participate in cholesteryl ester hydrolysis. Second, novel gene changes were observed in LXR-DKO mice that may impact lipid metabolism: a) Ces1d and Ces1e are significantly reduced, which may indicate a role in the partitioning of free versus esterified lipids; b) MTP was increased in LXR-DKO mice which correlates with the observed increases in both VLDL and chylomicron secretion.

Through both short-term and long-term high-fat diet feeding strategies, Ezetimibe clearly mitigates the development of hepatic steatosis independent of LXR and the initiating events do not involve a reduction in hepatic lipogenesis. However, the molecular mechanism regulating these events still remains unclear. Future studies to interrogate other lipid processes, i.e. fatty acid oxidation, or other regulators (HNF1α, PPARs, FXR) is warranted. The strategies used in these studies provide an excellent framework to interrogate the initiating events leading to hepatic steatosis, and the mechanism by which Ezetimibe mitigates this process.

CHAPTER THREE:

Delineation of biochemical, molecular, and physiological changes accompanying bile acid pool size restoration in *Cyp7a1*$^{-/-}$ mice fed low levels of cholic acid

Adapted from: Jones RD, Repa JJ, Russell DW, Dietschy JM, Turley SD. Delineation of biochemical, molecular and physiological changes accompanying bile acid pool size restoration in Cyp7a1-/- mice fed low levels of cholic acid. Am J Physiol. 2012;303:G263-G74.

3.1 ABSTRACT

Cholesterol 7α-hydroxylase (CYP7A1) is the initiating and rate limiting enzyme in the neutral pathway that converts cholesterol to primary bile acids (BA). CYP7A1-deficient mice (*Cyp7a1*$^{-/-}$) have a depleted BA pool, diminished intestinal cholesterol absorption, accelerated fecal sterol loss, and increased intestinal cholesterol synthesis. To determine the molecular and physiological effects of restoring the BA pool in this model, adult female *Cyp7a1*$^{-/-}$ and matching *Cyp7a1*$^{+/+}$ controls were fed diets containing cholic acid (CA) at modest levels (0.015, 0.030 and 0.060 % wt/wt) for 15-18 days. A level of just 0.03% provided a CA intake of about 12 umol (4.8mg)/day/100 g body wt and was sufficient in the *Cyp7a1*$^{-/-}$ mice to normalize BA pool size, fecal BA excretion, fractional cholesterol absorption and fecal sterol excretion but caused a significant rise in the cholesterol concentration in the small intestine and liver, as well as a marked inhibition of cholesterol synthesis in these organs. In parallel with these metabolic changes, there were marked shifts in intestinal and hepatic expression levels for many target genes of the BA sensor, farnesoid X receptor (FXR), as well as of genes involved in cholesterol transport, especially adenosine triphosphate-binding cassette transporter A1 (ABCA1) and ABCG8. In *Cyp7a1*$^{+/+}$ mice this level of CA supplementation did not significantly disrupt BA or cholesterol metabolism except for an increase in fecal BA excretion and marginal changes in the mRNA expression for some BA synthetic enzymes. These findings underscore the importance of using moderate dietary BA levels in studies with animal models.

3.2 INTRODUCTION

THE FORMATION OF bile acids from cholesterol in the liver and their eventual excretion in the stools represents a major route for the elimination of cholesterol from the body (Grundy and Bilheimer, 1984; McMurry et al., 1985; Vanhanen et al., 1992; von Bergmann et al., 1979). Bile acid synthesis occurs in the liver via several pathways, the predominant one usually being the classic or neutral pathway that is initiated by cholesterol 7α-hydroxylase (CYP7A1). There are also alternate pathways that involve an initial hydroxylation of the side chain via either sterol 27-hydroxylase (CYP27A1) or cholesterol 25-hydroxylase. Both 27-hydroxycholesterol and 25-hydroxycholesterol are substrates for CYP7B1, an oxysterol 7α-hydroxylase. In another pathway, 24-hydroxycholesterol, generated in the brain via cholesterol 24-hydroxylase (CYP46A1), is transported to the liver where it serves as a substrate for CYP39A1, another oxysterol 7α-hydroxylase. Each of these reactions, as well as all the subsequent steps in the bile acid synthetic pathway, and the mechanisms that ultimately control the amount of cholesterol being converted to bile acids, are discussed in recent reviews (Chiang, 2009; Norlin and Wikvall, 2007; Russell, 2009).

Bile acids, in conjugated form, are secreted via the bile into the lumen of the small bowel where they enter an intestinal pool, the preservation of which is essential for the absorption of sterols and various other classes of lipid including essential fatty acids and fat soluble vitamins (Carey and Cahalane, 1988). Indeed, it has long been known that one of the key factors influencing the amount of cholesterol that is absorbed from the small intestine and transported to the liver is the size and composition of the bile acid pool (Schwarz et al., 2001; Wang et al., 2003; Woollett et al., 2006). In the steady state, the fraction of bile acid in this pool that is excreted from the body each day is ordinarily replaced by an equal amount of newly synthesized bile acid. The bile acid pool undergoes continuous enterohepatic flux, a process that is facilitated through the action of multiple transporters (Alrefai and Gill, 2007; Dawson et al., 2009). Specifically, these proteins are responsible for either pumping bile acids across the canalicular membrane

into the bile (BSEP), reclaiming them from the ileum (ASBT and OSTα-OSTβ), or extracting them from the portal blood (NCTP). Long before these proteins were identified and their specific roles in bile acid handling delineated, the pharmacologic interruption of the enterohepatic circulation of bile acids was used as an effective strategy for lowering the plasma low density lipoprotein-cholesterol (LDL-C) concentration in the treatment of atherosclerosis (Grundy et al., 1971; Insull, 2006).

In recent years, new areas of research point to a more global role for bile acids in metabolic regulation beyond their critical involvement in the solubilization of lipids and the maintenance of cholesterol balance across the liver and the body as a whole (Amaral et al., 2009; Hylemon et al., 2009). This development stems largely from major advances in our knowledge of how bile acids serve as activators of several nuclear receptors such as farnesoid X receptor (FXR) and pregnane X receptor (PXR), and also of cell signaling pathways in the liver and gastrointestinal tract (Goodwin et al., 2003; Hylemon et al., 2009; Modica et al., 2010). One of the most clinically significant findings centers around the apparent relationship between bile acid metabolism, hepatic insulin resistance and glucose homeostasis, which may be mediated through both FXR-dependent and independent mechanisms (Kobayashi et al., 2007; Li et al., 2010; Watanabe et al., 2011; Zieve et al., 2007). To the contrary, a more recent study suggests that glucose and insulin may be regulators of bile acid synthesis (Li et al., 2012). These and other findings are driving a wave of research into the association between bile acid metabolism and various disorders such as type 2 diabetes and obesity. Many of these new areas of investigation utilize either animal models with genetically altered bile acid metabolism and/or experimental diets enriched with various bile acids. In most cases the level of bile acid incorporated into such diets is 0.5% (wt/wt) but in some studies the amount of supplementation has far exceeded this level (Biddinger et al., 2008; Cheng et al., 2007; Cho et al., 2010; Huang et al., 2011; Miyata et al., 2009; Wang et al., 2003; Wolters et al., 2002; Yu et al., 2000; Zhang and Klaassen, 2010). Depending on the design of the study, such high levels of supplementation could be considered unphysiological because the daily oral intake of bile acid is many-fold greater than the size of the animal's bile acid pool and vastly more than the basal rate of bile

acid synthesis in that animal, as measured by its daily excretion rate of acidic sterols. This practice arises in part because of the lack of published data defining the impact of graded increases in dietary bile acid supplementation on bile acid and cholesterol metabolism in the mouse and other species.

Mice deficient in cholesterol 7α-hydroxylase manifest a marked reduction in bile acid pool size and excretion, diminished intestinal cholesterol absorption, accelerated fecal neutral sterol excretion, and increased intestinal cholesterol synthesis (Erickson et al., 2003; Schwarz et al., 1998). In the present study we established a dietary cholic acid level that was sufficient to normalize these various parameters in this model. We then systematically quantitated, at a molecular and biochemical level, the changes in multiple components of intestinal and hepatic bile acid and sterol metabolism in both *Cyp7a1*$^{-/-}$ mice and also in their matching *Cyp7a1*$^{+/+}$ controls at this, as well as at lower and higher levels of cholic acid intake. Together, the data show that decisive shifts in bile acid and cholesterol metabolism occur in response to dietary bile acid levels far lower than those traditionally used to perturb the enterohepatic circulation of bile acids in animal models.

3.3 MATERIALS AND METHODS

Animals and diets. Cholesterol 7α-hydroxylase-deficient mice (*Cyp7a1*$^{-/-}$) were generated by crossing homozygous carriers (Ishibashi et al., 1996). The colony was maintained on a mixed strain background (C57BL/6:129/SvEv), and C57BL/6:129/SvEv hybrids (*Cyp7a1*$^{+/+}$) served as control animals. To increase the survival rate of homozygous pups, the diet of nursing females was routinely supplemented with cholic acid (0.25%, wt/wt) until the pups were weaned at 23-25 days of age. In all experiments the age of the mice at the time of study ranged from seven to 10 months, except those involving the measurement of cholesterol absorption and neutral sterol excretion where the mice were three to four months of age. All studies were done with female mice fed the meal from a cereal-based rodent diet (Wayne Lab Blox, No. 8604; Harland Teklad, Madison, WI), which contained 0.02% (wt/wt) cholesterol and ~5 % (wt/wt) total lipid. This regimen, referred to as the basal diet, was made to contain varying levels of cholic acid as detailed below. Depending on the metabolic parameter being measured, the mice were housed either individually or in groups of three or four in plastic colony cages with wood shavings in a light-cycled room. All animals were studied in the fed state toward the end of the dark phase of their light cycle. All experiments were approved by the Institutional Animal Care and Use Committee of the University of Texas Southwestern Medical School.

Establishment of dietary cholic acid levels to be tested in Cyp7a1$^{-/-}$ *and Cyp7a1*$^{+/+}$ *mice*. Mature female mice lacking cholesterol 7α-hydroxylase were documented to excrete about 5 µmol of bile acid/day/100 g body weight (bw) which represented only about 36% of the output seen in matching *Cyp7a1*$^{+/+}$ females (~14 µmol/day/100 g bw) (Schwarz et al., 2001). These mice, irrespective of genotype, consumed about 16 g of the basal diet/day/100 g bw (data not shown), which corresponds to the food intake we have reported previously for other mouse strains (Turley et al., 1998). From these data we thus determined that the addition of cholic acid (molecular weight of 408.6) to the diet at a level of 0.03% (wt/wt) ought to provide a daily intake of bile acid (ignoring that taken in through coprophagy) of about 11.7 µmol/day/100 g bw. This supplementation, on top of their basal rate of bile acid excretion of 5

μmol/day/100 g bw would raise the excretion rate in the *Cyp7a1*$^{-/-}$ mice to a level not very different from that typically found in their *Cyp7a1*$^{+/+}$ counterparts. Nevertheless, it was decided that, in addition to a level of 0.03% (wt/wt) cholic acid, we would also test the response of mice of both genotypes to half 0.015% (wt/wt), and twice this level 0.060% (wt/wt) of supplementation.

Bile acid pool size and composition and rate of fecal bile acid excretion. Pool size was determined as the total bile acid content of the small intestine, gallbladder, and liver combined. The bile acids were extracted in ethanol in the presence of [24-^{14}C] taurocholic acid (PerkinElmer, Inc,Waltham, MA) and analyzed by HPLC (Schwarz et al., 1998). Bile acids were detected by measurement of the refractive index and identified by comparison with authentic standards. For muricholic acids no attempt was made to determine whether the major peak identified as β-muricholic acid might have also represented unknown amounts of α and ω-muricholic acid. In all animals, cholic and muricholic acid together represented more than 90% of the bile acids in the pool, although the ratio of cholic to muricholic acid varied widely depending largely on the level of dietary cholic acid supplementation. Essentially all bile acids detected in the extracted pools were taurine conjugated. Pool size was expressed as μmol per 100 g bw. For the fecal bile acid measurements, stools collected over three days from individually housed mice were dried, weighed and ground to a fine powder. A 1-g aliquot of this material was used to determine total bile acid content by an enzymatic method previously described (Schwarz et al., 1998). The excretion rate of bile acids was expressed as μmol per day per 100 g bw.

Intestinal cholesterol absorption and rate of fecal neutral sterol excretion. Fractional cholesterol absorption was measured by a dual-isotope method. A mixture of 2μCi of [5,6-^{3}H]sitostanol (American Radiolabeled Chemicals, Inc., St. Louis, MO) and 1μCi of [4-^{14}C]cholesterol (PerkinElmer Inc.) in medium chain triglyceride oil (Mead Johnson, Evansville, IN) was administered intragastrically by gavage. Mice were housed individually and stools were collected over the next 3 days. Aliquots of stool and of the original dosing mixture were extracted, and fractional cholesterol absorption (%) was

calculated from the ratio of ^{14}C to ^{3}H as previously described (Schwarz et al., 1998). A second aliquot was used to quantitate the amounts of cholesterol, coprostanol, epicoprostanol, and cholestanone by gas chromatography (GC) and these data were used to calculate the rate of fecal neutral sterol excretion as μmol per day per 100 g bw.

Concentrations of total, unesterified and esterified cholesterol in liver and small intestine. Aliquots of liver and the whole small intestine were saponified and extracted and their total cholesterol concentrations were measured by GC using stigmastanol as an internal standard (Schwarz et al., 1998). In one study, additional aliquots of liver were extracted in chloroform:methanol (2:1 vol/vol) for the measurement of unesterified and esterified cholesterol concentrations as described (Turley et al., 2010).

Rates of cholesterol synthesis in liver and small intestine. These rates were measured in vivo using [^{3}H]water as detailed elsewhere (Schwarz et al., 1998). One hour after the mice were administered approximately 40 mCi of [^{3}H]water intraperitoneally, the liver and whole small intestine were removed, rinsed, blotted, and weighed. They were then saponified and the labeled sterols extracted and quantitated as described (Schwarz et al., 1998). The rate of cholesterol synthesis in each organ was calculated as the nmol of [^{3}H] water incorporated into sterols per hour per g of tissue.

Relative mRNA expression analysis. Small intestines were removed, flushed with ice-cold phosphate-buffered saline and then cut into three sections of similar length. The proximal and distal sections were opened longitudinally and the mucosae were removed by gentle scraping. These scrapings, along with aliquots of liver were quickly frozen in liquid nitrogen. mRNA levels were measured using a quantitative real-time PCR assay (Kurrasch et al., 2004a). All analyses were determined by the comparative cycle number at threshold method (User Bulletin No. 2, Perkin-Elmer Life Sciences) with cyclophilin as the internal control. The primer sequences used to measure RNA levels are given in Table 1. Relative mRNA levels in individual animals were determined by expressing the amount of mRNA found relative to that obtained for *Cyp7a1*$^{+/+}$ mice fed the basal diet alone, which in each case was

arbitrarily set at 1.0. For RNA blotting analyses, total RNA was prepared from various tissues of 4-10 mice (all male, except for ovary and uterus), equal amounts/animal were pooled, and polyA$^+$-enriched mRNA was purified. Five μgrams of this RNA/lane were loaded, separated by electrophoresis, transferred from gel to membrane, and hybridized with ^{32}P-cDNA probes as previously described (Goodwin et al., 2003).

Analysis of data. All data are reported as means ± SE for the specified number of animals. GraphPad Prism 5 software (GraphPad, San Diego, CA) was used to perform all statistical analyses. Differences between means were tested for statistical significance ($P < 0.05$) by either one-way or two-way analysis of variance with genotype and diet as factors. The Newman-Keuls multiple-comparison test for statistical significance was used for all one-way analyses of variance. Transformed data were used if unequal variance among the groups was evident by Bartlett's test.

3.4 RESULTS

Loss of Cyp7a1 function has a differential effect on the expression levels of mRNAs encoding other enzymes involved in bile acid biosynthesis. Although the *Cyp7a1*$^{-/-}$-deficient mouse has been widely studied, there is no documented information regarding how the expression levels of mRNA for other enzymes involved in the primary and alternate pathways of bile acid synthesis shift in the absence of cholesterol 7α-hydroxylase. Given that one of the objectives of this study was to determine the impact of modest cholic acid supplementation on the level of mRNA expression for enzymes in the hepatic bile acid biosynthetic pathways of adult *Cyp7a1*$^{-/-}$ and matching *Cyp7a1*$^{+/+}$ mice, we carried out a preliminary study to measure the mRNA levels for these enzymes in mice fed a basal diet. As shown in Fig. 3.1, the enzyme with the highest abundance of mRNA was 3α-hydroxysteroid dehydrogenase (AKR1C4). Thus this level was arbitrarily set at 1.0 and the mRNA levels for other enzymes were expressed relative to this baseline. Surprisingly, for the majority of enzymes, there was no significant difference in the relative mRNA level between the *Cyp7a1*$^{-/-}$ and *Cyp7a1*$^{+/+}$ mice. The clearest exception was the mRNA level for sterol 12α-hydroxylase (CYP8B1), which showed a decisive increase in the cholesterol 7α-hydroxylase–deficient mice. In contrast, there were modest reductions in the mRNA levels for sterol 27-hydroxylase (CYP27A1) and both of the oxysterol 7α-hydroxylases (CYP39A1 and CYP7B1). In a related figure (Fig. 3.2), the tissue distribution of eight of the key enzymes, as measured by RNA blotting, is shown. With the exception of cholesterol 25-hydroxylase (CH25H) and cholesterol 24-hydroxylase (CYP46A1), all enzymes were primarily localized to the liver. In the case of CH25H, the expression level was highest in the lung, and CYP46A1 was found almost exclusively in brain.

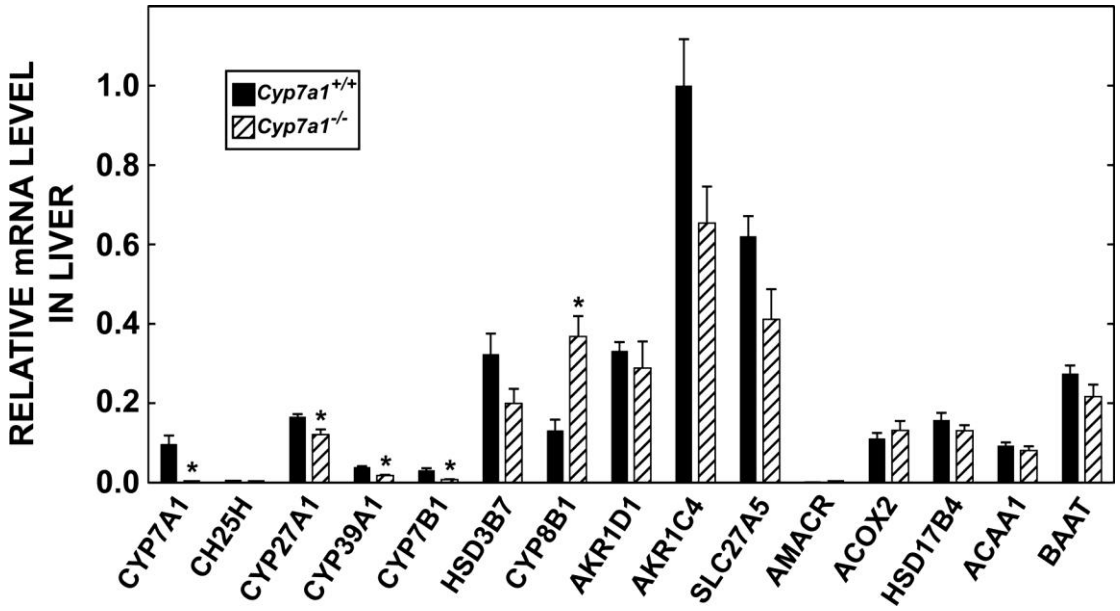

Fig 3.1. Relative levels of expression of mRNA for enzymes involved in the conversion of cholesterol to bile acids in *Cyp7a1*$^{+/+}$ and *Cyp7a1*$^{-/-}$ mice fed a basal rodent chow diet. Quantitative real-time PCR was used to measure the mRNA level of each enzyme in the livers of adult mice of both genotypes. The order in which the enzymes are listed follows that set out in a recent review (Russell, 2009). The full name, gene accession number, and primer sequence for each enzyme are given in Table A.2. The mRNA level for individual enzymes is expressed relative to that for 3α-hydroxysteroid dehydrogenase (AKR1C4), which was arbitrarily set at 1.0. Cholesterol 24-hydroxylase (CYP46A1) was omitted because this mRNA is expressed at very low levels in liver (Lund et al., 1999). In the case of cholesterol 25-hydroxylase (CH25H) and 2-methylacyl-CoA-racemase (AMACR) only trace amounts of mRNA were detected in both the *Cyp7a1*$^{+/+}$ and *Cyp7a1*$^{-/-}$ mice. Values are means ± SE of determinations in five mice of each genotype. An asterisk denotes that the value for the *Cyp7a1*$^{-/-}$ mice is significantly different from that for matching *Cyp7a1*$^{+/+}$ controls ($P < 0.05$).

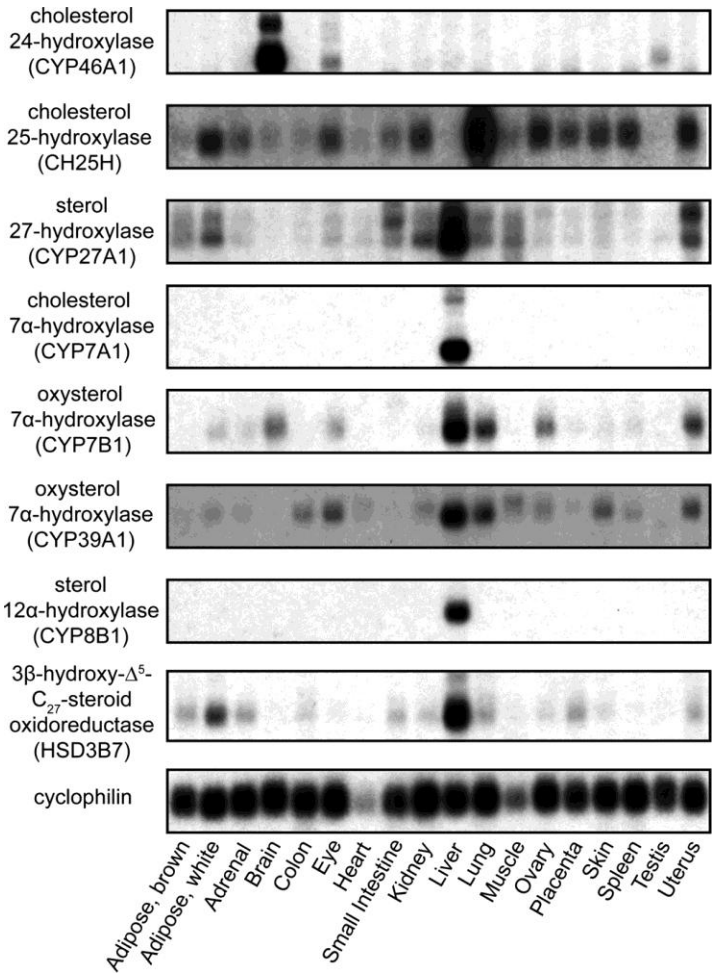

Fig. 3.2. Tissue distribution of key enzymes of bile acid biosynthesis in the mouse. PolyA$^+$-enriched RNA from various mouse tissues (all male, except for ovary and uterus) were resolved by electrophoresis, transferred to membrane and detected by ^{32}P-cDNA probes. The membrane was stripped and reprobed to detect RNAs encoding key enzymes of bile acid synthesis and the housekeeping gene, cyclophilin.

Low levels of dietary cholic acid supplementation cause dramatic changes in bile acid metabolism in Cyp7a1$^{-/-}$ mice with comparatively little effect in Cyp7a1$^{+/+}$ controls. The data in Fig. 3.3 reveal two notable findings with respect to how the major parameters of bile acid metabolism in CYP7A1-deficient mice change when small amounts of cholic acid are added to their diet. First, at a dietary cholic acid level of 0.030% (wt/wt), bile acid pool size (Fig. 3.3*A*) and fecal bile acid excretion (Fig. 3.3*C*) were restored to values very close to those found for *Cyp7a1*$^{+/+}$ mice fed the basal diet alone; however, at this level of supplementation there was a 6.4-fold increase in the ratio of cholic to muricholic acid in the pool of the CYP7A1-deficient mice (Fig. 3.3*B*). This rise, which reflected an increase in the

mass of cholic acid in the pool, far exceeded that in the matching *Cyp7a1*$^{+/+}$ mice where the ratio increased from 2.16 ± 0.14 on the basal diet alone to 3.05 ± 0.21 in the matching group given the diet containing 0.030% (wt/wt) cholic acid. Second, in *Cyp7a1*$^{+/+}$ mice, cholic acid supplementation, while having comparatively little impact on pool size and composition, consistently raised the rate of fecal bile acid excretion but the magnitude of change at each level of supplementation was never as pronounced as it was for matching *Cyp7a1*$^{-/-}$ mice (Fig. 3.3*C*).

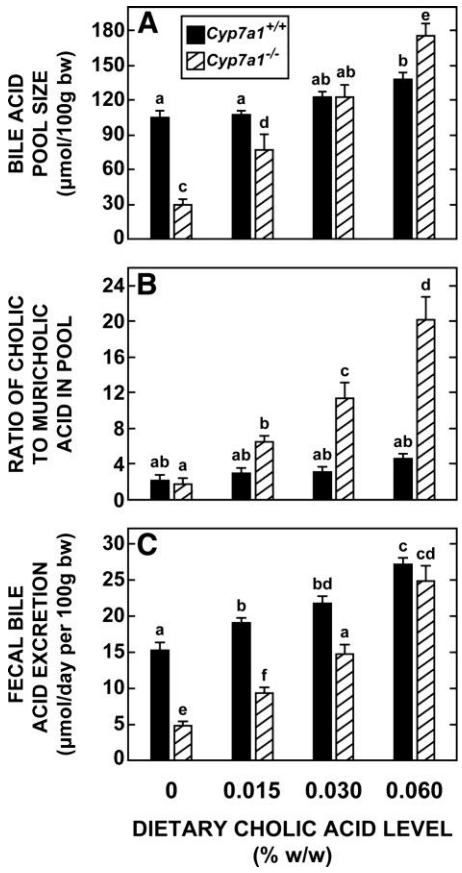

Fig. 3.3. Bile acid pool size and composition, and fecal bile acid excretion rate in *Cyp7a1*$^{-/-}$ and *Cyp7a1*$^{+/+}$ mice fed graded levels of cholic acid in their diet. Groups of adult female *Cyp7a1*$^{-/-}$ and matching *Cyp7a1*$^{+/+}$ mice were fed a basal rodent chow diet containing cholic acid at levels ranging from 0 to 0.060% (wt/wt) for 15-18 days. Values are means ± SE of data from eight mice in each group. Two-way ANOVA revealed significant interaction between diet and genotype, thus one-way ANOVA was performed, and bars designated with different letters denote statistically different values, $P < 0.05$.

Normalization of bile acid pool size in Cyp7a1$^{-/-}$ mice by cholic acid feeding restores cholesterol absorption and rate of cholesterol excretion, and is accompanied by a marked increase in hepatic cholesterol concentration. As shown in Fig. 3.4, the characteristically low level of cholesterol absorption and accelerated rate of fecal neutral sterol excretion evident in the *Cyp7a1*$^{-/-}$ mice fed the basal diet alone were restored by cholic acid feeding (0.030% wt/wt) to values seen in matching *Cyp7a1*$^{+/+}$ controls given the basal diet (Figs. 3.4*A* and 3.4*B*). This restoration was almost fully achieved at a cholic acid level of only 0.015% (wt/wt). Doubling the cholic acid level to 0.060% (wt/wt) did not have an additional effect on cholesterol absorption and excretion in the *Cyp7a1*$^{-/-}$ mice but it did marginally raise the fractional cholesterol absorption value in the *Cyp7a1*$^{+/+}$ controls. At the two higher levels of cholic acid there was a modest but significant increase in the total cholesterol concentration in the small intestine in mice lacking CYP7A1 but not in their corresponding controls (Fig. 3.4*C*). One of the most striking effects of these low levels of cholic acid supplementation in the *Cyp7a1*$^{-/-}$ mice was on their total cholesterol concentrations in the liver which increased 5.9-fold from 2.86 ± 0.15 mg/g on the basal diet alone to 17.01 ± 2.17 mg/g on the diet containing 0.060 % (wt/wt) cholic acid (Fig. 3.4*D*). The weight of the liver, expressed relative to body weight in this latter group of mice was 6.0 ± 0.2 % which was just above the range for all other mice in this study (5.1 to 5.6%) (data not shown).

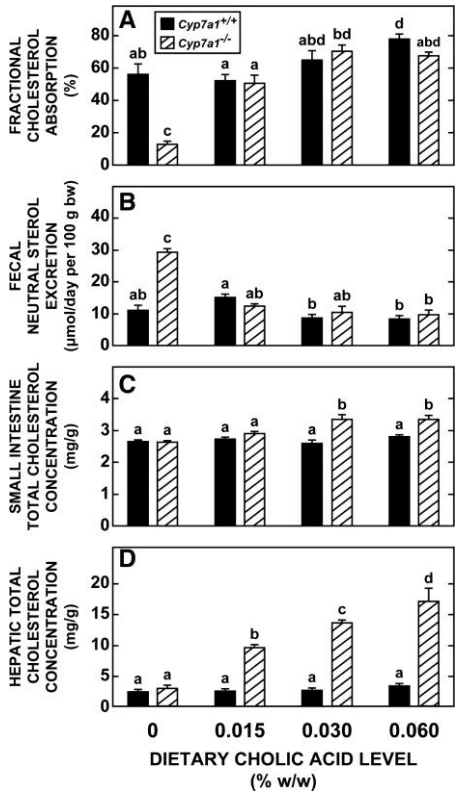

Fig. 3.4. Intestinal cholesterol absorption, fecal neutral sterol excretion and total cholesterol concentrations in small intestine and liver of *Cyp7a1*$^{-/-}$ and *Cyp7a1*$^{+/+}$ mice fed graded levels of cholic acid in their diet. Groups of adult female *Cyp7a1*$^{-/-}$ and matching *Cyp7a1*$^{+/+}$ mice were fed the same diets as described in the legend for Fig. 3.3. Three days before the end of the experiment mice were dosed with radiolabeled sterols and their stools were collected over the following three days for measurement of fractional cholesterol absorption and fecal neutral sterol excretion as described in MATERIALS AND METHODS. Values are means ± SE of data for four or five mice in each group in *A-C*, and eight mice per group in *D*. Two-way ANOVA revealed significant interaction between diet and genotype, thus one-way ANOVA was performed, and bars designated with different letters denote statistically significant values, $P < 0.05$.

Compensatory inhibition of hepatic and intestinal cholesterol synthesis accompanies increase in tissue cholesterol concentrations in Cyp7a1$^{-/-}$ *mice given cholic acid supplementation.* For the remaining studies it was decided to use only a single level of cholic acid supplementation (0.030 % wt/wt) based on the findings described in Figs. 3.3 and 3.4. The primary objective of these additional experiments was to determine how cholic acid supplementation affected the rate of hepatic and intestinal cholesterol synthesis, as well as the relative level of expression of mRNA for a constellation of enzymes, transcription factors and transporters involved in the synthesis and handling of bile acids, and of other proteins that regulate the intestinal synthesis and movement of cholesterol. The data in Fig. 3.5*A* show

that essentially all of the increase in hepatic cholesterol levels in *Cyp7a1*$^{-/-}$ mice given cholic acid (Fig. 3.4*D*) reflected a rise in the esterified fraction. Other groups of matching mice manifested a near complete inhibition of hepatic cholesterol synthesis (Fig. 3.5*B*), and a significantly lower level of hepatic mRNA expression for HMG CoA synthase (Fig. 3.5*C*) in parallel with the markedly expanded pool of cholesteryl ester. In the case of the *Cyp7a1*$^{+/+}$ mice fed the diet with cholic acid, there was a clear trend toward lower rates of hepatic cholesterol synthesis (Fig. 3.5*B*) and levels of mRNA expression for HMG CoA synthase (Fig. 3.5*C*) although these were not statistically significant.

Cholic acid feeding had comparatively little effect on intestinal cholesterol concentrations; however, as shown in Fig. 3.5*D*, in *Cyp7a1*$^{-/-}$ mice fed the diet with 0.03% (wt/wt) cholic acid, the total cholesterol concentration in the small intestine (3.36 ± 0.11 mg/g) was significantly higher than in either matching *Cyp7a1*$^{-/-}$ or *Cyp7a1*$^{+/+}$ mice fed the basal diet alone (2.70 ± 0.06 and 2.75 ± 0.10 mg/g, respectively). Although cholic acid feeding did not significantly affect either the rate of cholesterol synthesis or the mRNA level for HMG CoA synthase in the small intestine of the *Cyp7a1*$^{+/+}$ mice (Fig. 3.5*E* and 3.5*F*, respectively), this treatment did lower both of these parameters in the CYP7A1-deficient mice. As noted in the legend to Fig. 3.5, the mRNA data for the small intestine represent the distal third of the organ, whereas those for cholesterol synthesis are for the entire small intestine.

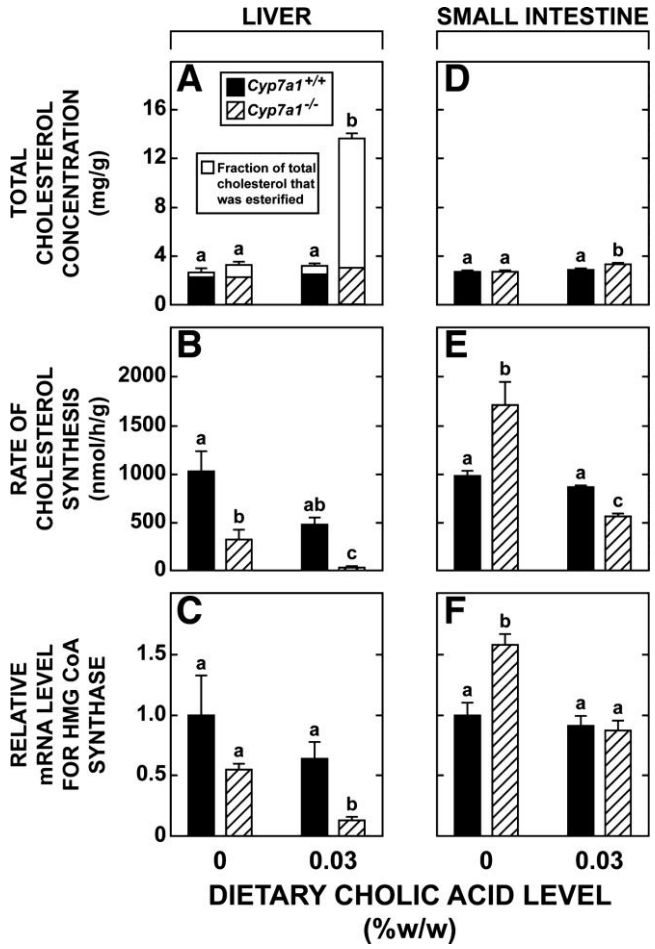

Fig. 3.5. Concentrations of unesterified and esterified cholesterol in the liver, and rates of cholesterol synthesis in the liver and small intestine of *Cyp7a1*$^{-/-}$ and *Cyp7a1*$^{+/+}$ mice fed a single level of cholic acid in their diet. In these experiments the level of dietary cholic acid supplementation was set at either 0 or 0.030% (wt/wt). All measurements were made in adult female mice fed their respective diets for 15-18 days. These data are derived from several experiments. The data in *A* are from the same animals used for the measurements in Fig. 3.4*D*. Other groups of matching mice were used for the measurement of total cholesterol concentration in intestine (*D*), the rates of hepatic and intestinal cholesterol synthesis (*B* and *E*), and the mRNA level for HMG CoA synthase (*C* and *F*). The liver and small intestine (distal third only) taken for these mRNA analyses came from the same animals used in the experiments described in Figs. 3.6 and 3.7. Values are means ± SE of data from five to eight mice in each group. In *A* the height of each bar defines the total cholesterol concentration and the relevant SE is shown. The SE for the esterified fraction is not indicated. Two-way ANOVA of data in *A*, *D* and *E* revealed significant interaction between diet and genotype, thus one-way ANOVA was performed, and bars designated with different letters denote statistically different values, $P < 0.05$.

Marked elevation in mRNA expression level for CYP8B1 in liver of Cyp7a1$^{-/-}$ *mice is abolished by cholic acid feeding*. Although the relative mRNA level for multiple proteins involved in the conversion of cholesterol to bile acids was measured, for the majority of these there was no change either as a function of genotype or of cholic acid intake. Therefore, in Fig. 3.6 (*A*-*F*), the mRNA expression levels of just six

of the 15 enzymes listed in Fig. 3.1 and Table A.2 are shown. The most striking changes associated with CYP7A1 deficiency were a 73% reduction in the relative mRNA level for an oxysterol 7α-hydroxylase (CYP7B1) (Fig. 3.6*D*), and a 2.8-fold increase in the mRNA for sterol 12α-hydroxylase (CYP8B1) (Fig. 3.6*E*). While this level of mRNA expression for CYP7B1 in the *Cyp7a1*$^{-/-}$ mice was unaltered by cholic acid feeding, in the case of CYP8B1, the supplementation lowered the mRNA expression level to just a fraction of that seen in the matching and unsupplemented *Cyp7a1*$^{-/-}$ mice, and also to levels well below those found in the *Cyp7a1*$^{+/+}$ mice fed either the basal diet alone or containing cholic acid. In parallel with the findings for CYP7B1, the mRNA level for CYP39A1 (the other oxysterol 7α-hydroxylase) in the *Cyp7a1*$^{-/-}$ mice was less than that in the matching *Cyp7a1*$^{+/+}$ controls, especially after cholic acid feeding (Fig. 3.6*C*). The dietary level of cholic acid that produced these changes in the mice lacking cholesterol 7α-hydroxylase had comparatively little effect on the matching *Cyp7a1*$^{+/+}$ controls with the exception of a 2-fold increase in the relative mRNA level for CYP39A1 (Fig. 3.6*C*) and a 43% reduction in that for CYP7B1 (Fig. 3.6*D*).

The remaining data in Fig. 3.6 (*G-L*) show the relative mRNA levels in liver for various regulatory transcription factors in bile acid metabolism (HNF4α, SHP, LRH-1) (Fig. 3.6, *G-I*), bile acid transporters (Fig. 3.6 *J,K*), and a canalicular sterol transporter, ABCG8 (Fig. 3.6*L*). The most notable changes associated with CYP7A1 deficiency alone were reductions of about 40 to 50% in the mRNA levels for SHP (Fig. 3.6*H*), BSEP (Fig. 3.6*J*), and ABCG8 (Fig. 3.6*L*), all of which were reversed to varying degrees by cholic acid supplementation. The most striking change in this regard was for ABCG8 where the mRNA level in the *Cyp7a1*$^{-/-}$ mice given cholic acid was 5.2-fold greater than it was in the unsupplemented *Cyp7a1*$^{-/-}$ controls, and 3.2-fold more than in the unsupplemented *Cyp7a1*$^{+/+}$ mice (Fig. 3.6*L*).

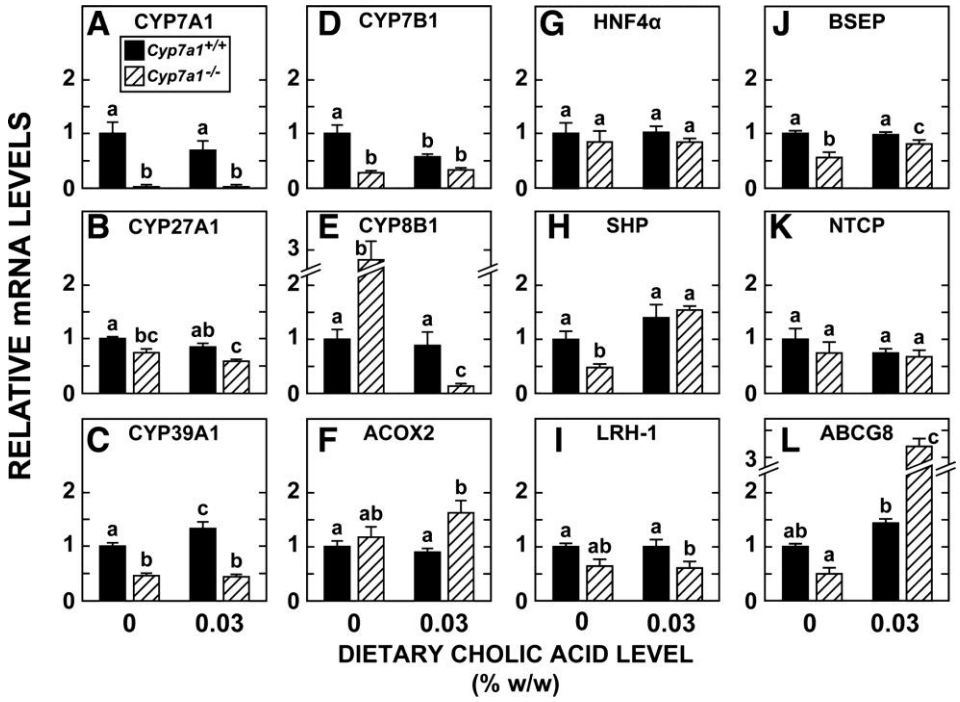

Fig. 3.6. Relative mRNA levels for various enzymes, transcription factors and transporters involved in bile acid metabolism in the livers of *Cyp7a1*$^{-/-}$ and *Cyp7a1*$^{+/+}$ mice fed a single level of cholic acid in their diet. Groups of adult female mice were fed the same diets used in the experiments described in Fig. 3.5. Their livers and small intestines were removed for RNA measurements as described in MATERIALS AND METHODS. The first set of data (*A*-*F*) are for six of the enzymes involved in the conversion of cholesterol to bile acids, whereas the second set (*G*-*L*) are for various proteins that play a role in bile acid synthesis and transport within the liver, or in the case of ABCG8, in facilitating hepatic cholesterol efflux. Values are the means ± SE of data for five or six mice in each group. Bars designated with different letters denote statistically different values, $P < 0.05$, as determined by one-way ANOVA.

Diminished intestinal expression of mRNA for various sterol and bile acid transporters and related proteins resulting from loss of CYP7A1 function is reversed to variable degree by cholic acid feeding. One of the main objectives of these studies was to define the impact of CYP7A1 deficiency and bile acid pool restoration on the expression of a constellation of genes involved in cholesterol and bile acid handling in the small intestine. The data in Fig. 3.7 show mRNA levels for multiple genes in the proximal and distal small intestine of the same mice used for mRNA analyses in the liver. The focus in the proximal region (Fig. 3.7 *A*-*F*) was on proteins that facilitate sterol movement across the enterocyte. For NPC1L1 (Fig. 3.7*A*), the expression level fell (32%) in the *Cyp7a1*$^{-/-}$ mice and this outcome changed little with cholic acid feeding. This was also the case in the *Cyp7a1*$^{+/+}$ controls given cholic acid.

Although flotillin-1 and flotillin-2 are believed to play a key role in NPC1L1-mediated cholesterol uptake (Ge et al., 2011), mRNA levels for these proteins remained unchanged in the *Cyp7a1*$^{-/-}$ animals and were unresponsive to cholic acid supplementation (Fig. 3.7*B*, *C*). This was also the case for SR-B1 (Fig. 3.7*D*). The pattern of mRNA expression for ABCG8 (Fig. 3.7*E*) followed that seen for liver (Fig. 3.6*L*), although the changes were not as large. In the case of ABCA1, the expression level in the *Cyp7a1*$^{-/-}$ mice on the basal diet alone was only 27% of that in the corresponding *Cyp7a1*$^{+/+}$ controls. Although cholic acid feeding did not significantly change the mRNA level for ABCA1 in the *Cyp7a1*$^{+/+}$ mice, in the case of those lacking CYP7A1 it caused a substantial increase.

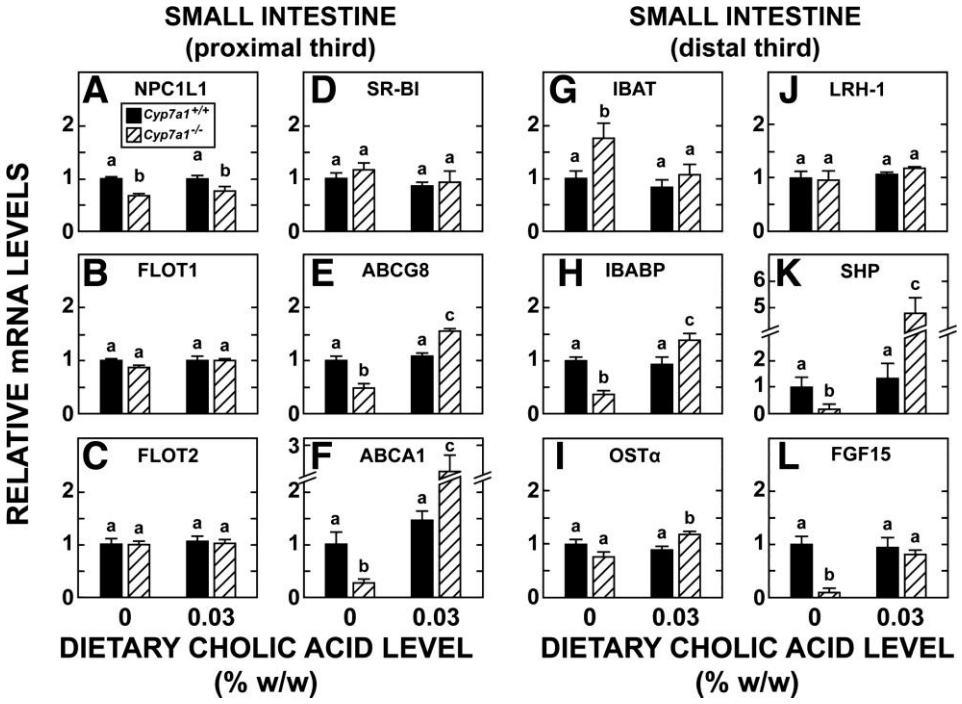

Fig. 3.7. Relative mRNA levels for various proteins involved in the movement of cholesterol, or in the synthesis and transport of bile acids, in the small intestine of *Cyp7a1*$^{-/-}$ and *Cyp7a1*$^{+/+}$ mice fed a single level of cholic acid in their diet. These analyses were carried out in mucosal scrapings from the proximal (*A*-*F*) and distal (*G*-*L*) sections of the small intestine of adult female *Cyp7a1*$^{-/-}$ and *Cyp7a1*$^{+/+}$ mice fed the same diets as described in Figs. 3.5 and 3.6. Values are means ± SE of data for five or six mice per group. Bars designated with different letters denote statistically different values, $P < 0.05$, as determined by one-way ANOVA.

In the distal small intestine the most pronounced change in mRNA expression levels resulting from CYP7A1 deficiency alone was seen for SHP (Fig. 3.7*K*) and FGF15 (Fig. 3.7*L*), with the relative mRNA level for both proteins being 80 to 90 % lower than in matching *Cyp7a1*$^{+/+}$ mice on the basal diet, and also for IBABP (Fig. 3.7*H*) where a reduction of 64% was seen. In the *Cyp7a1*$^{-/-}$ mice, cholic acid feeding essentially normalized the expression levels for IBABP and FGF15. However, for SHP it dramatically increased the relative mRNA in *Cyp7a1*$^{-/-}$ mice to a level that was 27-fold greater than that seen in their counterparts fed the basal diet alone, and 4.8-fold more than that found for the *Cyp7a1*$^{+/+}$ controls on the basal diet. The mRNA levels for OSTα (Fig. 3.7*I*) and LRH-1 (Fig. 3.7*J*) showed little change with either genotype or diet. In the case of the mRNA level for IBAT (Fig. 3.7*G*), there was a significant increase in the *Cyp7a1*$^{-/-}$ mice but this change was normalized with cholic acid feeding.

3.5 DISCUSSION

Several points relating to the objectives and design of these studies warrant elaboration. The first has to do with the experiments being run in both normal as well as *Cyp7a1*-deficient mice. This design allowed us to make a side by side comparison of the impact of giving small, graded increases of bile acid via the diet, not only to mice with normal bile acid pool sizes and intestinal cholesterol metabolism, but moreover, to mice with inherently small bile acid pools, altered rates of intestinal cholesterol absorption and synthesis as well as enhanced fecal sterol loss, all stemming from their lack of cholesterol 7α-hydroxylase. The *Cyp7a1*$^{-/-}$ mouse was selected mainly because this model has been defined more completely with respect to sterol metabolism than others with genetically altered bile acid metabolism (Erickson et al., 2003; Schwarz et al., 2001; Schwarz et al., 1998; Wolters et al., 2002). Another point concerns the selection of the bile acid species used for supplementation. While it would have been interesting to compare both cholic and chenodeoxycholic acid as has been done previously in a short-term feeding study with mice lacking sterol 12α-hydroxylase (CYP8B1) (Li-Hawkins et al., 2002), we focused specifically on cholic acid because it is a predominant bile acid in the pool of the mouse, and also because of its key role in the feedback regulation of bile acid biosynthesis (Beher et al., 1969; Li-Hawkins et al., 2002). We gauged the response of the mice to cholic acid supplementation through the measurement of a constellation of parameters that encompass the major steps involved in the synthesis, enterohepatic flux, and disposition of bile acids and cholesterol. Together, the data reveal informative findings about the widely differing sensitivity of *Cyp7a1*$^{-/-}$ mice and their *Cyp7a1*$^{+/+}$ counterparts to the delivery of physiological amounts of cholic acid into their intestinal pools from the diet.

Two major sets of conclusions can be drawn from these data. One of these relates to the changes in the synthesis, storage, transport and disposition of bile acids, while the other centers on the impact that these changes in bile acid metabolism had on the handling of cholesterol by the small intestine and liver. Although we had projected that a dietary cholic acid level as low as 0.03% (wt/wt) should be sufficient to restore bile acid pool size in mice lacking CYP7A1 to that found for *Cyp7a1*$^{+/+}$ mice fed the basal diet

alone, our initial experiments nevertheless also tested levels of cholic acid supplementation equal to half (0.015% wt/wt) and twice (0.060% wt/wt) this dose. While the intermediate level of supplementation, which provided an intake of cholic acid of just 4.8 mg (11.7 μmol) per day per 100 g bw did normalize the pool size in the *Cyp7a1*$^{-/-}$ mice (Fig. 3.3*A*), it also resulted in marked cholic acid enrichment of the pool (Fig. 3.3*B*). This enrichment had no discernible impact on the expression of mRNA for any of the three enzymes involved in the initiating steps of the alternate pathways of bile acid synthesis; CYP27A1 (Fig. 3.6B), CYP39A1 (Fig. 3.6*C*), and CYP7B1 (Fig. 3.6*D*). However, there was a large reduction in the level of mRNA expression of CYP8B1 (Fig. 3.6*E*), as well as a greater than 2-fold increase in the relative level of mRNA for SHP (Fig. 3.6*H*). There was also a marginal rise in the mRNA level for BSEP (Fig. 3.6*J*) but no discernible change in mRNA for NTPC (Fig. 3.6*K*). In the distal small intestine the impact of restoring the bile acid pool on the level of mRNA expression for several proteins that act as sensors of changes in bile acid flux, or that facilitate the transport of bile acids at various points in the enterohepatic cycle, was particularly striking. Thus, with the deficiency of bile acids now corrected, the mRNA level for the ileal bile acid transporter IBAT fell (Fig. 3.7*G*) while that for the cytosolic ileal bile acid binding protein IBABP (Fig. 3.7*H*) and for the organic solute transporter Ostα (Fig. 3.7*I*) increased significantly. In the case of SHP (Fig. 3.7*K*) and FGF15 (Fig. 3.7*L*), the expression level of mRNA for both proteins was many-fold greater in the *Cyp7a1*$^{-/-}$ mice given cholic acid than in those on the basal diet alone. While many of the changes accompanying pool restoration are directionally what might have been predicted for this model, what should be emphasized is the low level of dietary cholic acid content that precipitated these changes.

With respect to bile acid metabolism in the matching *Cyp7a1*$^{+/+}$ mice, their response to the intermediate level of cholic acid intake was more subtle. The relative mRNA level for CYP7A1 was only marginally lower ($P > 0.05$) in the cholic acid-fed *Cyp7a1*$^{+/+}$ mice (Fig. 3.6*A*), and there was also no consistent impact on the mRNA levels for CYP27A1 (Fig. 3.6*B*), CYP39A1 (Fig. 3.6*C*) or CYP7B1 (Fig. 3.6*D).* A suppression was nevertheless evident in the case of CYP7B1. Although mRNA measurements

were not made in the livers of any of the mice given the diet with 0.06 % (wt/wt) cholic acid, a more conspicuous change in the mRNA level for CYP7A1, and perhaps for other genes that regulate bile acid synthesis and handling might have been manifest at this level of supplementation because there were discernible changes in the size of the bile acid pool (Fig. 3.3*A*) and its composition (Fig. 3.3*B*). This possibility seems likely based on findings in other studies that when *Cyp7a1*$^{+/+}$ mice were fed diets containing significantly more cholic acid (0.10, 0.25 or 0.5 % wt/wt) there was a marked to complete suppression of expression of mRNA for CYP7A1 (Li-Hawkins et al., 2002; Schwarz et al., 1997; Wolters et al., 2002), and up to more than a 2-fold increase in the level of mRNA for SHP (Li-Hawkins et al., 2002). At a dietary cholic acid level of 0.5 % (wt/wt), the mRNA level for CYP7B1 was reduced by about 70% (Schwarz et al., 1997), and there was also a clear reduction in the mRNA level of the bile acid transporter, NCTP (Wolters et al., 2002).

The data in Fig. 3.6 *B, C* and *D* raise the general question of why the mRNA levels for CYP27A1, CYP39A1 and CYP7B1 were all consistently lower in the *Cyp7a1*$^{-/-}$ mice than in their matching *Cyp7a1*$^{+/+}$ controls, irrespective of whether they were given any cholic acid in their diet. This question cannot be answered from other measurements made in these mice, but what is clear from earlier studies done in cholesterol 7α-hydroxylase-deficient mice is that the amount of bile acid generated by the alternate pathways, while equal to about only a third of what is found when CYP7A1 is present, is sufficient to sustain the animals throughout life after the age of about three weeks (Erickson et al., 2003; Ishibashi et al., 1996; Schwarz et al., 1996; Schwarz et al., 2001). It is also known that the amount of bile acid made via these alternate pathways does not vary with gender and remains unchanged in the face of either a marked increase in dietary cholesterol intake or the disruption of the enterohepatic circulation of bile acids by feeding of cholestyramine (Schwarz et al., 2001). All of these various findings were based on the use of fecal bile acid excretion rates as a surrogate measure of the rate of bile acid synthesis in the intact animal. While this technique has been applied in many animal models and also in humans under a diverse set of experimental conditions (Grundy et al., 1971; Hahn et al., 1995; Mott et al., 1992; Turley et

al., 1997; Xie et al., 2000), its application to the measurement of bile acid synthesis rates in animals given even small levels of dietary bile acid supplementation is not valid because, with rare exception, there is no way to determine what fraction of the acidic sterols appearing in the stool come from new synthesis versus the diet. Given this caveat, a particular comment on what can be concluded from the fecal bile acid excretion rates in the present studies (Fig. 3.3*C*) is warranted. For both the *Cyp7a1*$^{+/+}$ and *Cyp7a1*$^{-/-}$ mice, the rate of fecal bile acid excretion increased significantly with almost every stepwise increment in the dietary cholic acid level starting at 0.015% (wt/wt). However, the magnitude of increase from one step to another was always higher in the *Cyp7a1*$^{-/-}$ mice than it was in their corresponding *Cyp7a1*$^{+/+}$ controls. One interpretation of this outcome is simply that with progressively greater degrees of inhibition of the cholesterol 7α-hydroxylase-mediated pathway paralleling cholic acid intake, the quantity of newly synthesized bile acid appearing in the stool of the *Cyp7a1*$^{+/+}$ mice fell proportionately but never to zero as it does in the *Cyp7a1*$^{-/-}$ mice.

The more important point to be taken from the data in Fig. 3.3*C* has to do with the practice of coprophagy by mice in general. In the early stages of maturity mice reingest at least 10% of their daily stool output (Brown and Donnelly, 2004). Clearly, the higher the level of dietary bile acid supplementation, the more bile acid will be taken in through consumption of stool, thus adding to the exogenous bile acid load that the small bowel and liver must deal with. Moreover, the species of bile acid in the stool may be quite variable and include the secondary bile acids deoxycholic and lithocholic acid (Erickson et al., 2003; Schwarz et al., 1996). Thus, when these points are considered together, the first major conclusion from these studies is that, depending partly on the genetic makeup of the animal, the feeding of exaggerated amounts of bile acid in the diet might well induce changes in one or more aspects of bile acid metabolism that do not represent a true physiological response.

The second major conclusion from this work has to do with the marked sensitivity of many parameters of cholesterol metabolism to changes in bile acid pool size and composition resulting from

dietary bile acid supplementation. The magnitudes of these changes are dictated largely by the extent to which cholesterol absorption and the amount of chylomicron-cholesterol delivered to the liver change as a consequence of shifts in bile acid pool size and composition. In the case of the *Cyp7a1*$^{+/+}$ mice, the only discernible change in cholesterol metabolism in response to the intermediate level of cholic acid supplementation was a trend toward a lower rate of hepatic cholesterol synthesis ($P > 0.05$) (Fig. 3.5*B* and 3.5*C*). Clearly, more decisive changes in this and other parameters of cholesterol metabolism might have been found in *Cyp7a1*$^{+/+}$ mice at twice the level of cholic acid supplementation (i.e., 0.06% wt/wt) because the subtle changes in bile acid pool size and composition seen at this dose (Fig. 3.3*A* and 3.3*B*) were accompanied by an increase in fractional cholesterol absorption from 56.5 ± 6.3 to 78.6 ± 3.0 % (Fig. 3.4*A*). Irrespective of whether this is the case, in the *Cyp7a1*$^{-/-}$ mice given cholic acid at the intermediate level there were striking changes in virtually every aspect of cholesterol metabolism measured. Normalization of bile acid pool size and the accompanying cholic acid enrichment of the pool (Fig. 3.3*A* and 3.3*B*) culminated in a major increase in hepatic cholesterol content, mainly in the esterified fraction (Fig. 3.4*D* and 3.5*A*). This outcome was likely due to the inability of the liver to convert cholesterol of intestinal origin to bile acids, not only because of the absence of cholesterol 7α-hydroxylase, but also because of the unresponsiveness of the alternate pathways of bile acid synthesis to an expanding intrahepatic pool of surplus cholesterol (Schwarz et al., 2001). In addition to esterifying much of this cholesterol, the liver exhibited the classic responses of completely repressing *de novo* synthesis (Fig. 3.5*B* and 3.5*C*) and accelerating cholesterol efflux via ABCG5/G8 (Fig. 3.6*L*). One unexpected finding was the impact that the intermediate dietary cholic acid level had on cholesterol metabolism in the small intestine of the *Cyp7a1*$^{-/-}$ mice. There was a modest but significant rise in the total cholesterol concentration (Fig. 3.4*C*), a marked inhibition of cholesterol synthesis (Fig. 3.5*E* and 3.5*F*), and an increase in the expression levels of mRNA for both ABCG8 and ABCA1 in the proximal region of the small intestine (Fig. 3.7*E* and 3.7*F*).

Taken together, the results from these studies point to the importance of using very low levels of bile acid in diets, especially when they are given to mouse models with genetic alterations in some aspect of their bile acid metabolism. Ideally, this level of bile acid supplementation should only be large enough to restore the pool size and activity of relevant metabolic pathways to physiological levels, and should not be so high as to induce pharmacological or, possibly, artifactual changes in a biological process of interest. The current studies illustrate how small the supplements should be in order to delineate with greater certainty the role that specific bile acid species might play in the pathogenesis and management of metabolic diseases such as obesity and type 2 diabetes (Kobayashi et al., 2007; Li et al., 2010; Watanabe et al., 2011; Zieve et al., 2007).

CHAPTER FOUR:

Carboxylesterases are uniquely expressed among tissues and regulated by nuclear hormone receptors in the mouse

Adapted from: Jones RD, Taylor AM, Tong EY, Repa JJ. Carboxylesterases are uniquely expressed among tissues and regulated by nuclear hormone receptors in the mouse. Drug Metab Dispos. 2013;41(1):40-9. PMCID: 3533427.

4.1 ABSTRACT

Carboxylesterases (CES) are a well recognized, yet incompletely characterized family of proteins that catalyze neutral lipid hydrolysis. Some CES have well-defined roles in xenobiotic clearance, pharmacologic pro-drug activation, and narcotic detoxification. In addition, emerging evidence suggests other CES may have roles in lipid metabolism. Humans have six *CES* genes, while mice have 20 *Ces* genes grouped into five isoenzyme classes. Perhaps due to the high sequence similarity shared by the mouse *Ces* genes, the tissue-specific distribution of expression for these enzymes has not been fully addressed. Therefore, we performed studies to provide a comprehensive tissue distribution analysis of mouse *Ces* mRNAs. These data demonstrated that while the mouse *Ces* family 1 is highly expressed in liver and family 2 in intestine, many *Ces* genes have a wide and unique tissue distribution defined by relative mRNA levels. Furthermore, evaluating *Ces* gene expression in response to pharmacologic activation of lipid and xenobiotic-sensing nuclear hormone receptors (NHR) showed differential regulation. Finally, specific shifts in *Ces* gene expression were seen in peritoneal macrophages following LPS treatment and in a steatotic liver model induced by high-fat feeding, two model systems relevant to disease. Overall these data show that each mouse *Ces* gene has its own distinctive tissue expression pattern and suggest that some CES may have tissue-specific roles in lipid metabolism and xenobiotic clearance.

4.2 INTRODUCTION

Carboxylesterases (CES) comprise a family of proteins that catalyze neutral lipid hydrolysis (Holmes and Cox, 2011; Hosokawa et al., 2007; Williams et al., 2010). Substrate specificity among CES is often broad, overlapping, or yet to be identified leading to difficulty in performing comprehensive functional assays (Staudinger et al., 2010). Still, certain CES have long been recognized to play important roles in the biotransformation of ester- and amide-containing compounds to affect the detoxification and/or activation of a variety of xenobiotics, narcotics, and pharmacologic agents in liver and intestine (Satoh and Hosokawa, 1998; Satoh and Hosokawa, 2006). In addition, growing evidence suggests that some CES enzymes may contribute to aspects of lipid metabolism through triglyceride, cholesteryl ester, or retinyl ester hydrolysis (Ghosh, 2012; Parathath et al., 2011; Quiroga and Lehner, 2011b; Schreiber et al., 2009).

The CES family has been organized into five isoenzyme classes based on sequence similarity and gene structure (Holmes and Cox, 2011; Holmes et al., 2010b; Hosokawa et al., 2007; Williams et al., 2010). The six human *CES* genes, including one pseudogene, reside on chromosome 16; and the 20 mouse *Ces* genes, also including one pseudogene, are located on chromosome 8. The large number of *Ces* genes in rodents is believed to have arisen by tandem duplication. Thus, the sequence similarities of mouse *Ces* mRNA species and protein products are quite high, particularly within an isoenzyme class, which complicates the selective detection of *Ces* members *in vivo*.

With the recent description of a standardized nomenclature for mammalian carboxylesterases (Holmes et al., 2010b) and the advent of technologies that allow for quantitative and specific detection of closely related mRNA species (Valasek and Repa, 2005), we undertook a comprehensive survey of *Ces* mRNA expression in the mouse. Our goals were to: firstly, determine the tissue distribution of mouse *Ces* mRNAs to identify organs beyond liver and intestine that express various *Ces* family members; secondly, evaluate the regulation of *Ces* gene expression by various nuclear hormone receptors (NHR) that serve as lipid and xenobiotic-sensing transcription factors, as well as pharmacologic targets (Chawla

et al., 2001); and finally, to interrogate *Ces* expression in cell and organ systems relevant to disease, the macrophage and the steatotic liver. This *Ces* expression survey reveals novel tissues and regulation of family members, suggesting potential role(s) for these enzymes in lipid metabolism, xenobiotic clearance in extrahepatic tissues, as well as in the pharmacologic response to NHR activation by synthetic ligands.

4.3 MATERIALS AND METHODS

Materials

The liver X receptor (LXR) agonist, T0901317 (T1317, (Repa et al., 2000b)), was purchased from Cayman Chemical (Ann Arbor, MI); pregnane X receptor (PXR) agonist, pregnenolone-16α-carbonitrile (PCN, (Jones et al., 2000)) and the constitutive androstane receptor (CAR) agonist, 1,4-Bis-[2-(3,5-dichloro-pyridyloxy)]benzene, 3,3',5,5'-Tetrachloro-1,4-bis(pyridyloxy)benzyne (TCPOBOP, (Tzameli et al., 2000)), were obtained from Sigma-Aldrich Chemical (St. Louis, MO). Ligands for the peroxisome proliferator-activated receptors (PPARα-GW7647, (Brown P. J. et al., 2001); PPARβ-GW0742, (Sznaidman et al., 2003) ; and PPARγ-GW7845, (Henke et al., 1998)) and FXR (GW4064, (Maloney et al., 2000)) were provided by Timothy M. Willson (Glaxo SmithKline), and the retinoid X receptor (RXR) agonist LG268 (Mukherjee et al., 1997) from Richard A. Heyman (Aragon Pharmaceuticals).

Animals and treatments

Mice were housed in a temperature-controlled environment with 12h light/dark cycles (light: 06:00-18:00) and allowed free access to water and a cereal-based rodent diet (#7001; Teklad Diets, Madison, WI). For establishing the tissue distribution of *Ces* mRNAs, three male C57Bl/6 mice were euthanized (at 10:00, 4h after lights on) by xsanguinations under deep anesthesia, and tissues were harvested. For evaluating NHR regulation of *Ces* gene expression, male A129/SvJ mice received ligands by oral gavage, as this strain of mice has been previously used for similar studies where drug doses were established (Cha and Repa, 2007). Agonists were suspended in 1% w/v methylcellulose and 1% v/v Tween-80 (vehicle) to deliver the following quantities of ligand in each dose using 10 µl/g body weight: LG268, 30 mg/kg body weight (mpk); GW7647, 10 mpk; GW0742, 10 mpk; GW7845, 20 mpk; T1317, 30 mpk; GW4064, 100 mpk; PCN, 50 mpk, and TCPOBOP, 3 mpk. For gavage-dosing, treatments were administered at the beginning of the dark cycle (at 18:00) and again 12h later at the beginning of the light cycle (at 06:00), at which point food was removed. After 4h (at 10:00), mice were euthanized, and tissues harvested. For the high-fat diet study, male C57BL/6 mice were fed either high-fat diet containing 58

kcal% fat provided by soybean and coconut oils (#D12331; Research Diets, New Brunswick, NJ), or a cereal-based rodent diet (#7001, Teklad) for 16 weeks before livers were harvested at 10:00.

All animal experiments were approved by the Institutional Animal Care and Use Committee of the University of Texas Southwestern Medical Center in accordance with the Guide for the Care and Use of Laboratory Animals as adopted and promulgated by the National Institutes of Health.

Cell culture

All cells were cultured in a 37°C humidified incubator with 5% CO_2.

Cell lines: The adenoma-derived glucagonoma cell line αTC1-clone 9 ([CRL-2350], (Powers et al., 1990)) was obtained from American Type Culture Collection (Manassas, VA). The insulin-secreting MIN6 cell line, passage #24 (Miyazaki et al., 1990) was kindly provided by Melanie Cobb (UT Southwestern). αTC1 cells were cultured in DMEM with 4 mM L-glutamine adjusted to contain 1.5 g/L sodium bicarbonate and 3 g/L glucose with 10% heat-inactivated dialyzed FBS, further supplemented with 15 mM HEPES, 0.1 mM non-essential amino acids and 0.02% BSA. MIN6 cells were maintained in DMEM (4.5g/L glucose) with 2 mM L-glutamine, 1 mM sodium pyruvate and 10% heat-inactivated FBS.

Islets: Mouse pancreatic islets were prepared as previously described (Chuang et al., 2008). Briefly, the pancreata from three C57Bl/6 male mice were perfused and digested with liberase R1 (Roche, Indianapolis, IN). Islets were then isolated using Ficoll gradient centrifugation and hand-selection under a stereomicroscope for transfer to RPMI 1640 medium (11.1 mM glucose) supplemented with 10% (v/v) heat-inactivated FBS, 100 IU/ml penicillin, and 100 µg/ml streptomycin. Islets were allowed to recover overnight before RNA was isolated.

Macrophages: Male A129/SvJ mice received an intraperitoneal injection of 1 ml 3%-thioglycollate (autoclaved and aged for 3 months) to elicit macrophages. Three days later, mice were euthanized and macrophages were withdrawn by sterile lavage using ice-cold saline. Cells were collected by gentle centrifugation and plated at $1x10^5$ cells/cm^2 in high-glucose DMEM containing 10% heat-inactivated FBS

and 100 IU/ml penicillin/100 µg/ml streptomycin. After 6h, cells were washed with sterile PBS and provided fresh media containing saline (vehicle, 0.1% v/v) or 100 ng/ml lipopolysaccharide (LPS, Sigma). Cells were harvested 4h later for RNA isolation.

Preparation of samples for RNA measurements

Mice were anesthetized and exsanguinated via the inferior vena cava. Small intestines were removed, flushed with ice-cold saline, and cut into three sections of equal length which we denote as duodenum, jejunum, and ileum. The sections were slit lengthwise, and the mucosae were obtained by gentle scraping. Intestinal mucosa, liver, adrenal glands, brain, epididymal white adipose tissue, intrascapular brown adipose tissue, kidneys, lung, skeletal muscle (quadriceps), and spleen samples were flash-frozen in liquid nitrogen and stored at -80°C. Total RNA was isolated from tissue samples, cultured cells, and islets using RNA STAT-60 (Tel-Test, Inc., Friendswood, TX) as previously described (Kurrasch D. M. et al., 2004b). RNA concentration was determined by absorbance at 260 nm, and RNA quality by the 260/280 ratio.

Quantitative real-time PCR

Quantitative real-time PCR (qPCR) was performed using an Applied Biosystems 7900HT sequence detection system as described (Kurrasch D. M. et al., 2004b; Valasek and Repa, 2005). Briefly, total RNA was treated with Dnase I (Rnase-free; Roche Molecular Biochemicals) and reverse-transcribed with random hexamers using SuperScript II (Invitrogen) to generate cDNA. Primers for each gene were designed using a variety of primer design algorithms: Dlux (Invitrogen, https://orf.invitrogen.com/lux/); PrimerBlast (NCBI, http://www.ncbi.nlm.nih.gov/ tools/primer-blast) and Integrated DNA Technology (http://www.idtdna.com/scitools/ applications/RealTimePCR/default.aspx) to ensure that for each target: primers spanned an intron; primers did not anneal to unanticipated off-site cDNA or genomic sequences, and primers exhibited maximal 3' mismatch for closely related CES family members to achieve target specificity. All primer pairs were validated by: analysis of template titration (acceptable primers

exhibited slopes of -3.3 ± 0.1 for plot of C_q vs log[cDNA, ng], (Bustin et al., 2009)); appearance of a single peak upon a graded temperature dissociation analysis; and the absence of PCR product upon omission of template cDNA. Of note, no discernible PCR product was generated using three different primer sets designed for *Ces1b*, using template cDNA from liver, intestine, kidney, and a universal RNA mixture. It is likely that *Ces1b* mRNA is expressed at levels too low to detect by qPCR or expressed in minor cell or tissue types. Finally, while multiple transcript isoforms, generated by alternative promoter usage and/or alternative splicing of exons, have been described for human *CES* genes, this is not yet the case for mouse *Ces* genes, thus our qPCR primer designs are consistent with the current GenBank reference sources, and all primer sequences and gene annotations are provided in Supplemental Table 1.

Each qRT-PCR was analyzed in duplicate and contained in a final volume of 10 µl: 25 ng of cDNA, each primer at 150 nM, and 5 µl of 2x SYBR Green PCR Master Mix (Applied Biosystems). Results were evaluated by the comparative cycle number at threshold method (Schmittgen and Livak, 2008) using cyclophilin as the invariant reference gene (Dheda et al., 2004; Kosir et al., 2010).

Analysis of data

Data are reported as means ± SEM for the number of animals per tissue and/or treatment group, as specified in each figure legend. GraphPad Prism 5 software (GraphPad Software, Inc., San Diego, CA) was used to perform all statistical analyses. For the multi-agonist study, statistical differences were determined by one-way ANOVA with Dunnett's *post hoc* analysis, which compares each treatment group to the vehicle-treated control group (significantly different groups denoted by an asterisk *, $p<0.05$; **, $p<0.01$; ***, $p<0.001$). A Student's *t*-test was used for comparison of only 2 groups.

4.4 RESULTS

The CES1 family is highly expressed in liver and the CES2 family in intestine, but these and other CES members are present in a wide variety of tissues and cells in the mouse.

Numerous reports have appeared describing the distribution, regulation and function of various carboxylesterases in the mouse model (Holmes et al., 2010a; Holmes et al., 2009; Poole et al., 2001; Staudinger et al., 2010; Xu et al., 2009; Zhang Y. et al., 2012). However, with the confusion regarding nomenclature and ortholog assignment, and the nonselectivity of some oligonucleotide and antibody probes, the reliability of these findings has been uncertain. With the standardization of *Ces* nomenclature (Holmes et al., 2010b) and the target specificity available using quantitative real-time PCR (qPCR), we have now performed a comprehensive survey of *Ces* expression in the mouse. The utility of our qPCR method is readily apparent by the distinct expression patterns of *Ces* mRNAs, thus confirming the specificity of primers. In addition, the rank order of *Ces* mRNA levels in liver tissue observed in our studies is consistent with recently published findings for 11 *Ces* members using a branched-DNA signal amplification assay (Zhang Y. et al., 2012). Hence our qPCR method provides a reliable means to determine steady-state levels of *Ces* mRNA in the mouse.

The mouse *Ces1* family consists of eight genes *Ces1a*-*Ces1h* (Fig. 4.1) located in tandem on chromosome 8 (between coordinates 95,544,116 – 95,903,624). Each mouse *Ces1* gene contains 13-14 exons and encodes a protein with a predicted mass of 62 kDa. The *Ces1* family has been reported to be expressed predominantly in liver (reviewed in (Holmes et al., 2010b)), and indeed all detected *Ces1* members were present in liver; however, we noted four important points. Firstly, there was no detectable expression of *Ces1b* mRNA in any tissue tested, including liver, despite our efforts to identify primer sets and tissues that would yield a qPCR product by this method. Secondly, *Ces1d* mRNA was detectable in liver, but was far more abundant in brown (BAT, denoted as "X" in Fig. 4.1) and white adipose tissue (WAT, W in Fig. 4.1). Thirdly, *Ces1f* mRNA levels were greatest in kidney, a tissue that expressed high

levels of many *Ces* members. Finally, while the highest mRNA levels for *Ces1h* are found in mouse lung, it should be noted that the quantification cycle (C_q, (Bustin et al., 2009)) observed for this PCR product is nearly at the limit of detection. Thereby this mRNA species is found only at very low levels in all mouse tissues in which it was expressed. Thus, in line with previous studies describing the *Ces1* family members as the hepatic carboxylesterases, four of the seven detectable mRNAs (*Ces1a, Ces1c, Ces1e, and Ces1g*) were most highly expressed in liver compared to 15 other mouse tissues and cell types.

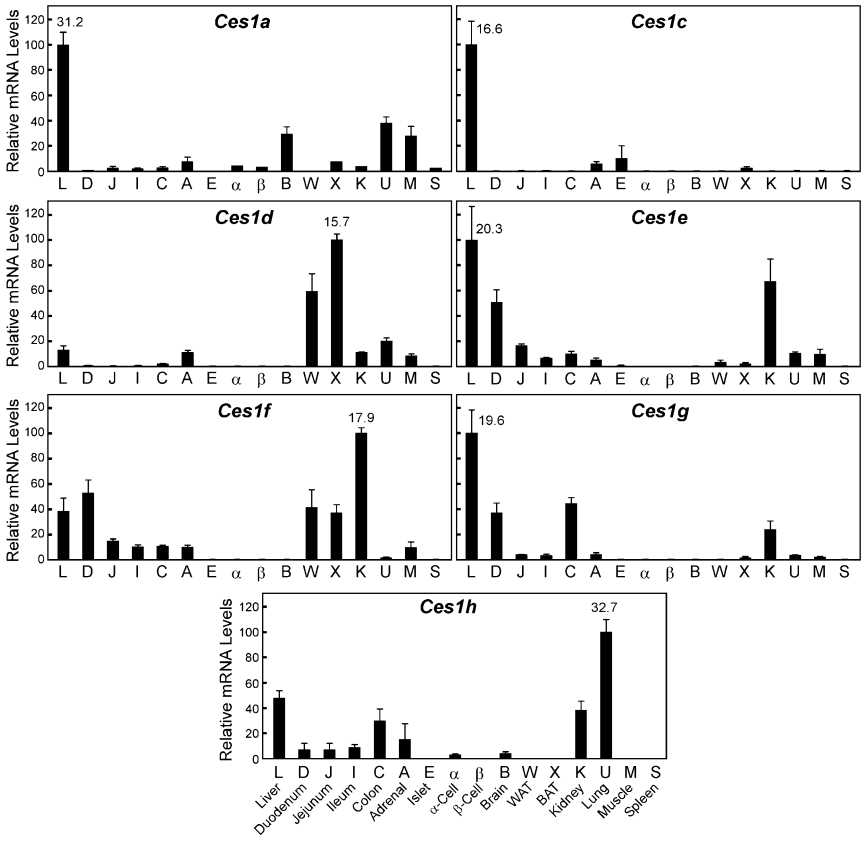

Figure 4.1. *Tissue Distribution of the Carboxylesterases: Family 1.* The relative mRNA levels are depicted for mouse liver (L), duodenum (D), jejunum (J), ileum (I), colon (C), adrenal (A), islet (E),α-cell line (αTC1, α), and β-cell line (MIN6, β), brain (B), epididymal white adipose tissue (WAT, W), intrascapular brown adipose tissue (BAT, X), kidney (K), lung (U), muscle (M), and spleen (S). Tissues were obtained from adult (3-5 months of age) C57Bl/6 mice that were fed *ad libitum* a standard low-fat rodent diet. Individual mRNA values were calculated relative to cyclophilin and the mean values were arithmetically adjusted to depict the highest-expressing tissue as a unit of 100. Values represent the means ± SEM of three independent samples for each tissue or cell line. Note, that as these data are portrayed, comparisons can only be made between the different tissues for a single *Ces* mRNA family member, not between the various *Ces* mRNA species (see Fig. 4 for this comparison). The average cycle-at-threshold (C_q) value used for quantification is provided for the tissue showing the most abundant mRNA level for each *Ces*.

The mouse *Ces2* family contains eight members (*Ces2a*-*Ces2h*) with one, *Ces2d*, identified as a pseudogene (excluded in our survey). In line with previous studies which have shown that family 2 encodes the intestinal carboxylesterases (reviewed in (Holmes et al., 2010b)), almost all the *Ces2* members were most highly expressed in segments of the small intestine (Fig. 4.2). The only exception was *Ces2h*, which exhibited the highest mRNA levels in kidney, followed closely by the small intestine. For all *Ces2* members, there was a cephalocaudal distribution of mRNA with highest levels in the

proximal third (duodenum) of the small intestine, and decreasing amounts throughout the rest of the small bowel and into the colon. Of note, although *Ces2* mRNA levels are highest in the intestine, there is also relatively high expression in other organs including liver (*Ces2a, 2e*), kidney (*Ces2c*), and spleen (*Ces2g*). *Ces2f* mRNA levels were extremely low in all tissues tested.

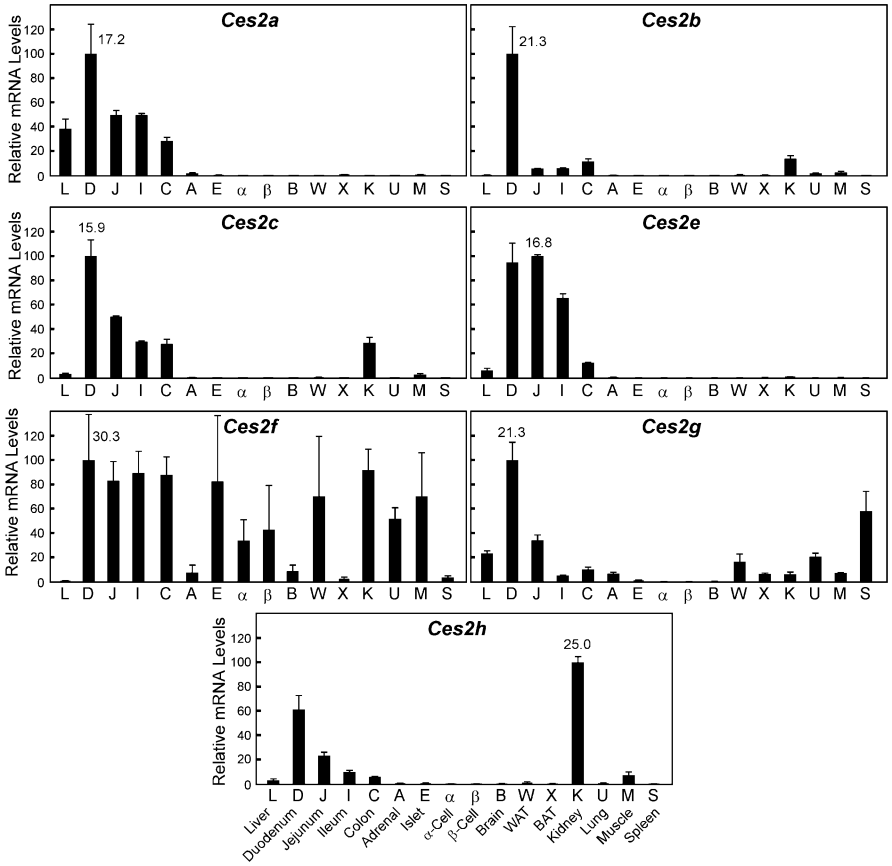

Figure 4.2. *Tissue Distribution of the Carboxylesterases: Family 2.* Refer to the legend of Fig.4.1 for details.

The mouse *Ces3* family includes two genes, *Ces3a* and *Ces3b,* which are almost exclusively expressed in liver (Fig. 4.3). **Families 4 and 5** have only one member each, *Ces4a* and *Ces5a*. *Ces4a* mRNA levels are highest in liver, and *Ces5a* expression is evident in WAT, brain, and the glucagonoma alpha-cell line (αTC1).

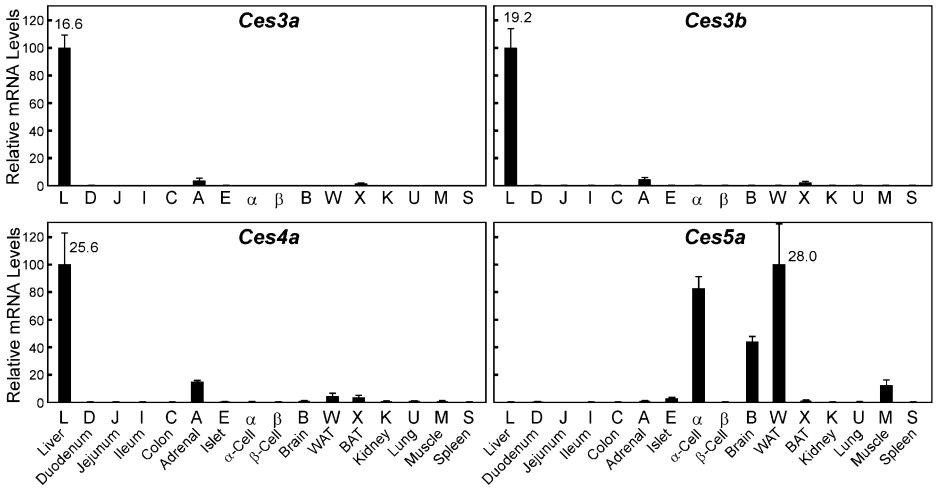

Figure 4.3. *Tissue Distribution of the Carboxylesterases: Families 3, 4 and 5.* Refer to the legend of Fig.4.1 for details.

The rank order of *Ces* mRNA levels within tissues reveals that members outside of family 1 are likely to play an important role in liver, and kidney and brain exhibit unique expression patterns of *Ces* mRNA species.

Our experimental strategy allowed for a rank order determination of mRNA levels for *Ces* members within a given tissue (Fig. 4.4). The PCR primers were designed to provide equivalent PCR amplification efficiency for all *Ces* targets and showed no product formation in the absence of template cDNA. Therefore, as the same samples were used for all *Ces* mRNA analyses, we could compare the relative expression of all 18 *Ces* members to one another in a given tissue or cell type. Viewing the data in this rank order format for liver reveals that in addition to the "liver" CES1 family of enzymes, CES2A, CES3A, and CES3B proteins may play some role in hepatic lipid metabolism and/or xenobiotic response. The "intestine" *Ces2* family are by far the most abundant *Ces* members expressed in the duodenum (*Ces2c* >> *Ces2a*=*Ces2e*). In lung, *Ces1d* mRNA levels are so abundant (C_q=17.2) that other *Ces* members (*Ces1e*, *1f*, and *2g*), which exhibit significant (C_q <24) expression, and *Ces1h*, which is found nearly exclusively in this tissue, are barely evident. The kidney and brain express a unique complement of "liver" *Ces1* (*Ces1d* and *1f*) and "intestine" *Ces*2 (*Ces2c*) mRNA species, and brain is the only tissue

among those we examined that exhibits appreciable relative levels of *Ces5a* mRNA, which encodes a secreted carboxylesterase member also known as cauxin, previously identified in urine and epididymal fluid (Holmes et al., 2008). For all other mouse tissues tested, except cells of the endocrine pancreas which do not appear to abundantly express any carboxylesterase mRNA, the rank order data resemble those of lung and white adipose tissue, with other CES members dwarfed by *Ces1d* expression (data not shown).

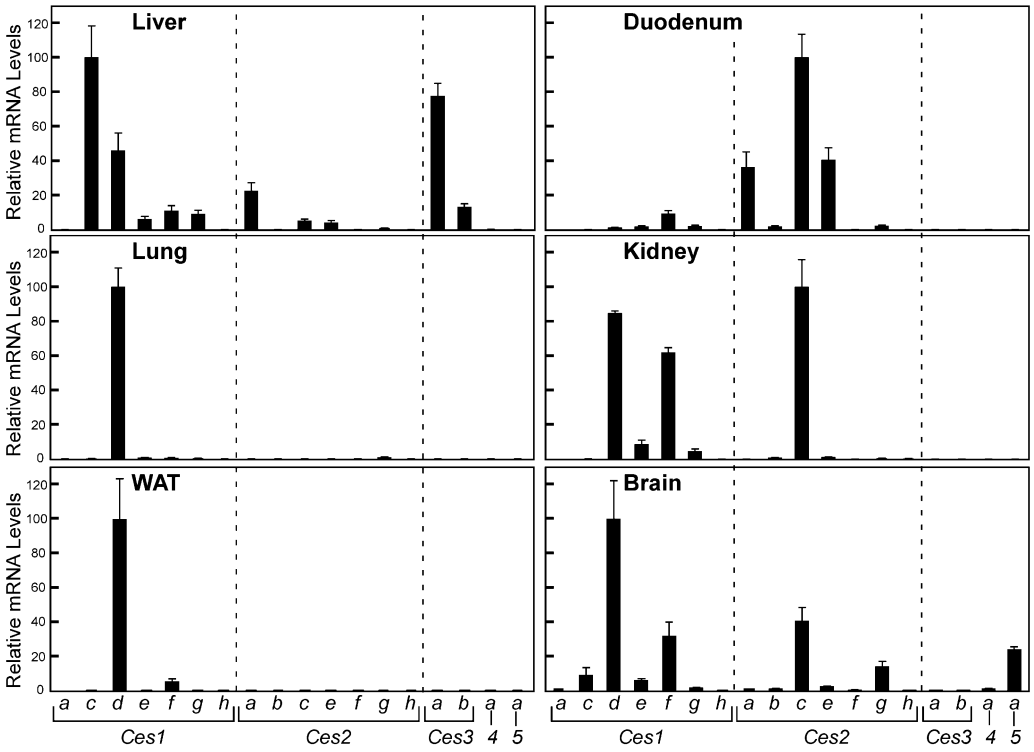

Figure 4.4. *Comparative Expression Levels of mRNA for Carboxylesterases of Liver, Duodenum, Kidney and Lung.* The relative mRNA levels of all *Ces* family members are provided for each tissue. Individual values were calculated relative to cyclophilin and the means were arithmetically adjusted to depict the highest-expressed *Ces* mRNA species for each tissue as a unit of 100. Values represent the means ± SEM of three independent samples for each tissue.

Short-term administration of synthetic agonists for nuclear hormone receptors results in differential expression of *Ces* family members.

A subset of the NHR superfamily of ligand-activated transcription factors has been characterized as lipid or xenobiotic sensors (Chawla et al., 2001). For these NHRs (LXRs, FXR, PPARs, PXR and CAR), ligand-activation induces the expression of genes encoding transporters, enzymes and binding proteins to modulate the intracellular levels for a receptor's respective ligand. To test whether *Ces* mRNA expression is subject to this regulation, and perhaps reveal novel lipid metabolic pathway(s) affected by *Ces* gene products, we evaluated *Ces* expression in a variety of tissues from mice treated with NHR agonists. Potent synthetic agonists which have been developed for pharmacologic activation of specific NHRs were administered to mice by oral gavage twice, 16h and 4h prior to harvesting tissues, to allow sufficient time for direct gene activation or repression by NHRs. The efficacy of this dosing regimen was confirmed by the measurement of known hepatic target genes for these NHRs (Fig. 4.5A). Cholesterol 7α-hydroxylase (*Cyp7a1*) mRNA levels were increased 9.7-fold by an LXR agonist and decreased by ligands for RXR (to 1%), FXR (to 7%), and PXR (to 22%), changes consistent with previous reports (Repa et al., 2000b). The PPAR target gene, cytochrome P450 4A14 (*Cyp4a14*, (Patsouris et al., 2006)) exhibited greater hepatic mRNA levels in mice treated with a PPARα agonist (GW7647, 34-fold), a PPARβ ligand (GW0742, 10.5-fold) and an RXR drug (LG268, 11.3-fold). Finally, administration of ligands for the xenobiotic receptors, PXR and CAR, resulted in enhanced expression of the drug-metabolizing enzyme, cytochrome P450 3A11 (5.2-fold for PXR, 2.7-fold for CAR). Thus, this relatively short-term (16h) dosing method delivered sufficient NHR agonists to affect gene transcription.

In liver, we observed numerous changes in *Ces* mRNA levels following administration of NHR ligands to mice (Fig. 5B). PPARα activation resulted in increased expression of *Ces1d* (5.2-fold), *Ces1e* (4.7-fold), *Ces1f* (3.4-fold), *Ces2c* (3.3-fold), and *Ces2e* (1.7-fold). PPARβ activation significantly increased the expression of *Ces1e* (2.3-fold), and *Ces2e* (1.7-fold). Administration of agonists for LXR, PXR, and CAR all resulted in increased hepatic mRNA levels of *Ces2a* (3-, 7.6- and 4.8-fold

respectively), while PXR activation significantly decreased expression of *Ces3a* (to 76%). *Ces2c* was the most responsive hepatic carboxylesterase to NHR activation, as its expression was increased by agonists for RXR (4.8-fold), PPARα (3.3-fold), LXR (2.4-fold), and CAR (2.9-fold). *Ces4a* expression was significantly increased upon RXR (3.1-fold) activation alone. Of note, the hepatic expression of *Ces1d*, *Ces1e*, and *Ces1f* due to NHR activation had very similar patterns (Fig. 4.5B), even though they have unique tissue distribution profiles (Fig. 4.1). In mucosa obtained from the proximal third of the small intestine (duodenum), the mRNA levels of two *Ces* members were altered by NHR activation (Fig. 4.5C). Duodenal *Ces2a* mRNA levels were increased by agonists for LXR (2.4-fold), FXR (4.3-fold), PXR (7.1-fold), and CAR (2.1-fold); whereas *Ces2c* was significantly upregulated by only PXR activation (1.6-fold). Finally, in the lung, *Ces* mRNA levels were largely unaffected by NHR ligand treatment, with only a modest, but significant, increase observed for *Ces1e* mRNA levels. It is of interest that certain genes such as *Ces2c* and *Ces1d* respond differently to NHR activation in different organs, suggesting there is tissue-specific regulation of these carboxylesterases.

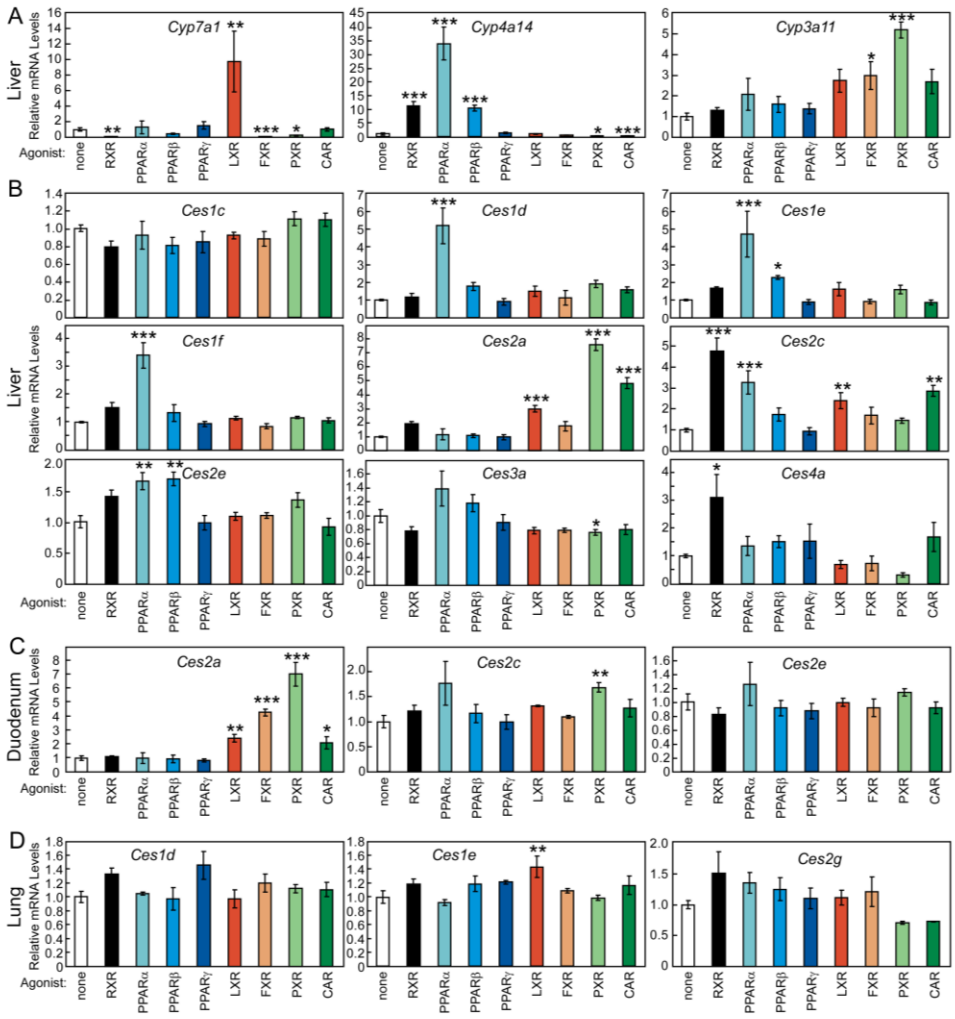

Figure 4.5. *Regulation of Carboxylesterase mRNA Levels by Nuclear Hormone Receptor Agonists.* Relative mRNA levels are depicted for adult (3-5 months of age) A129/SvJ mouse liver, duodenum and lung. Tissues were harvested from mice that had received two doses of nuclear receptor agonist by oral gavage (16h and 4h before tissue collection). Each dose provided agonist of a given nuclear hormone receptor as follows: Vehicle (1% w/v methylcellulose, 1% v/v tween-80), 30 mg/kg body weight, "mpk" LG268 (RXR), 10 mpk GW7647 (PPARα), 10 mpk GW0742 (PPARβ), 20 mpk GW7845 (PPARγ), 30 mpk T1317 (LXR), 100 mpk GW4064 (FXR), 50 mpk PCN (PXR), and 3 mpk TCPOBOP (CAR). Individual values were calculated relative to cyclophilin and the mean values were arithmetically adjusted to depict the vehicle-treated group at a unit of 1. **A.** Changes in the hepatic expression of selected cytochrome P450 enzymes confirm the efficacy of this dosing regimen. *Ces* mRNA levels are shown for liver (**B**), duodenum (**C**), and lung (**D**). Values reflect the means ± SEM (n=4). *, $P < 0.05$; **, *P<0.01;* ***, *P<0.001* compared with the vehicle-treated group (white bar), as determined by one-way ANOVA with Dunnett's post-hoc comparison.

Differential expression of *Ces* in LPS-activated macrophages and in steatotic livers of high-fat fed mice.

We extended this *Ces* expression survey to cells and tissues associated with disease: the activated macrophage (atherosclerosis and inflammatory disease) and the steatotic liver (insulin resistance and the metabolic syndrome). As these disease-associated conditions have also been the subject of transcriptomic and lipidomic analyses (Barish et al., 2005; Dennis et al., 2010; Fu S. et al., 2011; Joseph et al., 2003; Welch et al., 2003), the concomitant regulation of *Ces* members may reveal pathways of lipid metabolism affected by these enzymes.

A carboxylesterase cloned from human monocytes (*CES1*) has been characterized and found to promote cholesteryl ester hydrolysis when overexpressed in macrophages or mice (Ghosh, 2000; Ghosh, 2012; Zhao et al., 2007). However, a functional ortholog of this enzyme in the mouse macrophage has not yet been identified (reviewed in (Quiroga and Lehner, 2011b)). More recently, human *CES3* has also been implicated in cholesteryl ester hydrolysis in macrophages (Zhao et al., 2012), and the expression of this CES member appears to be dependent on the abundance of CES1. Again, however, it is unclear which mouse *Ces* member may impart this CES3 function in macrophages. Thus we evaluated the expression of all mouse *Ces* mRNAs in primary mouse macrophages (Fig. 4.6A). Thioglycollate-elicited peritoneal macrophages were harvested from mice and then treated in culture for 4h with either vehicle (saline) or lipopolysaccharide (LPS) to activate an inflammatory response as demonstrated by an increase in mRNA levels for the cytokines, interleukin 1β (*Il1β*) and tumor necrosis factor (*Tnf*) (Fig. 4.6A inset). *Ces1c*, *Ces2f*, and *Ces2g* were the most abundant carboxylesterase mRNA species in unstimulated mouse macrophages. After LPS treatment, a significant decrease in the expression of *Ces1c* and a nearly significant decline in *Ces2f* mRNA levels (p=0.06) occurred, making *Ces2g* the most plentiful carboxylesterase in the activated macrophage. It should be noted that the mRNA level for the most abundant macrophage carboxylesterase, *Ces1c* (qPCR C_q=28.8) represents less than 1% of the mRNA level for *Ces1c* observed in liver (qPCR C_q= 16.6), which suggests a low abundance of these enzymes in

the mouse macrophage. Future studies will be required to ascertain the functional contribution of mouse *Ces* members to macrophage lipid biology, in analogy to the reports regarding the roles of *CES1* and *CES3* in human macrophage cholesterol homeostasis (Ghosh, 2000; Ghosh, 2011; Zhao et al., 2012; Zhao et al., 2007).

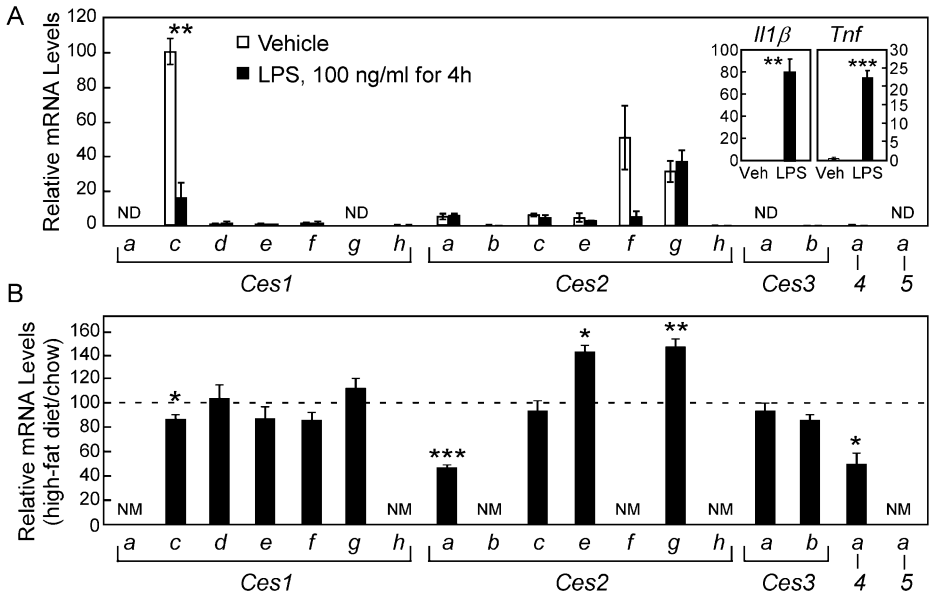

Figure 4.6. *Comparative Expression of Carboxylesterases in Thioglycollate-elicited Mouse Peritoneal Macrophages and in the Livers of High Fat Diet Fed Mice.* **A.** The relative mRNA levels of *Ces* are depicted for thioglycollate-elicited mouse macrophages, treated in culture for 4h with saline (vehicle, 0.1% v/v, white bars) or 100 ng/ml LPS (black bars). Increased expression of *Il1β* and *Tnf* mRNA demonstrate efficacy of LPS administration (inset). Results depict the mean ± SEM for three wells per treatment. All values were mathematically adjusted relative to the most abundant value (*Ces1c*, vehicle) set at 100%, so all bars in this graph can be compared. * $P < 0.05$, significant effect of LPS treatment by Student's *t*-test. **B.** Hepatic levels of *Ces* mRNA in mice fed for 16 weeks a high-fat diet relative to mice fed a low-fat control diet, which is represented by the hatched line, set at 100%. Expressed in this manner, comparisons cannot be made between CES members in this panel. Results depict the mean ± SEM for n=6 mice per dietary group, * $P < 0.05$; **, $P<0.01$; ***, $P<0.001$ significant effect of high-fat feeding as determined by Student's *t*-test. ND, not detected. NM, not measured.

Finally, to complement our survey of *Ces* gene regulation by lipid-sensing transcription factors, we elected to evaluate *Ces* mRNA levels in a steatotic liver model induced by feeding a high-fat diet. Male C57Bl/6 mice were fed *ad libitum* a diet containing 58 kcal% fat (soybean and coconut oils) for 16 weeks. Compared to mice fed a standard chow diet, the mice fed high-fat had greater body weight (1.67-fold), increased liver weight (1.31-fold), and impaired glucose tolerance (increased fasting glucose, and more profound glucose excursion following an oral glucose challenge) (data not shown). The "liver" *Ces1*

family showed very little change in mRNA levels, except the most abundant member, *Ces1c* (see Fig. 4.4), for which mRNA levels were reduced about 20% by high-fat feeding. The steatotic livers of these high-fat fed mice also exhibited increased *Ces2e* and *Ces2g* mRNA, while *Ces2a* and *Ces4a* mRNA levels were decreased.

4.5 DISCUSSION

To our knowledge this is the first comprehensive analysis of *Ces* expression in the mouse. This project was largely instigated by the recent report recommending a standardized nomenclature for *Ces* genes (Holmes et al., 2010b), and the fact that these genes repeatedly appear in microarray data, where it is often unclear which *Ces* member(s) is represented. We elected to perform this survey in mice, as these are widely used subjects in lipid and xenobiotic research, for which a large collection of genetic, dietary, and drug-induced models of lipid-related disease are available. In addition, the mouse has 20 *Ces* genes, the largest number of any mammalian species reported to date (Williams et al., 2010), thus making the selectivity and sensitivity of our qPCR method especially appropriate.

The first important and quite surprising finding was that these 20 *Ces* members exhibit very distinct expression patterns. It is thought that the 20 mouse *Ces* genes arose through tandem duplication, and indeed, they share remarkable sequence similarity and gene structure. They even reside in a cluster on mouse chromosome 8, which would suggest that they might share enhancer elements and regulatory sequences to dictate their expression levels, as seen for hepatic *Ces1d*, *Ces1e*, and *Ces1f* due to NHR activation (Fig. 4.5). However, while there are some general patterns (*Ces1*s enriched in liver, *Ces2*s abundant in intestine), each *Ces* member is expressed in a unique set of tissues (Figs. 4.1-4.4), and many show selective changes in gene expression by drug (Fig. 4.5, Fig. 4.6A) or diet (Fig. 4.6B) treatment. These data provide valuable insight regarding potential xenobiotic activity of CES in organs other than the intestine and liver. While major questions still remain about these enzymes including the identification of substrates, which remains difficult, and the localization of activity, this report will inform future studies.

The second finding is that the mRNA levels of several *Ces* members are regulated by the lipid-sensing nuclear hormone receptors. The role of carboxylesterases in drug metabolism has been widely appreciated, and previous work from the Klasseen and Staudinger groups has convincingly shown that the xenobiotic nuclear hormone receptors PXR and CAR increase expression of *Ces2a* (previously *Ces6*) and

Ces2c (Staudinger et al., 2010; Xu et al., 2009; Zhang Y. et al., 2012). Our work confirms these findings (Fig. 4.5) and extends these analyses to reveal that NHRs traditionally associated with fatty acid and/or sterol regulation can likewise regulate the expression of *Ces* mRNAs:

Bile acids/FXR. A previous report suggested that modifying bile acid homeostasis in mice by depletion using cholestyramine or supplementation with sodium cholate increased hepatic levels of *Ces1g* mRNA (previously called ES-x, (Ellinghaus et al., 1998)). Our specific, synthetic agonist, GW4064, for the bile acid nuclear receptor, FXR, did not recapitulate these findings in liver, nor were changes in *Ces1g* mRNA observed in mouse intestine (data not shown), suggesting that alternate bile acid-responsive, non-FXR mechanisms may be responsible for differential *Ces1g* expression.

Fatty acids & fibrates/PPARs. Early studies in mice and rats demonstrated that certain drugs that enhanced hepatic peroxisome proliferation also caused an increase in microsomal carboxylesterase activity (Ashour et al., 1987; Hosokawa and Satoh, 1993; Mentlein et al., 1986; Parker et al., 1996). In particular, treating rodents with the PPARα ligands clofibrate, WY14,653, or perfluorinated fatty acids resulted in increased CES enzyme activity of 5-6 subclasses defined by substrate specificity. Most recently two reports have demonstrated that fibrate treatment of C57/Bl6 mice for 5 days to 2 weeks does not upregulate hepatic *Ces1d* mRNA levels (Dolinsky et al., 2003; Zhang Y. et al., 2012). These recent findings differ from our results showing that administration of the potent, specific PPARα agonist GW7647 to A129/SvJ mice is associated with increased expression of *Ces1d*, *Ces1e*, *Ces1f*, *Ces2c* and *Ces2e* mRNA in liver. These differing findings could be due to drug specificity (Thomas et al., 2002); duration of dosing, and/or mouse strain (although our studies were not designed and optimized for direct comparison of strains, the C_q relative to reference cyclophilin gene expression suggests that C57Bl/6 mice exhibit higher basal *Ces1d* mRNA levels than A129/SvJ, which may preclude them from exhibiting robust upregulation of this Ces family member).

Oxysterols/LXR. Treatment with ligands for the "sterol-sensing" LXRs resulted in increased expression of hepatic and intestinal *Ces2a* and *Ces2c*. In addition, a synthetic ligand for the common

heterodimer partner, RXR, caused a robust increase in *Ces2c* and *Ces4a* mRNA levels. These results suggest either a combinatorial effect of RXR with other regulators (PPARα, LXR in the case of *Ces2c*), or a novel transcriptional mechanism involving RXR homodimers and/or other RXR heterodimer partners not interrogated in our experiments (such as RARs, VDR, or NGFIB). It should be noted that T1317, the LXR agonist used in these studies, has been shown to function as a potent ligand for human PXR (Xue et al., 2007), and to exhibit some activity towards mouse PXR and FXR (Mitro et al., 2007; Repa et al., 2000b). While we did not detect a significant increase in the mRNA levels of *Cyp3a11*, the surrogate marker of PXR activation used to define drug specificity and potency in our studies (Fig. 4.5A), we can not rule out the possibility that PXR mediates some of the effects of T1317 in regulating hepatic *Ces2a* expression.

The mammalian carboxylesterases have become enzymes of increasing interest, particularly in regards to potential activities as cholesteryl ester and/or triacylglyceride hydrolases (Ghosh, 2012; Quiroga and Lehner, 2011a; Zechner et al., 2012). Recombinant mouse *Ces1e* (called Es22) enzyme shows robust retinyl ester hydrolysis activity and modest, albeit significant, activity as a cholesteryl ester hydrolase (Schreiber et al., 2009). It has been noted that several tissues exhibit triglyceride hydrolysis activity that cannot be accounted for by known lipases (e.g. ATGL, HSL, and others), thus supporting the existence of additional neutral lipases (Zechner et al., 2012). Mouse *Ces1d* (also called TGH or Ces3) has been identified as a triglyceride hydrolase (Dolinsky et al., 2001), and mice lacking this enzyme show dramatic changes in energy expenditure, plasma lipoprotein profiles and hepatic steatosis (Wei et al., 2010). Thus a number of *Ces* members have been implicated in regulation of lipid hydrolysis, however except for *Ces1d*, it is not clear if or which mouse *Ces* gene(s) may show similar activities. This report reveals many other *Ces* genes which may be involved in these processes, based solely on evidence from gene expression changes due to lipid-sensing transcription factors, and disease models. Acute activation of fatty acid-sensing transcription factors (RXRs, PPARs see Fig. 4.5) results in increased hepatic RNA levels of *Ces1*members (*1d, 1e, and 1f*), although chronic high-fat feeding of mice does not result in

altered expression of these genes in the steatotic liver (Fig. 4.6B). The *Ces2* members exhibit both acute (*Ces2a, Ces2c, and Ces2e)* effects due to short-term administration of ligands to the lipid-sensing nuclear hormone receptors, and differential mRNA levels in the steatotic liver (*Ces2e* and *Ces2g*). Finally, two *Ces* genes exhibited altered expression in LPS-treated mouse macrophages (*Ces1c* and *Ces2f*), suggesting that these carboxylesterases may play a role in the lipid biology of this important cell type, as previously reported for other *CES* members in human macrophages (Ghosh, 2000; Ghosh, 2011; Zhao et al., 2012; Zhao et al., 2007).

While it is clear that there are many post-transcriptional levels of regulation which limit the interpretation of mRNA expression data, this survey offers valuable information to guide future studies of the CES family of enzymes. Given the current lack of CES-selective substrates and/or antibodies for the 19 mouse enzymes, a comprehensive analysis of protein abundance or activity is not yet possible. Therefore this description of mouse distribution and regulation of *Ces* mRNA expression provides a framework for future research into the pharmacologic response, and extrahepatic xenobiotic clearance capacity of the highly similar, yet variably regulated carboxylesterases.

CHAPTER FIVE:

Conclusions and Recommendations

5.1 Summary and rationale

Metabolic pathways consist of an interconnected series of regulatory events involving the synthesis, storage, transportation, and catabolism of various essential nutrients. This is especially true for lipids, which are used for many functions such as energy storage, structural components of membranes, and hormone signaling. When proper lipid balance is lost, it results in a pathological state which very often leads to disease.

One example of this metabolic dysfunction is hepatic steatosis and its sequelae termed nonalcoholic fatty liver disease (NAFLD). NAFLD is a disease of the aberrant accumulation of triglycerides (TGs) in the liver, which can progress to an inflammatory state, cirrhosis, and in some cases hepatocellular carcinoma. There are few treatment options for this disease, and it affects a very large proportion of the United States. There has been an interesting observation, in both mice and humans, that blocking cholesterol absorption with the drug Ezetimibe mitigates hepatic steatosis. Understanding this process was the main focus of CHAPTER TWO of this dissertation, with an emphasis on the early events leading to hepatic triglyceride accumulation before confounding factors such as obesity and insulin resistance became involved.

Another example of lipid dysfunction is seen with a depletion of bile acid pool size through a mutation in the rate limiting enzyme for bile acid biosynthesis. Mice that lack cholesterol 7α-hydroxylase (Cyp7a1) have a depleted bile acid pool size, and as a result they have a cholesterol absorption deficiency, diminished FXR signaling, and altered cholesterol synthesis rates. As shown in CHAPTER THREE, the bile acid pool size in these animals was restored through dietary administration of one of the primary bile acid species, cholic acid, at a physiological dose. This provided valuable information regarding the role of bile acids in total lipid balance.

One powerful approach used to identify potential molecular mediators of metabolic dysfunction is gene expression analysis, because many processes in lipid metabolism are regulated by transcription factors. One high-throughput method to interrogate global gene expression is the microarray analysis. Thus, I used microarrays to identify genes regulated in the liver and intestine from mice studied in the experiments of hepatic steatosis described in CHAPTER TWO. These analyses revealed a family of enzymes called carboxylesterases (CES), which are involved in neutral lipid hydrolysis, which were highly regulated in tissues of these mice. There are 20 CES genes in the mouse that share significant sequence homology, and therefore I developed quantitative real-time PCR methods to measure these gene products. This led to a series of studies classifying the entire family of CES for differential expression in mouse tissues and for regulation by lipid sensing transcription factors in CHAPTER FOUR.

5.2 Conclusion 1: Ezetimibe and Hepatic Steatosis

Many studies have demonstrated an effect of Ezetimibe treatment to prevent the accumulation of triglycerides in the liver. In nearly all repots, the mechanism of this effect has been hypothesized to involve an alteration in LXR activity to affect hepatic *de novo* lipogenesis. One of the primary aims of this dissertation was to test this hypothesis by using mice lacking both LXRα and LXRβ (LXR DKO), to determine if LXR was required for this process. To do this, mice were fed high-fat diet or high-fat high-cholesterol diet with or without Ezetimibe for 12 days. This short-term treatment was used to observe the development of hepatic steatosis prior to the onset of diet-induced insulin resistance and obesity, which could confound interpretation of the data.

The results from these studies clearly demonstrate two main points: first, that the Ezetimibe-mediated protection from hepatic steatosis is independent of LXR; and second, that there is actually a paradoxical increase in hepatic lipogenesis, despite reduced hepatic TG levels, in mice treated with Ezetimibe within the first 12 days of dietary administration. The molecular mechanism regulating this

effect of Ezetimibe is still unclear, however the prevailing hypotheses of LXR-dependence and insulin resistance have now been carefully excluded through this work.

Additionally, in these studies there was an observed genotype difference in the rates of cholesterol synthesis, in which the LXR DKO mice had greater liver cholesterol concentrations, yet still maintained high rates of *de novo* sterol synthesis. SREBP-2 and SREBP-1c have different functions, however when one is absent, there could be compensation by the other, or perhaps by SREBP-1a which drives both cholesterol and fatty acid biogenesis. The hepatic expression of SREBP-1c is dramatically reduced in LXR-DKO mice, which could lead to this compensation which would explain the increase in cholesterol synthesis. However, cholesterol synthesis rates are also increased in the intestine of the LXR-DKO mice, which have a higher expression of SREBP-1c compared to wildtype mice. An alternative explanation is that some target gene of LXR could be involved in intracellular transport or hydrolysis of cholesterol esters, and when LXR is missing, the cell loses its capacity to accurately gauge its cholesterol levels. Two genes, *Ces1d* and *Ces1e*, were expressed at significantly lower levels in LXR-DKO mice, and it is possible that these could participate in cholesteryl ester hydrolysis.

Future recommendations

Based on the results presented in CHAPTER TWO, there are many new questions that arise. Primarily, the mechanism regulating the Ezetimibe-mediated protection from hepatic steatosis is still unclear. To address these questions, I recommend more detailed examination of lipid balance measurements, especially in short-term feeding studies. A measurement of fatty acid β-oxidation should be done in liver slices or isolated primary hepatocytes taken from mice treated with Ezetimibe to delineate the rate at which triglycerides are catabolized in the liver. Sensitive lipid absorption assays should be carried out to determine more accurately the uptake and perhaps distribution of absorbed TGs. Chylomicron distribution, secretion rates, and composition should be examined, as the dynamics may be altered due to diminished availability of intestinal cholesterol. The composition of fatty acids and

cholesterol metabolites in the liver could be interrogated to find any potential differences in fatty acid saturation or oxysterol production due to Ezetimibe treatment.

I would also recommend this same feeding and treatment strategy with mice lacking other lipid-sensing nuclear hormone receptors such as PPARα (Hashimoto et al., 2000; Ip et al., 2003), PPARγ (Gavrilova et al., 2003; Kumadaki et al., 2011), FXR (Herrema et al., 2010; Watanabe M. et al., 2011), or other transcription factors impacting hepatic steatosis such as C/EBPα (Inoue et al., 2004), HNF1α (Rebouissou et al., 2007), or XBP1 (Lee et al., 2008). This could potentially elucidate one of these receptors as the molecular mediator regulating the effect of Ezetimibe on hepatic steatosis.

Finally, a lot of evidence regarding Ezetimibe and hepatic steatosis in humans has been collected from small cohorts of patients. I believe a large clinical trial should be conducted with the effect of Ezetimibe on NAFLD progression as the main outcome measured. Although the mechanism driving this effect is still unknown, the facts that Ezetimibe is already widely used, and that NAFLD lacks effective treatment options provide an impetus for a large-scale clinical trial.

5.3 Conclusion 2: Restoration of bile acid pool size in *Cyp7a1*$^{-/-}$ mice

In characterizing the phenotype of the bile acid deficient *Cyp7a1*$^{-/-}$ mice, some very interesting observations were made after restoration of the bile acid pool size. First, pool size restoration was achieved by feeding cholic acid in the diet at much lower concentrations than most research groups use to test bile acid signaling (.5-5% of diet). This low level of cholic acid (0.03% of diet) not only restored pool size, but also resulted in a restoration of cholesterol absorption, fecal neutral sterol excretion, and FXR signaling. An unforeseen consequence of restoring cholesterol absorption in these animals was that due to the lack of Cyp7a1, they were still unable to convert cholesterol to bile acids, which resulted in a large dose-dependent accumulation in hepatic cholesterol concentration. Additionally, due to our choice to provide cholic acid to these mice, their bile acid pools became enriched for this bile acid species, which has superior lipid solubilizing effects, resulting in a greater capacity to absorb cholesterol.

Future Directions

Due to the dramatic effects seen when restoring the bile acid pool size with cholic acid, it would also be interesting to test similar pool size restoration with the other primary bile acid chenodeoxycholic acid (CDCA), which the mice would metabolize to create a bile acid pool rich in muricholic acid (MCA). Chenodeoxycholic acid (and MCA) rich pools are generally recognized to diminish intestinal cholesterol absorption. This would also allow for a comparison between bile acid ligands, CA versus CDCA, as effectors for FXR, PXR, VDR, CAR, and TGR5 signalling. Much of the data for this series of experiments has already been completed but will not be presented here.

5.4 Conclusion 3: The distribution and regulation of carboxylesterases

The results from this survey of CES gene expression and regulation reveal many interesting points. One of the most important findings was that even though many of the genes lie in tandem on the chromosome, they still exhibit differential patterns of expression and regulation. While it is clear that there are many post-transcriptional levels of regulation which limit the interpretation of mRNA expression data, this survey offers valuable information to guide future studies of the CES family of enzymes. Given the current lack of CES-selective substrates and/or antibodies for the 19 mouse enzymes, a comprehensive analysis of protein abundance or activity is not yet possible. Therefore this description of mouse distribution and regulation of *Ces* mRNA expression provides a framework for future research into the pharmacologic response, and extrahepatic xenobiotic clearance capacity of the highly similar, yet variably regulated carboxylesterases. In addition as lipid hydrolytic activities are identified and/or confirmed for members of this family, this survey will implicate particular members in the regulation of lipid homeostasis.

APPENDIX A: Primers used for Quantitative Real-time PCR

Table A.1 PCR primers used to quantify mouse mRNA levels from Chapter 2

Gene	Gene Name	NCBI Accession Number	Sequence of Primers (5' to 3')	Amplicon Nucleotide Numbers
Primers for mouse gene expression				
Rpl19	Ribosomal Protein L19	NM_009078	F: GTATCACAGCCTGTACCTGA R: AGACTGATCCACATGAGGCC	419-709
Lxrα	Liver X Receptor alpha aka *Nr1h3*	NM_013839	F: AGGAGTGTCGACTTCGCAAA R: CTCTTCTTGCCGCTTCAGTTT	788-888
Lxrβ	Liver X Receptor beta aka *Nr1h2*	NM_009473	F: AAGCAGGTGCCAGGGTTCT R: TGCATTCTGTCTCGTGGTTGT	1084-1204
Abca1	ATP binding cassette member A1	NM_013454	F: CGTTTCCGGGAAGTGTCCTA R: GCTAGAGATGACAAGGAGGATGGA	6805-6883
Abcg5	ATP binding cassette member G5	NM_031884	F: TGGATCCAACACCTCTATGCTAAA R: GGCAGGTTTTCTCGATGAACTG	1817-1893
Ces1d	Carboxylesterase 1D aka *Ces3*	NM_053200	F: ATATGGCTTTCTCTTGCTGCG R: CCCAGGACTTTGCCTTTAACAGT	104-189
Ces1e	Carboxylesterase 1E aka *Es22*	NM_133660	F: GATTGGGGATGTGGTATTCG R: GGGCTCCGGCATCTCTATGT	1455-1522
Fas	Fatty acid synthase aka *Fasn*	NM_007988	F: GCTGCGGAAACTTCAGGAAAT R: AGAGACGTGTCACTCCTGGACTT	7058-7141
HMG CoA Syn	Hydroxymethyl glutaryl CoA synthase aka *Hmgcs1*	NM_145942	F: GCCGTGAACTGGGTCGAA R: GCATATATAGCAATGTCTCCTGCAA	536-612
Ldlr	Low density lipoprotein receptor	NM_010700	F: GAGGAACTGGCGGCTGAA R: GTGCTGGATGGGGAGGTCT	2638-2876
Mtp	Microsomal triglyceride transfer protein aka *Mttp*	NM_008642	F: CCTACCAGGCCCAACAAGAC R: CGCTCAATTTTGCATGTATCC	607-670
Npc1l1	Niemann-Pick Type C1-like protein 1	NM_207242	F: TGGACTGGAAGGACCATTTCC R: GACAGGTGCCCCGTAGTCA	1547-1650
Pcsk9	Proprotein convertase subtilisin/kexin type 9	NM_153565	F: CAGGCGGCCAGTGTCTATG R: GCTCCTTGATTTTGCATTCCA	2198-2261
Perilipin	Perilipin 1 aka *Plin1*	NM_175640	F: TGCTGGATGGAGACCTC R: ACCGGCTCCATGCTCCA	131-332
Scd1	Stearoyl-Coenzyme A desaturase 1	NM_009127	F: CCGGAGACCCCTTAGATCGA R: TAGCCTGTAAAAGATTTCTGCAAACC	3934-4022
Srebp-1c	Sterol regulatory element-binding protein 1c aka *Srebf1c*	NM_011480 NT_096135 (Genomic seq.)	F: GGAGCCATGGATTGCACATT R: GGCCCGGGAAGTCACTGT	10438-10419 7291-7308
Srebp-2	Sterol regulatory element-binding protein 2 aka *Srebf2*	NM_033218	F: GCGTTCTGGAGACCATGGA R: ACAAAGTTGCTCTGAAAACAAATCA	157-287

Table A.2 PCR primers used to quantify mouse mRNA levels from Chapter 3				
Gene	Gene Name	NCBI Accession Number	Sequence of Primers (5' to 3')	Amplicon Nucleotide Numbers
Bile Acid Synthetic Enzymes				
Cyp7a1	Cholesterol 7α-hydroxylase	NM_007824	F: AGCAACTAAACAACCTGCCAGTACTA R: GTCCGGATATTCAAGGATGCA	1073-1154
Ch25h	Cholesterol 25-hydroxylase	NM_009890	F: CACAAGGTGCATCACCAGAACT R: CGAAGAAGGTCAGCGAAAGC	478-565
Cyp27a1	Sterol 27-hydroxylase	NM_024264	F: GCCTCACCTATGGGATCTTCA R: TCAAAGCCTGACGCAGATG	485-547
Cyp39a1	Oxysterol 7α-hydroxylase	NM_018887	F: GGTAGTGAAGCCAGTTAAAATTCTGA R: CTGTGTAGCCAGAATGGAGACAA	1228-1308
Cyp7b1	Oxysterol 7α-hydroxylase	NM_007825	F: TAGCCCTCTTTCCTCCACTCATA R: GAACCGATCGAACCTAAATTCCT	1298-1374
Hsd3b7	3β-Hydroxy-Δ5-C_{27} steroid oxidoreductase	NM_133943	F: CCAGGTAGTTGGCAAAACTGATT R: TGTTCCTCCCTGCTTGAGAAA	1464-1542
Cyp8b1	Sterol 12α-hydroxylase	NM_010012	F: GCCTTCAAGTATGATCGGTTCCT R: GATCTTCTTGCCCGACTTGTAGA	1252-1326
Akr1d1	Δ4-3-Oxosteroid 5β-reductase	NM_145364	F: GAACGTCTCTTCTCCACCCTTGT R: TCCCTCGCTGGATGTTGAA	762-871
Akr1c4	3α-Hydroxysteroid dehydrogenase	NM_030611	F: TGCCTTGTGCCAGATGTCA R: CAGAAGCTTGGATTAGGGTGATATG	1037-1129
Slc27a5	Bile acid CoA ligase	NM_009512	F: GACCACTGGACTCCCAAAGC R: GACAGCACGTTGCTCACTTGT	976-1044
Amacr	2-Methylacyl-CoA-racemase	NM_008537	F: GTGGATGAACAGCAATGAAGTCA R: CGCAATCGTTATCGTGTAACCA	1279-1356
Acox2	Branched-chain acyl-CoA oxidase	NM_053115	F: GACGGTCCTGAACGCATTT R: CATTCATGGCAATACCATGTAAGTT	484-562
Hsd17b4	D-Bifunctional protein	NM_008292	F: CACTGTGTGCTGTTAAAGGAGTCA R: CACTCCTGTGGATCGCAGAA	2240-2319
Acaa1	Peroxisomal thiolase	NM_130864	F: GCAGAAGCAGGATGACTTTGC R: CAATCTCAGCACGGAGCAT	809-891
Baat	Bile acid CoA: Amino acid N-acyltransferase	NM_007519	F: AGCACCACTCCTCACTTCCATAG R: TCCATCCTCCTGTATTTTCTTGTG	1517-1605
Genes Involved in the Enterohepatic Flux of Cholesterol and Bile Acid				
Abca1	ATP binding cassette member A1	NM_013454	F: CGTTTCCGGGAAGTGTCCTA R: GCTAGAGATGACAAGGAGGATGGA	6805-6883

Abcb11	Bile salt export pump (BSEP)	NM_021022	F: AAGCTACATCTGCCTTAGACACAGAAA R: CAATACAGGTCCGACCCTCTCT	3858-3941
Abcg8	ATP binding cassette member G8	NM_026180	F: TGCCCACCTTCCACATGTC R: ATGAAGCCGGCAGTAAGGTAGA	1759-1831
Fabp6	Ileal bile acid binding protein (IBABP)	NM_008375	F: CAAGGCTACCGTGAAGATGGA R: CCCACGACCTCCGAAGTCA	240-317
Fgf15	Fibroblast growth factor 15	NM_008003	F: ACGGGCTGATTCGCTACTC R: TGTAGCCTAAACAGTCCATTTCCT	497-562
Flot1	Flotillin 1	NM_008027	F: CAAGAGTGAAAAGGTTTATACCCG R: CCTTGTTCTGGCCCTGGATTT	309-394
Flot2	Flotillin 2	NM_008028	F: AGGTGACATCAGAAGTAAACCG R: GGGTATCTTTGAAAGGTCCACACC	1383-1468
Hmgcs1	Hydroxymethyl glutaryl CoA synthase 1	NM_145942	F: GCCGTGAACTGGGTCGAA R: GCATATATAGCAATGTCTCCTGCAA	536-612
Npc1l1	Niemann-Pick Type C1-like protein 1	NM_207242	F: TGGACTGGAAGGACCATTTCC R: GACAGGTGCCCCGTAGTCA	1547-1650
Nr0b2	Short heterodimer partner (SHP)	NM_011850	F: CAGCGCTGCCTGGAGTCT R: AGGATCGTGCCCTTCAGGTA	492-565
Nr2a1	Hepatic nuclear factor 4α (HNF4α)	NM_008261	F: CCAACCTCAATTCATCCAACA R: CCCGGTCGCCACAGAT	254-316
Nr5a2	Liver receptor homolog 1 (LRH-1)	NM_030676	F: TGGGAAGGAAGGGACAATCTT R: CGAGACTCAGGAGGTTGTTGAA	1406-1506
Ostα	Organic solute transporter α	NM_145932	F: AACAGAACATGGGATCCAAGTTT R: CAGGGCGGTCAGGATGA	1103-1161
Slc10a1	Sodium taurocholate cotransporter polypeptide (NTCP)	NM_011387	F: GAAGTCCAAAAGGCCACACTATGT R: ACAGCCACAGAGAGGGAGAAAG	568-645
Slc10a2	Ileal bile acid transporter (IBAT)	NM_011388	F: TGGGTTTCTTCCTGGCTAGACT R: TGTTCTGCATTCCAGTTTCCAA	768-848
ScarbI	Scavenger receptor Type BI (SRBI)	NM_016741	F: TCCCCATGAACTGTTCTGTGAA R: TGCCCGATGCCCTTGA	1331-1397

Table A.3 PCR primers used to quantify mouse mRNA levels from Chapter 4				
Gene	Name(s)	Accession Number	Sequence of Primers (5' to 3')	Amplicon position
Carboxylesterase Genes				
Ces1a	Carboxylesterase 1A aka *EG244595*	NM_001013764	F: CCCTACAGACCTGACAAGCAAAGA R: ATGCTCCACCAGAGAGTAAACCG	453-532
Ces1c	Carboxylesterase 1C aka *Es1, Ces-N*	NM_007954	F: GCACTACGCTGGGTCCAAGAT R: AAAGATGGTCACGGAATCCG	614-679
Ces1d	Carboxylesterase 1D aka *Ces3*	NM_053200	F: ATATGGCTTTCTCTTGCTGCG R: CCCAGGACTTTGCCTTTAACAGT	104-189
Ces1e	Carboxylesterase 1E aka *Es22*	NM_133660	F: GATTGGGGATGTGGTATTCG R: GGGCTCCGGCATCTCTATGT	1455-1522
Ces1f	Carboxylesterase 1F aka *CesML1, TGH-2*	NM_144930	F: TTTCAAAGAACAGTAGGCTACCG R: AGAGAGCCCGTCCATCAAAGC	416-508
Ces1g	Carboxylesterase 1G aka *Ces1*	NM_021456	F: CGAGTCAGCAGGAGGTGAAAGT R: TTGAAAATGACACTACTCTGAGCG	712-810
Ces1h	Carboxylesterase 1H aka *AK009689*	XM_134476	F: CTTTGTGAAGAATGCCACCTCG R: TCTGCCCTAACACTGCATCTTG	225-286
Ces2a	Carboxylesterase 2A aka *Ces6*	NM_133960	F: CTCACAGCCGGCCATGT R: AGATTCATTTCCTTCGCATCCT	336-401
Ces2b	Carboxylesterase 2B aka *BC015286*	NM_198171	F: TCTGAGATGGTCTCCACTACG R: GCAGGGATCATCTGGACAAGC	818-954
Ces2c	Carboxylesterase 2C aka *Ces2*	NM_145603	F: GCTGAATGCTGGGTTCTTCG R: GCTGCCTTGGATCTGTCCTGT	92-203
Ces2e	Carboxylesterase 2E aka *Ces5*	NM_172759	F: CTTGTCTTTGGCTACCAGTTCG R: TTGCTCCTCTTCCTCAGTGTAAGG	1448-1507
Ces2f	Carboxylesterase 2F	NM_001079865	F: TTCAGCGTTCCCATGCTCCT R: CTTGAGTAAACTGGACCTATGCTG	1306-1367
Ces2g	Carboxylesterase 2G	NM_197999	F: TCTCTGAGGTGGTTTACCAAACG R: CCTCTCAGACAGCGCACCAG	870-954
Ces2h	Carboxylesterase 2H	XM_488149	F: AACTGTCTACGAGGCAAAAGCG R: GAGGATGTCTGGGCAGGAAGAT	865-967
Ces3a	Carboxylesterase 3A aka *Es31*	NM_198672	F: GATGGCCTGTCTGCTCCTGATA R: CAGGAAGACATTTACCATGCG	73-214
Ces3b	Carboxylesterase 3B aka *Es31L*	NM_144511	F: GGATTGTCACGACCATTATGATG R: CAGAGCCACAGGCCACAGAA	796-879
Ces4a	Carboxylesterase 4A aka *Ces8*	NM_146213	F: TCTCAGCAGAGGAGGTGACG R: CACTGGGCTCAGGAACCACAC	1036-1136
Ces5a	Carboxylesterase 5A aka *Ces7*	NM_001003951	F: GTTGTCACCATCCAGTACCG R: GTCCCAGAAGGCCCAATTCC	508-594
Other genes				
Cyclo	Cyclophilin, peptidyl-prolyl isomerase B	NM_011149	F: TGGAGAGCACCAAGACAGACA R: TGCCGGAGTCGACAATGAT	642-707
Cyp3a11	Cytochrome P450 3a11	NM_007818	F: AAACTGCAGGATGAGATCGATGA R: TCCAGGTATTCCATCTCCATCAC	1069-1151
Cyp4a14	Cytochrome P450 4a14	NM_007822	F: CCCCTCTAGATTTGCACCAGAT R: TCCCAATGCAGTTCCTTGATC	1315-1397
Cyp7a1	Cytochrome P450 7a1, Cholesterol 7α-hydroxylase	NM_007824	F: AGCAACTAAACAACCTGCCAGTACTA R: GTCCGGATATTCAAGGATGCA	1073-1154
Il1β	Interleukin 1β	NM_008361	F: CAACCAACAAGTGATATTCTCCATG R: GATCCACACTCTCCAGCTGCA	527-678
Tnf	Tumor necrosis factor	NM_013693	F: CTGAGGTCAATCTGCCCAAGTAC R: CTTCACAGAGCAATGACTCCAAAG	791-866

BIBLIOGRAPHY

Abumrad NA and Davidson NO (2012) Role of the gut in lipid homeostasis. *Physiol Rev* **92:** 1061-1085.

Alrefai WA and Gill RK (2007) Bile acid transporters: structure, function, regulation and pathophysiological implications. *Pharm Res* **24:** 1803-1823.

Altmann SW, Davis HR, Zhu L-j, Yao X, Hoos LM, Tetzloff G, Iyer SPN, Maguire M, Golovko A, Zeng M, Wang L, Murgolo N and Graziano MP (2004) Niemann-Pick C1 like 1 protein is critical for intestinal cholesterol absorption. *Science* **303:** 1201-1204.

Amaral JD, Viana RJS, Ramalho RM, Steer CJ and Rodrigues CMP (2009) Bile acids: regulation of apoptosis by ursodeoxycholic acid. *J Lipid Res* **50:** 1721-1734.

Ashour M-BA, Moody DE and Hammock BD (1987) Apparent induction of microsomal carboxylesterase activities in tissues of clofibrate-fed mice and rats. *Toxicology and Applied Pharmacology* **89:** 361-369.

Barish GD, Downes M, Alaynick WA, Yu RT, Ocampo CB, Bookout AL, Mangelsdorf DJ and Evans RM (2005) A nuclear receptor atlas: macrophage activation. *Molecular Endocrinology* **19:** 2466-2477.

Beher WT, Filus AM, Rao B and Beher ME (1969) A comparative study of bile acid metabolism in the rat, mouse, hamster, and gerbil. *Proc Soc Exp Biol Med* **130:** 1067-1074.

Biddinger SB, Haas JT, Yu BB, Bezy O, Jing E, Zhang W, Unterman TG, Carey MC and Kahn CR (2008) Hepatic insulin resistance directly promotes formation of cholesterol gallstones. *Nat Med* **14:** 778-782.

Brown CJ and Donnelly TM (2004) Rodent husbandry and care. *Vet Clin North Am Exot Anim Pract* **7:** 201-225.

Brown MS and Goldstein JL (2008) Selective versus total insulin resistance: a pathogenic paradox. *Cell Metabolism* **7:** 95-96.

Brown PJ, Stuart LW, Hurley KP, Lewis MC, Winegar DA, Wilson JG, Wilkison WO, Ittoop OR and Willson TM (2001) Identification of a subtype selective human PPARα agonist through parallel-array synthesis. *Bioorganic & Medicinal Chemistry Letters* **11:** 1225-1227.

Browning JD, Szczepaniak LS, Dobbins RL, Nuremberg P, Horton JD, Cohen JC, Grundy SM and Hobbs HH (2004) Prevalence of hepatic steatosis in an urban population in the United States: impact of ethnicity. *Hepatology* **40:** 1387-1395.

Bustin SA, Benes V, Garson JA, Hellemans J, Huggett JF, Kubista M, Mueller R, Nolan T, Pfaffl MW, Shipley GL, Vandesompele J and Wittwer CT (2009) The MIQE guidelines: Minimum information for publication of quantitative real-time PCR experiments. *Clinical Chemistry* **55:** 611-622.

Calkin AC and Tontonoz P (2012) Transcriptional integration of metabolism by the nuclear sterol-activated receptors LXR and FXR. *Nature Reviews Molecular Cell Biology* **on-line:**

Carey MC and Cahalane MJ (1988) Enterohepatic Circulation. *Raven Press, Ltd.* 573-616.

Cha J-Y and Repa JJ (2007) The liver X receptor (LXR) and hepatic lipogenesis: the carbohydrate-response element-binding protein is a target gene of LXR. *Journal of Biological Chemistry* **282:** 743-751.

Chan DC, Watts GF, Gan SK, Ooi EMM and Barrett PHR (2010) Effect of Ezetimibe on hepatic fat, inflammatory markers, and apolipoprotein B-100 kinetics in insulin-resistant obese subjects on a weight loss diet. *Diabetes Care* **33:** 1134-1139.

Chawla A, Repa JJ, Evans RM and Mangelsdorf DJ (2001) Nuclear receptors and lipid physiology: opening the X-files. *Science* **294:** 1866-1870.

Cheng X, Buckley D and Klaassen CD (2007) Regulation of hepatic bile acid transporters Ntcp and Bsep expression. *Biochem Pharmacol* **74:** 1665-1676.

Chiang JYL (2009) Bile acids: regulation of synthesis. *J Lipid Res* **50:** 1955-1966.

Cho J-Y, Matsubara T, Kang DW, Ahn S-H, Krausz KW, Idle JR, Luecke H and Gonzalez FJ (2010) Urinary metabolomics in *Fxr*-null mice reveals activated adaptive metabolic pathways upon bile acid challenge. *J Lipid Res* **51:** 1063-1074.

Chuang J-C, Cha J-Y, Garmey JC, Mirmira RG and Repa JJ (2008) Nuclear hormone receptor expression in the endocrine pancreas. *Molecular Endocrinology* **22:** 2353-2363.

Clader JW (2004) The discovery of Ezetimibe: a view from outside the receptor. *Journal of Medicinal Chemistry* **47:** 1-9.

Cohen JC, Boerwinkle E, Mosley TH and Hobbs HH (2006) Sequence variations in *PCSK9*, low LDL, and protection against coronary heart disease. *New England Journal of Medicine* **354:** 1264-1272.

Cohen JC, Horton JD and Hobbs HH (2011) Human fatty liver disease: old questions and new insights. *Science* **332:** 1519-1523.

Collins JL, Fivush AM, Watson MA, Galardi CM, Lewis MC, Moore LB, Parks DJ, Wilson JG, Tippin TK, Binz JG, Plunket KD, Morgan DG, Beaudet EJ, Whitney KD, Kliewer SA and Willson TM (2002) Identification of a nonsteroidal liver X receptor agonist through

parallel array synthesis of tertiary amines. *Journal of Medicinal Chemistry* **45:** 1963-1966.

Costet P (2010) Molecular pathways and agents for lowering LDL-cholesterol in addition to statins. *Pharmacology & Therapeutics* **126:** 263-278.

Dawson PA, Lan T and Rao A (2009) Bile acid transporters. *J Lipid Res* **50:** 2340-2357.

de Bari O, Neuschwander-Tetri BA, Liu M, Portincasa P and Wang D-Q-H (2011) Ezetimibe: its novel effects on the prevention and the treatment of cholesterol gallstones and nonalcoholic fatty liver disease. *Journal of Lipids* **2012:** article 302847.

Dennis EA, Deems RA, Harkewicz R, Quehenberger O, Brown HA, Milne SB, Myers DS, Glass CK, Hardiman G, Reichart D, Merrill AH, Sullards MC, Wang E, Murphy RC, Raetz CRH, Garrett T, Guan Z, Ryan AC, Russell DW, McDonald JG, Thompson BM, Shaw WA, Sud M, Zhao Y, Gupta S, Maurya MR, Fahy E and Subramaniam S (2010) A mouse macrophage lipidome. *Journal of Biological Chemistry* **285:** 39976-39985.

Deushi M, Nomura M, Kawakami A, Haraguchi M, Ito M, Okazaki M, Ishii H and Yoshida M (2007) Ezetimibe improves liver steatosis and insulin resistance in obese rat model of metabolic syndrome. *FEBS Lett.* **581:** 5664-5670.

Dheda K, Huggett JF, Bustin SA, Johnson MA, Rook G and Zumla A (2004) Validation of housekeeping genes for normalizing RNA expression in real-time PCR. *BioTechniques* **37:** 112-119.

Dietschy JM and Spady DK (1984) Measurement of rates of cholesterol synthesis using tritiated water. *Journal of Lipid Research* **25:** 1469-1476.

Dolinsky VW, Gilham D, Hatch GM, Agellon LB, Lehner R and Vance DE (2003) Regulation of triacylglycerol hydrolase expression by dietary fatty acids and peroxisomal proliferator-activated receptors. *Biochimica Biophysica Acta* **1635:** 20-28.

Dolinsky VW, Sipione S, Lehner R and Vance DE (2001) The cloning and expression of a murine triacylglycerol hydrolase cDNA and the structure of its corresponding gene. *Biochimica Biophysica Acta* **1532:** 162-172.

Ellinghaus P, Seedorf U and Assmann G (1998) Cloning and sequencing of a novel murine liver carboxylase cDNA. *Biochimica Biophysica Acta* **1397:** 175-179.

Erickson SK, Lear SR, Deane S, Dubrac S, Huling SL, Nguyen L, Bollineni JS, Shefer S, Hyogo H, Cohen DE, Shneider B, Sehayek E, Ananthanarayanan M, Balasubramaniyan N, Suchy FJ, Batta AK and Salen G (2003) Hypercholesterolemia and changes in lipid and bile acid metabolism in male and female cyp7A1-deficient mice. *J Lipid Res* **44:** 1001-1009.

Expert Panel on Detection E, and Treatment of High Blood Cholesterol in Adults. (2001) Executive summary of the third report of the National Cholesterol Education Program (NCEP) expert panel on detection, evalutaion, and treatment of high blood cholesterol in adults (Adult Treatment Panel III). *Journal of the American Medical Association* **285:** 2486-2497.

Filippatos TD and Elisaf MS (2011) Role of ezetimibe in non-alcoholic fatty liver disease. *World Journal of Hepatology* **3:** 265-267.

Forman BM, Goode E, Chen J, Oro AE, Bradley DJ, Perlmann T, Noonan DJ, Burka LT, McMorris T, Lamph WW, Evans RM and Weinberger C (1995) Identification of a nuclear receptor that is activated by farnesol metabolites. *Cell* **81:** 687-693.

Fu S, Yang L, Li P, Hofmann O, Dicker L, Hide W, Lin X, Watkins SM, Ivanov AR and Hotamisligil GS (2011) Aberrant lipid metabolism disrupts calcium homeostasis causing liver endoplamsic reticulum stress in obesity. *Nature* **473:** 528-531.

Fu X, Menke JG, Chen Y, Zhou G, MacNaul KL, Wright SD, Sparrow CP and Lund EG (2001) 27-Hydroxycholesterol is an endogenous ligand for LXR in cholesterol-loaded cells. *Journal of Biological Chemistry* **276:** 38378-38387.

Fukuda M, Nakamura T, Kataoka K, Nako H, Tokutomi Y, Dong Y-F, Yasuda O, Ogawa H and Kim-Mitsuyama S (2010) Ezetimibe ameliorates cardiovascular complications and hepatic steatosis in obese and type 2 diabetic *db/db* mice. *Journal of Pharmacology and Experimental Therapeutics* **335:** 70-75.

Garcia-Calvo M, Lisnock J, Bull HG, Hawes BE, Burnett DA, Braun MP, Crona JH, Davis HR, Dean DC, Detmers PA, Graziano MP, Hughes M, MacIntyre DE, Ogawa A, O'Neill KA, Iyer SPN, Shevell DE, Smith MM, Tang YS, Makarewicz AM, Ujjainwalla F, Altmann SW, Chapman KT and Thornberry NA (2005) The target of ezetimibe is Niemann-Pick C1-like 1 (NPC1L1). *Proceedings of the National Academy of Sciences USA* **102:** 8132-8137.

Gavrilova O, Haluzik M, Matsusue K, Cutson JJ, Johnson L, Dietz KR, Nicol CJ, Vinson C, Gonzalez FJ and Reitman ML (2003) Liver peroxisome proliferator-activated receptor γ contributes to hepatic steatosis, triglyceride clearance, and regulation of body fat mass. *Journal of Biological Chemistry* **278:** 34268-34276.

Ge L, Qi W, Wang L-J, Miao H-H, Qu Y-X, Li B-L and Song B-L (2011) Flotillins play an essential role in Niemann-Pick C1-like 1-mediated cholesterol uptake. *Proc Natl Acad Sci U S A* **108:** 551-556.

Ghosh S (2000) Cholesteryl ester hydrolase in human monocyte/macrophage: cloning, sequencing, and expression of full-length cDNA. *Physiological Genomics* **2:** 1-8.

Ghosh S (2012) Early steps in reverse cholesterol transport: Cholesteryl ester hydrolase and other hydrolases. *Current Opinion in Endocrinology, Diabetes and Obesity* **19:** 136-141.

Ghosh S (2011) Macrophage cholesterol homeostasis and metabolic diseases: critical role of cholesteryl ester mobilization. *Expert Reviews in Cardiovascular THerapy* **9:** 329-340.

Goldstein JL, Hobbs HH and Brown MS (1995) Familial hypercholesterolemia. *McGraw-Hill, IOnc.* 2073-2099.

Goodwin B, Gauthier KC, Umetani M, Watson MA, Lochansky MI, Collins JL, Leitersdorf E, Mangelsdorf DJ, Kliewer SA and Repa JJ (2003) Identification of bile acid precursors as endogenous ligands for the nuclear xenobiotic pregnane X receptor. *Proc Natl Acad Sci U S A* **100:** 223-228.

Goodwin BJ, Zuercher WJ and Collins JL (2008) Recent advances in liver X receptor biology and chemistry. *Current Topics in Medicinal Chemistry* **8:** 781-791.

Grundy SM, Ahrens EH, Jr. and Salen G (1971) Interruption of the enterohepatic circulation of bile acids in man: comparative effects of cholestyramine and ileal exclusion on cholesterol metabolism. *J. Lab. Clin. Med.* **78:** 94-121.

Grundy SM and Bilheimer DW (1984) Inhibition of 3-hydroxy-3-methlyglutaryl-CoA reductase by mevinolin in familial hypercholesterolemia heterozygotes: effects on cholesterol balance. *Proc Natl Acad Sci U S A* **81:** 2538-2542.

Grundy SM, Cleeman JI, Merz CNB, Brewer HB, Clark LT, Hunninghake DB, Pasternak RC, Smith SC and Stone NJ (2004) Implications of recent clinical trials for the National

Cholesterol Education Program Adult Treatment Panel III guidelines. *Circulation* **110:** 227-239.

Hahn C, Reichel C and von Bergmann K (1995) Serum concentration of 7α-hydroxycholesterol as an indication of bile acid synthesis in humans. *J Lipid Res* **36:** 2059-2066.

Hashimoto T, Cook WS, Qi C, Yeldandi AV, Reddy JK and Rao MS (2000) Defect in peroxisome proliferator-activated receptor α-inducible fatty acid oxidation determines the severity of hepatic steatosis in response to fasting. *Journal of Biological Chemistry* **275:** 28918-28928.

Hebbard L and George J (2011) Animal models of nonalcoholic fatty liver disease. *Nature Reviews: Gastroenterology & Hepatology* **8:** 34-44.

Henke BR, Blanchard SG, Brackeen MF, Brown KK, Cobb JE, Collins JL, Harrington WW, Hashim MA, Hull-Ryde EA, Kaldor I, Kliewer SA, Lake DH, Leesnitzer LM, Lehmann JM, Lenhard JM, Orband-Miller LA, Miller JF, Mook RA, Noble SA, Oliver WO, Parks DJ, Plunket KD, Szewczyk JR and Willson TM (1998) *N*-(2-Benzoylphenyl)-L-tyrosine PPARγ agonists. 1. Discovery of a novel series of potent antihyperglycemic and antihyperlipidemic agents. *Journal of Medicinal Chemistry* **41:** 5020-5036.

Herrema H, Meissner M, van Dijk TH, Brufau G, Boverhof R, Oosterveer MH, Reijngoud D-J, Muller M, Stellaard F, Groen AK and Kuipers F (2010) Bile salt sequestration induces hepatic de novo lipogenesis through farnesoid X receptor- and liver X receptor alpha-controlled metabolic pathways in mice. *Hepatology* **51:**

Hillgartner FB, Salati LM and Goodridge AG (1995) Physiological and molecular mechanisms involved in nutritional regulation of fatty acid synthesis. *Physiol Rev* **75:** 47-76.

Holmes RS and Cox LA (2011) Comparative structures and evolution of vertebrate carboxyl ester lipase (CEL) genes and proteins with a major role in reverse cholesterol transport. *Cholesterol* **2011:** 1-15.

Holmes RS, Cox LA and VandeBerg JL (2010a) Mammalian carboxylesterase 3: comparative genomics and proteomics. *Genetica* 695-708.

Holmes RS, Cox LA and VandeBerg JL (2008) Mammalian carboxylesterase 5: Comparative biochemistry and genomics. *Comparative Biochemistry and Physiology Part D Genomics Proteomics* **3:** 195-204.

Holmes RS, Cox LA and VandeBerg JL (2009) A new class of mammalian carboxylesterase CES6. *Comparative Biochemistry and Physiology Part D Genomics Proteomics* **4:** 209-217.

Holmes RS, Wright MW, Laulederkind SJF, Cox LA, Hosokawa M, Imai T, Ishibashi S, Lehner R, Miyazaki M, Perkins EJ, Potter PM, Redinbo MR, Robert J, Satoh T, Yamashita T, Yan B, Yokoi T, Zechner R and Maltais LJ (2010b) Recommended nomenclature for five mammalian carboxylesterase gene families: human, mouse, and rat genes and proteins. *Mammalian Genome* **21:** 427-441.

Horton JD, Goldstein JL and Brown MS (2002) SREBPs: activators of the complete program of cholesterol and fatty acid synthesis in the liver. *Journal of Clinical Investigation* **109:** 1125-1131.

Hosokawa M, Furihata T, Yaginuma Y, Yamamoto N, Koyano N, Fujii A, Nagahara Y, Satoh T and Chiba K (2007) Genomic structure and transcriptional regulation of the rat, mouse, and human carboxylesterase genes. *Drug Metabolism Reviews* **39:** 1-15.

Hosokawa M and Satoh T (1993) Differences in the induction of carboxylesterase isozymes in rat liver microsomes by perfluorinated fatty acids. *Xenobiotica* **23:** 1125-1133.

Huang W, Bansode RR, Xie Y, Rowland L, Mehta M, Davidson NO and Mehta KD (2011) Disruption of the murine protein kinase Cβ gene promotes gallstone formation and alters biliary lipid and hepatic cholesterol metabolism. *J Biol Chem* **286:** 22795-22805.

Hussain MM, Fatma S, Pan X and Iqbal J (2005) Intestinal lipoprotein assembly. *Current Opinion in Lipidology* **16:** 281-285.

Hylemon PB, Zhou H, Pandak WM, Ren S, Gil G and Dent P (2009) Bile acids as regulatory molecules. *J Lipid Res* **50:** 1509-1520.

Inagaki T, Choi M, Moschetta A, Peng L, Cummins CL, McDonald JG, Luo G, Jones SA, Goodwin B, Richardson JA, Gerard RD, Repa JJ, Mangelsdorf DJ and Kliewer SA (2005) Fibroblast growth factor 15 functions as an enterohepatic signal to regulate bile acid homeostasis. *Cell Metabolism* **2:** 217-225.

Inoue Y, Inoue J, Lambert G, Yim SH and Gonzalez FJ (2004) Disruption of hepatic C/EBPα results in impaired tolerance and age-dependent hepatosteatosis. *Journal of Biological Chemistry* **(on-line Aug. 2):**

Insull W, Jr. (2006) Clinical utility of bile acid sequestrants in the treatment of dyslipidemia: a scientific review. *South. Med. J.* **99:** 257-273.

Ip E, Farrell GC, Robertson G, Hall P, Kirsch R and Leclercq I (2003) Central role of PPARα-dependent hepatic lipid turnover in dietary steatohepatitis in mice. *Hepatology* **38:** 123-132.

Iqbal J and Hussain MM (2009) Intestinal lipid absorption. *Am J Physiol Endocrinol Metab* **296:** E1183-1194.

Ishibashi S, Schwarz M, Frykman PK, Herz J and Russell DW (1996) Disruption of cholesterol 7α-hydroxylase gene in mice: I. Postnatal lethality reversed by bile acid and vitamin supplementation. *J. Biol. Chem.* **271:** 18017-18023.

Janowski BA, Grogan MJ, Jones SA, Wisely GB, Kliewer SA, Corey EJ and Mangelsdorf DJ (1999) Structural requirements of ligands for the oxysterol liver X receptors LXRα and LXRβ. *Proceedings of the National Academy of Sciences USA* **96:** 266-271.

Janowski BA, Willy PJ, Devi TR, Falck JR and Mangelsdorf DJ (1996) An oxysterol signalling pathway mediated by the nuclear receptor LXRα. *Nature* **383:** 728-731.

Jelinek DF, Andersson S, Slaughter CA and Russell DW (1990) Cloning and regulation of cholesterol 7α-hydroxylase, the rate-limiting enzyme in bile acid biosynthesis. *Journal of Biological Chemistry* **265:** 8190-8197.

Jia L, Ma Y, Rong S, Betters JL, Xie P, Chung SK, Wang N, Tang W and Yu L (2010) Niemann-Pick C1-like 1 deletion in mice prevents high-fat diet-induced fatty liver by reducing lipogenesis. *Journal of Lipid Research* **51:** 3135-3144.

Jones SA, Moore LB, Shenk JL, Wisely GB, Hamilton GA, McKee DD, Tomkinson NCO, LeCluyse EL, Lambert MH, Willson TM, Kliewer SA and Moore JT (2000) The pregnane X receptor: a promiscuous xenobiotic receptor that has diverged during evolution. *Molecular Endocrinology* **14:** 27-39.

Joseph SB, Castrillo A, Laffitte BA, Mangelsdorf DJ and Tontonoz P (2003) Reciprocal regulation of inflammation and lipid metabolism by liver X receptors. *Nature Medicine* **9:** 213-219.

Kalaany NY, Gauthier KC, Zavacki AM, Mammen PPA, Kitazume T, Peterson JA, Horton JD, Garry DJ, Bianco AC and Mangelsdorf DJ (2005) LXRs regulate the balance between fat storage and oxidation. *Cell Metabolism* **1:** 231-244.

Kobayashi M, Ikegami H, Fujisawa T, Nojima K, Kawabata Y, Noso S, Babaya N, Itoi-Babaya M, Yamaji K, Hiromine Y, Shibata M and Ogihara T (2007) Prevention and treatment of obesity, insulin resistance, and diabetes by bile acid-binding resin. *Diabetes* **56:** 239-247.

Kosir R, Acimovic J, Golicnik M, Perse M, Majdic G, Fink M and Rozman D (2010) Determination of reference genes for circadian studies in different tissues and mouse strains. *BMC Molecular Biology* **11:** 60.

Kosoglou T, Statkevich P, Johnson-Levonas AO, Paolini JF, Bergman AJ and Alton KB (2005) Ezetimibe: A review of its metabolism, pharmacokinetcis and drug interactions. *Clinical Pharmacokinetics* **44:** 467-494.

Kumadaki S, Karasawa T, Matsuzaka T, Ema M, Nakagawa Y, Nakakuki M, Saito R, Yahagi N, Iwasaki H, Sone H, Takekoshi K, Yatoh S, Kobayashi K, Takahashi A, Suzuki H, Takahashi S, Yamada N and Shimano H (2011) Inhibition of ubiquitin ligase F-box and WD repeat domain-containing 7α (Fbw7α) causes hepatosteatosis through the Kruppel-like factor 5 (KLF5)/PPARγ2 pathway, but not SREBP-1c in mice. *Journal of Biological Chemistry* **on-line Sept. 12:**

Kurrasch DM, Huang J, Wilkie TM and Repa JJ (2004a) Quantitative real-time polymerase chain reaction measurement of regulators of G-protein signaling mRNA levels in mouse tissues. *Methods Enzymol.* **389:** 3-15.

Kurrasch DM, Huang J, Wilkie TM and Repa JJ (2004b) Quantitative real-time polymerase chain reaction measurement of regulators of G-protein signaling mRNA levels in mouse tissues. *Methods in Enzymology* **389:** 3-15.

Laffitte BA, Joseph SB, Walczak R, Pei L, Wilpitz DC, Collins JL and Tontonoz P (2001) Autoregulation of the human liver X receptor α promoter. *Molecular and Cellular Biology* **21:** 7558-7568.

Lee A-H, Scapa EF, Cohen DE and Glimcher LH (2008) Regulation of hepatic lipogenesis by the transcription factor XBP1. *Science* **320:** 1492-1496.

Lehmann JM, Kliewer SA, Moore LB, Smith-Oliver TA, Oliver BB, Su J-L, Sundseth SS, Winegar DA, Blanchard DE, Spencer TA and Willson TM (1997) Activation of the nuclear receptor LXR by oxysterols defines a new hormone response pathway. *Journal of Biological Chemistry* **272:** 3137-3140.

Li-Hawkins J, Gåfvels M, Olin M, Lund EG, Andersson U, Schuster G, Björkhem I, Russell DW and Eggertsen G (2002) Cholic acid mediates negative feedback regulation of bile acid synthesis in mice. *J Clin Invest* **110:** 1191-1200.

Li T, Franci JM, Boehme S, Ochoa A, Zhang Y, Klaassen CD, Erickson SK and Chiang JYL (2012) Glucose and insulin induction of bile acid synthesis: mechanisms and implication in diabetes and obesity. *J Biol Chem* **287:** 1861-1873.

Li T, Owsley E, Matozel M, Hsu P, Novak CM and Chiang JYL (2010) Transgenic expression of cholesterol 7α-hydroxylase in the liver prevents high-fat diet–induced obesity and insulin resistance in mice. *Hepatology* **52:** 678-690.

Liang G, Yang J, Horton JD, Hammer RE, Goldstein JL and Brown MS (2002) Diminished hepatic response to fasting/refeeding and liver X receptor agonists in mice with selective

deficiency of sterol regulatory element-binding protein-1c. *Journal of Biological Chemistry* **277:** 9520-9528.

Lu TT, Repa JJ and Mangelsdorf DJ (2001) Orphan nuclear receptors as eLiXiRs and FiXeRs of sterol metabolism. *Journal of Biological Chemistry* **276:** 37735-37738.

Lund EG, Guileyardo JM and Russell DW (1999) cDNA cloning of cholesterol 24-hydroxylase, a mediator of cholesterol homeostasis in the brain. *Proc Natl Acad Sci U S A* **96:** 7238-7243.

Makishima M, Okamoto AY, Repa JJ, Tu H, Learned RM, Luk A, Hull MV, Lustig KD, Mangelsdorf DJ and Shan B (1999) Identification of a nuclear receptor for bile acids. *Science* **284:** 1362-1365.

Maloney PR, Parks DJ, Haffner CD, Fivush AM, Chandra G, Plunket KD, Creech KL, Moore LB, Wilson JG, Lewis MC, Jones SA and Willson TM (2000) Identification of a chemical tool for the orphan nuclear receptor FXR. *Journal of Medicinal Chemistry* **43:** 2971-2974.

McGarry JD (2002) Dysregulation of fatty acid metabolism in the etiology of type 2 diabetes. *Diabetes* **51:** 7-18.

McMurry MP, Connor WE, Lin DS, Cerqueira MT and Connor SL (1985) The absorption of cholesterol and the sterol balance in the Tarahumara Indians of Mexico fed cholesterol-free and high cholesterol diets. *Am. J. Clin. Nutr.* **41:** 1289-1298.

Mentlein R, Lembke B, Vik H and Berge RK (1986) Different induction of microsomal carboxylesterases, palmitoyl-CoA hydrolase and acyl-$_{L}$-carnitine hydrolase in rat liver after treatment with clofibrate. *Biochemical Pharmacology* **35:** 2727-2730.

Mitro N, Vargas L, Romeo R, Koder A and Saez E (2007) T0901317 is a potent PXR ligand: implications for the biology ascribed to LXR. *FEBS Letters* **581:** 1721-1726.

Miyata M, Matsuda Y, Nomoto M, Takamatsu Y, Sato N, Hamatsu M, Dawson PA, Gonzalez FJ and Yamazoe Y (2009) Cholesterol feeding prevents hepatic accumulation of bile acids in cholic acid-fed farnesoid X receptor (FXR)-null mice: FXR-independent suppression of intestinal bile acid absorption. *Drug Metab Dispos* **37:** 338-344.

Miyazaki J, Araki K, Yamato E, Ikegami H, Asano T, Shibasaki Y, Oka Y and Yamamura K (1990) Establishment of a pancreatic beta cell line that retains glucose-inducible insulin secretion: special reference to expression of glucose transporter isoforms. *Endocrinology* **127:** 126-132.

Modica S, Gadaleta RM and Moschetta A (2010) Deciphering the nuclear bile acid receptor FXR paradigm. *Nucl Recept Signal* **8:** e005.

Mott GE, Jackson EM, McMahan CA and McGill HC, Jr. (1992) Dietary cholesterol and type of fat differentially affect cholesterol metabolism and atherosclerosis in baboons. *J. Nutr.* **122:** 1397-1406.

Mukherjee R, Davies PJA, Crombie DL, Bischoff ED, Cesario RM, Jow L, Hamann LG, Boehm MF, Mondon CE, Nadzan AM, Paterniti JR and Heyman RA (1997) Sensitization of diabetic and obese mice to insulin by retinoid X receptor agonists. *Nature* **386:** 407-410.

Muraoka T, Aoki K, Iwasaki T, Shinoda K, Nakamura A, Aburatani H, Mori S, Tokuyama K, Kubota N, Kadowaki T and Terauchi Y (2011) Ezetimibe decreases SREBP-1c expression in liver and reverses hepatic insulin resistance in mice fed a high-fat diet. *Metabolism Clinical and Experimental* **60:** 617-628.

Norlin M and Wikvall K (2007) Enzymes in the conversion of cholesterol into bile acids. *Curr. Mol. Med.* **7:** 199-218.

Parathath S, Dogan S, Joaquin VA, Ghosh S, Guo L, Weibel GL, Rothblat GH, Harrison EH and Fisher EA (2011) Rat carboxylesterase ES-4 enzyme functions as a major hepatic neutral cholesteryl ester hydrolase. *Journal of Biological Chemistry* **286:** 39683-39692.

Park H, Shima T, Yamaguchi K, Mitsuyoshi H, Minami M, Yasui K, Itoh Y, Yoshikawa T, Fukui M, Hasegawa G, Nakamura N, Ohta M, Obayashi H and Okanoue T (2011) Efficacy of long-term ezetimibe therapy in patients with nonalcoholic fatty liver disease. *Journal of Gastroenterology* **46:** 101-107.

Parker AG, Pinot F, Grant DF, Spearow J and Hammock BD (1996) Regulation of mouse liver microsomal esterases by clofibrate and sexual hormones. *Biochemical Pharmacology* **51:** 677-685.

Parks DJ, Blanchard SG, Bledsoe RK, Chandra G, Consler TG, Kliewer SA, Stimmel JB, Willson TM, Zavacki AM, Moore DD and Lehmann JM (1999) Bile acids: natural ligands for an orphan nuclear receptor. *Science* **284:** 1365-1368.

Patsouris D, Reddy JK, Muller M and Kersten S (2006) Peroxisome prliferator-activated receptor α mediates the effects of high-fat diet on hepatic gene expression. *Endocrinology* **147:** 1508-1516.

Poole M, Bridgers K, Alexson SEH and Corton JC (2001) Altered expression of the carboxylesterases ES-4 and ES-10 by peroxisome proliferator chemicals. *Toxicology* **165:** 109-119.

Powers AC, Efrat S, Mojsov S, Spector D, Habener JF and Hanahan D (1990) Proglucagon processing similar to normal islets in pancreatic α-like cell line derived from transgenic mouse tumor. *Diabetes* **39:** 406-414.

Quiroga AD and Lehner R (2011a) Liver triacylglycerol lipases. *Biochimca Biophysica Acta* **1821:** 762-769.

Quiroga AD and Lehner R (2011b) Role of endoplasmic reticulum neutral lipid hydrolases. *Trends in Endocrinology and Metabolism* **22:** 218-225.

Rebouissou S, Imbeaud S, Balabaud C, Boulanger V, Bertrand-Michel J, Terce F, Auffray C, Bioulac-Sage P and Zucman-Rossi J (2007) HNF1α inactivation promotes lipogenesis in human hepatocellular adenoma independently of SREBP-1 and ChREBP activation. *Journal of Biological Chemistry* **282:** 14437-14446.

Repa JJ, Berge KE, Pomajzl C, Richardson JA, Hobbs HH and Mangelsdorf DJ (2002a) Regulation of ATP-binding cassette sterol transporters ABCG5 and ABCG8 by the liver X receptors α and β. *Journal of Biological Chemistry* **277:** 18793-18800.

Repa JJ, Dietschy JM and Turley SD (2002b) Inhibition of cholesterol absorption by SCH 58053 in the mouse is not mediated via changes in the expression of mRNA for ABCA1, ABCG5 or ABCG8 in the enterocyte. *Journal of Lipid Research* **43:** 1864-1874.

Repa JJ, Liang G, Ou J, Bashmakov Y, Lobaccaro J-MA, Shimomura I, Shan B, Brown MS, Goldstein JL and Mangelsdorf DJ (2000a) Regulation of mouse sterol regulatory element-binding protein-1c gene (SREBP-1c) by oxysterol receptors, LXRα and LXRβ. *Genes & Development* **14:** 2819-2830.

Repa JJ and Mangelsdorf DJ (2000) The role of orphan nuclear receptors in the regulation of cholesterol homeostasis. *Annu Rev Cell Dev Biol* **16:** 459-481.

Repa JJ, Turley SD, Lobaccaro J-MA, Medina J, Li L, Lustig K, Shan B, Heyman RA, Dietschy JM and Mangelsdorf DJ (2000b) Regulation of absorption and ABC1-mediated efflux of cholesterol by RXR heterodimers. *Science* **289:** 1524-1529.

Repa JJ, Turley SD, Quan G and Dietschy JM (2005) Delineation of molecular changes in intrahepatic cholesterol metabolism resulting from diminished cholesterol absorption. *Journal of Lipid Research* **46:** 779-789.

Russell DW (2003) The enzymes, regulation, and genetics of bile acid synthesis. *Annual Reviews in Biochemistry* **72:** 137-174.

Russell DW (2009) Fifty years of advances in bile acid synthesis and metabolism. *J Lipid Res* **50:** S120-S125.

Satoh T and Hosokawa M (1998) The mammlian carboxylesterases: From molecules to functions. *Annual Reviews in Pharmacology and Toxicology* **38:** 257-288.

Satoh T and Hosokawa M (2006) Structure, function and regulation of carboxylesterases. *Chemico-Biological Interactions* **162:** 195-211.

Schmittgen TD and Livak KJ (2008) Analyzing real-time PCR data by the comparative C_T method. *Nature Protocols* **3:** 1101-1108.

Schreiber R, Taschler U, Wolinski H, Seper A, Tamegger SN, Graf M, Kohlwein SD, Haemmerle G, Zimmermann R, Zechner R and Lass A (2009) Esterase 22 and beta-glucuronidase hydrolyze retinoids in mouse liver. *Journal of Lipid Research* **50:** 2514-2523.

Schultz JR, Tu H, Luk A, Repa JJ, Medina JC, Li L, Schwendner S, Wang S, Thoolen M, Mangelsdorf DJ, Lustig KD and Shan B (2000) Role of LXRs in control of lipogenesis. *Genes & Development* **14:** 2831-2838.

Schwarz M, Lund EG, Lathe R, Björkhem I and Russell DW (1997) Identification and characterization of a mouse oxysterol 7α-hydroxylase cDNA. *J. Biol. Chem.* **272:** 23995-24001.

Schwarz M, Lund EG, Setchell KDR, Kayden HJ, Zerwekh JE, Björkhem I, Herz J and Russell DW (1996) Disruption of cholesterol 7α-hydroxylase gene in mice: II. Bile acid deficiency overcome by induction of oxysterol 7α-hydroxylase. *J. Biol. Chem.* **271:** 18024-18031.

Schwarz M, Russell DW, Dietschy JM and Turley SD (2001) Alternate pathways of bile acid synthesis in the cholesterol 7α-hydroxylase knockout mouse are not upregulated by either cholesterol or cholestyramine feeding. *J. Lipid Res.* **42:** 1594-1603.

Schwarz M, Russell DW, Dietschy JM and Turley SD (1998) Marked reduction in bile acid synthesis in cholesterol 7α-hydroxylase-deficient mice does not lead to diminished tissue cholesterol turnover or to hypercholesterolemia. *J. Lipid Res.* **39:** 1833-1843.

Shimano H, Horton JD, Hammer RE, Shimomura I, Brown MS and Goldstein JL (1996) Overproduction of cholesterol and fatty acids causes massive liver enlargement in transgenic mice expressing truncated SREBP-1a. *Journal of Clinical Investigation* **98:** 1575-1584.

Sinal CJ, Tohkin M, Miyata M, Ward JM, Lambert G and Gonzalez FJ (2000) Targeted disruption of the nuclear receptor FXR/BAR impairs bile acid and lipid homeostasis. *Cell* **102:** 731-744.

Staudinger JL, Xu C, Cui YJ and Klaassen CD (2010) Nuclear receptor-mediated regulation of carboxylesterase expression and activity. *Expert Opinion in Drug Metabolism and Toxicology* **6:** 261-271.

Szczepaniak LS, Nurenberg P, Leonard D, Browning JD, Reingold JS, Grundy S, Hobbs HH and Dobbins RL (2005) Magnetic resonance spectroscopy to measure hepatic triglyceride content: prevalence of hepatic steatosis in the general population. *Am J Physiol Endocrinol Metab* **288:** E462-468.

Sznaidman ML, Haffner CD, Maloney PR, Fivush AM, Chao E, Goreham D, Sierra ML, LeGrumelec C, Xu HE, Montana VG, Lambert MH, Willson TM, Oliver WR and Sternbach DD (2003) Novel selective small molecule agonists for peroxisome proliferator-activated receptor δ (PPARδ) - Synthesis and biological activity. *Bioorganic & Medicinal Chemistry Letters* **13:** 1517-1521.

Temel RE and Brown JM (2010) A new framework for reverse cholesterol transport: Non-biliary contributions to reverse cholesterol transport. *World Journal of Gastroenterology* **16:** 5946-5952.

Thomas JW, Bramlett KS, Montrose C, Foxworthy P, Eacho PI, McCann D, Cao G, Kiefer A, McCowan J, Yu K, Grese T, Chin WW, Burris TP and Michael LF (2002) A chemical switch regulates fibrate specificity for PPARα versus LXR. *Journal of Biological Chemistry* **278:** 2403-2410.

Turley SD, Schwarz M, Spady DK and Dietschy JM (1998) Gender-related differences in bile acid and sterol metabolism in outbred CD-1 mice fed low- and high-cholesterol diets. *Hepatology* **28:** 1088-1094.

Turley SD, Spady DK and Dietschy JM (1997) Regulation of fecal bile acid excretion in male Golden Syrian hamsters fed a cereal-based diet with and without added cholesterol. *Hepatology* **25:** 797-803.

Turley SD, Valasek MA, Repa JJ and Dietschy JM (2010) Multiple mechanisms limit the accumulation of unesterified cholesterol in the small intestine of mice deficient in both ACAT2 and ABCA1. *Am J Physiol Gastrointest Liver Physiol* **299:** G1012-G1022.

Tzameli I, Pissios P, Schuetz EG and Moore DD (2000) The xenobiotic compound 1,4-bis[2-(3,5-dichloropyridyloxy)]benzene is an agonist ligand for the nuclear receptor CAR. *Molecular and Cellular Biology* **20:** 2951-2958.

Ushio M, Nishio Y, Sekine O, Nagai Y, Maeno Y, Ugi S, Yoshizaki T, Morino K, Kume S, Kashiwagi A and Maegawa H (2013) Ezetimibe prevents hepatic steatosis induced by a high-fat but not a high-fructose diet. *Am J Physiol Endocrinol Metab*

Uyeda K and Repa JJ (2006) Carbohydrate response element binding protein, ChREBP, a transcription factor coupling hepatic glucose utilization and lipid synthesis. *Cell Metabolism* **4:** 107-110.

Valasek MA, Clarke SL and Repa JJ (2007) Fenofibrate reduces intestinal cholesterol absorption via PPARα-dependent modulation of NPC1L1 expression in mouse. *Journal of Lipid Research* **48:** 2725-2735.

Valasek MA and Repa JJ (2005) The power of real-time PCR. *Advances in Physiology Education* **29:** 151-159.

Valasek MA, Repa JJ, Quan G, Dietschy JM and Turley SD (2008) Inhibiting intestinal NPC1L1 activity prevents diet-induced increase in biliary cholesterol in Golden Syrian hamsters. *American Journal of Physiology* **295:** G813-G822.

van der Velde AE, Brufau G and Groen AK (2010) Transintestinal cholesterol efflux. *Current Opinion in Lipidology* **21:** 167-171.

van der Velde AE, Vrins CLJ, van den Oever K, Seeman I, Oude Elferink RPJ, van Eck M, Kuipers F and Groen AK (2008) Regulation of direct transintestinal cholesterol excretion in mice. *American Journal of Physiology* **295:** G203-G208.

Vance JE (2012) Dysregulation of cholesterol balance in the brain: contribution to neurodegenerative diseases. *Dis Model Mech* **5:** 746-755.

Vanhanen H, Kesäniemi YA and Miettinen TA (1992) Pravastatin lowers serum cholesterol, cholesterol-precursor sterols, fecal steroids, and cholesterol absorption in man. *Metabolism* **41:** 588-595.

von Bergmann K, Mok HY, Hardison WGM and Grundy SM (1979) Cholesterol and bile acid metabolism in moderately advanced, stable cirrhosis of the liver. *Gastroenterology* **77:** 1183-1192.

Vrins CLJ (2010) From blood to gut: Direct secretion of cholesterol *via* transintestinal cholesterol efflux. *World Journal of Gastroenterology* **16:** 5953-5957.

Wang DQ-H, Tazuma S, Cohen DE and Carey MC (2003) Feeding natural hydrophilic bile acids inhibits intestinal cholesterol absorption: studies in the gallstone-susceptible mouse. *Am. J. Physiol. Gastrointest. Liver Physiol.* **285:** G494-G502.

Wang DQ (2007) Regulation of intestinal cholesterol absorption. *Annu Rev Physiol* **69:** 221-248.

Watanabe M, Horai Y, Houten SM, Morimoto K, Sugizaki T, Arita E, Mataki C, Sato H, Tanigawara Y, Schoonjans K, Itoh H and Auwerx J (2011) Lowering bile acid pool size with a synthetic farnesoid X receptor (FXR) agonist induces obesity and diabetes through reduced energy expenditure. *J Biol Chem* **286:** 26913-26920.

Wei E, Ali YB, Lyon J, Wang H, Nelson R, Dolinsky VW, Dyck JRB, Mitchell G, Korbutt GS and Lehner R (2010) Loss of TGH/Ces3 in mice decreases blood lipids , improves glucose tolerance, and increases energy expenditure. *Cell Metabolism* **11:** 183-193.

Welch JS, Ricote M, Akiyama TE, Gonzalez FJ and Glass CK (2003) PPARγ and PPARδ negatively regulate specific subsets of lipopolysaccharide and IFN-γ target genes in macrophages. *Proceedings of the National Academy of Sciences USA* **100:** 6712-6717.

Whitney KD, Watson MA, Goodwin B, Galardi CM, Maglich JM, Wilson JG, Willson TM, Collins JL and Kliewer SA (2001) Liver X receptor (LXR) regulation of the *LXRα* gene in human macrophages. *Journal of Biological Chemistry* **276:** 43509-43515.

Williams ET, Wang H, Wrighton SA, Qian Y-W and Perkins EJ (2010) Genomic analysis of the carboxylesterases: Identification and classification of novel forms. *Molecular Phylogenetic and Evolution* **57:** 23-34.

Wolters H, Elzinga BM, Baller JFW, Boverhof R, Schwarz M, Stieger B, Verkade HJ and Kuipers F (2002) Effects of bile salt flux variations on the expression of hepatic bile salt transporters in vivo in mice. *J Hepatol* **37:** 556-563.

Woollett LA, Wang Y, Buckley DD, Yao L, Chin S, Granholm N, Jones PJH, Setchell KDR, Tso P and Heubi JE (2006) Micellar solubilisation of cholesterol is essential for absorption in humans. *Gut* **55:** 197-204.

Xiao C, Hsieh J-C, Adeli K and Lewis GF (2011) Gut-liver interaction in triglyceride-rich lipoprotein metabolism. *American Journal of Physiology* **301:** E429-E446.

Xie C, Turley SD and Dietschy JM (2000) Centripetal cholesterol flow from the extrahepatic organs through the liver is normal in mice with mutated Niemann-Pick type C protein (NPC1). *J Lipid Res* **41:** 1278-1289.

Xu C, Wang X and Staudinger JL (2009) Regulation of tissue-specific carboxylesterase expression by pregnane X receptor and constitutive androstane receptor. *Drug Metabolism and Disposition* **37:** 1539-1547.

Xue Y, Chao E, Zuercher WJ, Willson TM, Collins JL and Redinbo MR (2007) Crystal structure of the PXR-T1317 complex provides a scaffold to examine the potential for receptor antagonism. *Bioorganic & Medicinal Chemistry* **15:** 2156-2166.

Yang C, McDonald JG, Patel A, Zhang Y, Umetani M, Xu F, MAngelsdorf DJ, Westover EJ, Covey DF, Cohen JC and Hobbs HH (2006) Sterol intermediates from cholesterol biosynthetic pathway as LXR ligands. *Journal of Biological Chemistry* **on-line July 20:**

Yu C, Wang F, Kan M, Jin C, Jones RB, Weinstein M, Deng C-X and McKeehan WL (2000) Elevated cholesterol metabolism and bile acid synthesis in mice lacking membrane tyrosine kinase receptor FGFR4. *J Biol Chem* **275:** 15482-15489.

Zechner R, Zimmermann R, Eichmann TO, Kohlwein SD, Haemmerle G, Lass A and Madeo F (2012) FAT SIGNALS - Lipases and lipolysis in lipid metabolism and signaling. *Cell Metabolism* **15:** 279-291.

Zelcer N, Hong C, Boyadjian R and Tontonoz P (2009) LXR regulates cholesterol uptake through Idol-dependent ubiquitination of the LDL receptor. *Science* **on-line June 11:**

Zhang Y, Cheng X, Aleksunes LM and Klaassen CD (2012) Transcription factor-mediated regulation of carboxylesterase enzymes in livers of mice. *Drug Metabolism and Disposition* **40:** 1191-1197.

Zhang Y and Klaassen CD (2010) Effects of feeding bile acids and a bile acid sequestrant on hepatic bile acid composition in mice. *J Lipid Res* **51:** 3230-3242.

Zhao B, Bie J, Wang J, Marqueen SA and Ghosh S (2012) Identification of a novel intracellular cholesteryl ester hydrolase (carboxylesterase 3) in human macrophages: compensatory increase in its expression after carboxylesterase 1 silencing. *American Journal of Physiology* **303:**

Zhao B, Song J, Chow WN, St. Clair RW, Rudel LR and Ghosh S (2007) Macrophage-specific transgenic expression of cholesteryl ester hydrolase significantly reduces atherosclerosis and lesion necrosis in Ldlr-/- mice. *Journal of Clinical Investigation* **117:** 2983-2992.

Zheng S, Hoos L, Cook J, Tetzloff G, davis HR, van Heek M and Hwa JJ (2008) Ezetimibe improves high fat and cholesterol diet-induced non-alcoholic fatty liver disease in mice. *European Journal of Pharmacology*

Zieve FJ, Kalin MF, Schwartz SL, Jones MR and Bailey WL (2007) Results of the glucose-lowering effect of WelChol study (GLOWS): A randomized, double-blind, placebo-controlled pilot study evaluating the effect of colesevelam hydrochloride on glycemic control in subjects with type 2 diabetes. *Clin Ther* **29:** 74-83.